Dissertations and Theses (Open Access)

MD Anderson UTHealth Houston Graduate School

8-2012

The Functional Organization Of Synaptic Vesicle Pools In A Retinal Bipolar Neuron

Proleta Datta

THE FUNCTIONAL ORGANIZATION OF SYNAPTIC VESICLE POOLS IN A

RETINAL BIPOLAR NEURON

by

Proleta Datta, M.B.B.S.

APPROVED:

_____
Ruth Heidelberger, M.D., Ph.D.
Supervisory Professor

_____
Roger Janz, Ph.D.

_____
Michael Beierlein, Ph.D.

_____
Ellen Lumpkin, Ph.D.

_____
John Putkey, Ph.D.

APPROVED

_____
Dean, The University of Texas,

Graduate School of Biomedical Sciences

THE FUNCTIONAL ORGANIZATION OF SYNAPTIC VESICLE POOLS IN A

RETINAL BIPOLAR NEURON

A DISSERTATION

Presented to the Faculty of The University of Texas Health Science Center at Houston and

The University of Texas M. D. Anderson Cancer Center

Graduate School of Biomedical Sciences

in Partial Fulfillment of the Requirements

for the Degree of

DOCTOR OF PHILOSOPHY

by

Proleta Datta, M.B.B.S

August 2012

This work is dedicated to my grandmother

who taught me how to add

and my daughter

who finds everything interesting

ACKNOWLEDGEMENTS

THE FUNCTIONAL ORGANIZATION OF SYNAPTIC VESICLE POOLS IN A

RETINAL BIPOLAR NEURON

Publication No-

Proleta Datta, M.B.B.S.

Supervisory Professor: Ruth Heidelberger, M.D. Ph.D.

Ribbon synapses are found in sensory systems and are characterized by 'ribbon-like' organelles that tether synaptic vesicles. The synaptic ribbons co-localize with sites of calcium entry and vesicle fusion, forming ribbon-style active zones. The ability of ribbon synapses to maintain rapid and sustained neurotransmission is critical for vision, hearing and balance. At retinal ribbon synapses, three vesicle pools have been proposed. A rapid pool of vesicles that are docked at the plasma membrane, and whose fusion is limited only by calcium entry, a releasable pool of ATP-primed vesicles whose size also correlates with the number of ribbon-tethered vesicles, and a reserve pool of non-ribbon-tethered cytoplasmic vesicles. However evidence of vesicle fusion at sites away from ribbon-style active zones questions this organization. Another fundamental question underlying the mechanism of vesicle fusion at these synapses is the role of SNARE (Soluble N-ethylmaleimide sensitive factor Attachment Protein Receptor) proteins. Vesicles at conventional neurons undergo SNARE complex-mediated fusion. However a recent study has suggested that ribbon synapses involved in hearing can operate independently of neuronal SNAREs. We used the well-characterized goldfish bipolar neuron to investigate the organization of vesicle pools

and the role of SNARE proteins at a retinal ribbon synapse. We blocked functional refilling of the releasable pool and then stimulated bipolar terminals with brief depolarizations that triggered the fusion of the rapid pool of vesicles. We found that the rapid pool draws vesicles from the releasable pool and that both pools undergo release at ribbon-style active zones. To assess the functional role of SNARE proteins at retinal ribbon synapses, we used peptides derived from SNARE proteins that compete with endogenous proteins for SNARE complex formation. The SNARE peptides blocked fusion of reserve vesicles but not vesicles in the rapid and releasable pools, possibly because both rapid and releasable vesicles were associated with preformed SNARE complexes. However, an activity-dependent block in refilling of the releasable pool was seen, suggesting that new SNARE complexes must be formed before vesicles can join a fusion-competent pool. Taken together, our results suggest that SNARE complex-mediated exocytosis of serially-organized vesicle pools at ribbon-style active zones is important in the neurotransmission of vision.

TABLE OF CONTENTS

LIST OF FIGURES

LIST OF TABLES

CHAPTER I

GENERAL INTRODUCTION

One of the most intriguing questions in neuroscience is how do nerve cells process and transmit information? The search for the answer began more than one hundred and twenty years ago (1886-90), when work by several neuroanatomists including Ramon Y Cajal, His, Purkinje and Forel suggested that nerve cells were independent biological units (1, 2). In 1891 Wilhelm von Waldeyer coined the term 'neuron' derived from the Greek word for sinew for the unitary nerve cell (3). The "neuron doctrine" was proposed by Cajal which asserts that "nerve tissue is composed of individual cells, which are genetic, anatomic, functional and trophic units". One of the assumptions of the neuron theory was that "neurons must enter into functional connections by contiguity, not continuity"(4). These sites of 'contiguity' were suggested to be sites where transmission of information occurred and were termed as 'synapses' by Sherrington in 1897(5).

Our current understanding of neurotransmission is that nerve cells communicate with each other by two main mechanisms: via chemical messengers molecules called neurotransmitters at chemical synapses and the direct transmission of electrical signals via gap junctions at electrical synapses (1). In a chemical synapse, neurotransmitter release occurs extremely rapidly (within milliseconds) and is restricted to an area of less than a micrometer square (6). Transmission of signals occurs via calcium-dependent fusion of neurotransmitter-laden vesicles with the outer membrane of the nerve cell; a process called exocytosis. Exocytosis is mediated by several protein-protein interactions.

A unique type of chemical synapse called 'ribbon synapse' is found in sensory neurons. Specialized organelles, so called ribbons to which synaptic vesicles tether, are found in the pre synaptic neurons of these synapses. These specialized synapses are found in photoreceptors and bipolar cells in the retina (7–10), other sensory systems such as the

cochlea and vestibular organ of balance (11), the electro-sensory organs and the receptors in the lateral line in fish (12). They are also found in pinealocytes of the pineal gland (13). Ribbon synapses are unique because they have the ability to respond to stimuli that are graded and can accurately transmit information over a broad range of stimulus intensities and over prolonged time periods. A human photoreceptor cell, which releases neurotransmitter tonically can detect a single photon of light and can also transmit changes in the intensity of light over a wide dynamic range of 10^{10} (14–16).

The overall aim of this dissertation is to study the mechanisms underlying neurotransmitter release at these specialized ribbon synapses, specifically the functional organization of synaptic vesicles. In this chapter I will briefly introduce 1) the synaptic vesicle cycle: the basic pre synaptic mechanism underlying neurotransmitter release and the proteins regulating it. 2) Different types of synaptic release. 3) Synaptic vesicle pools and 4) a short note on ribbon synapses. More detailed backgrounds of the relevant topics are found in the introductions to the respective chapters. Finally, I will propose the working hypothesis of this thesis, which will be tested in the following chapters.

The synaptic vesicle cycle

In its most classical and simplest form neurotransmitter release occurs during the synaptic vesicle cycle at the presynaptic nerve terminal. The synaptic vesicle cycle helps the neuron maintain repetitive release by recycling vesicles. The first step of this cycle is the active transport of the neurotransmitter into secretory vesicles relying on a proton gradient (17). A cohort of vesicles then dock at the active zone. The active zone is site at which protein-protein interactions that mediate exocytosis occur and is also the site of voltage dependent calcium channels. Once docked, the vesicles undergo multiple 'priming' steps in

preparation for release. The docking and priming steps of the cycle are regulated by several proteins and nucleotides (18–24). The final step in fusion requires the depolarization of the neuron which opens the voltage gated calcium channels and allows for an influx of calcium that triggers exocytosis. A number of proteins have been identified that aid in this process (6, 25–27). After exocytosis the vesicles are retrieved via endocytosis. Endocytosis occurs either via a fast pathway where the vesicle is reused locally without entering an endosomal recycling step or via a slower process where the protein clathrin assists in retrieving the vesicle, which then recycles via an endosomal pathway (28) completing the synaptic vesicle cycle.

Exocytosis is aided by four families of proteins: SNARE (Soluble N-ethylmaleimide-sensitive factor Attachment protein Receptor) proteins, SM (Sec1/Munc 18-like) proteins, Rab proteins and Rab effector proteins (26). The SNARE proteins, syntaxin, SNAP 25, (both traditionally considered to be found on the plasma membrane, or target SNAREs / t SNAREs) and synaptobrevin, also called VAMP, (found on the vesicle or v-SNAREs) form the minimum fusion machinery for neuronal exocytosis. These three proteins form a stable complex called the SNARE complex, allowing the vesicles to fuse with the plasma membrane. The SNARE proteins contain a 60 residue sequence called the SNARE domain which interacts with each other to form a tight coiled helical bundle. Syntaxin and synaptobrevin contribute one domain each while SNAP 25 contributes two. The formation of this SNARE complex is thought to bring the two membranes (vesicle and plasma membrane) together, destabilize the negatively charged membranes, allow intermixing of the hydrophobic lipid interiors and thus provide the energy for membrane fusion (29).
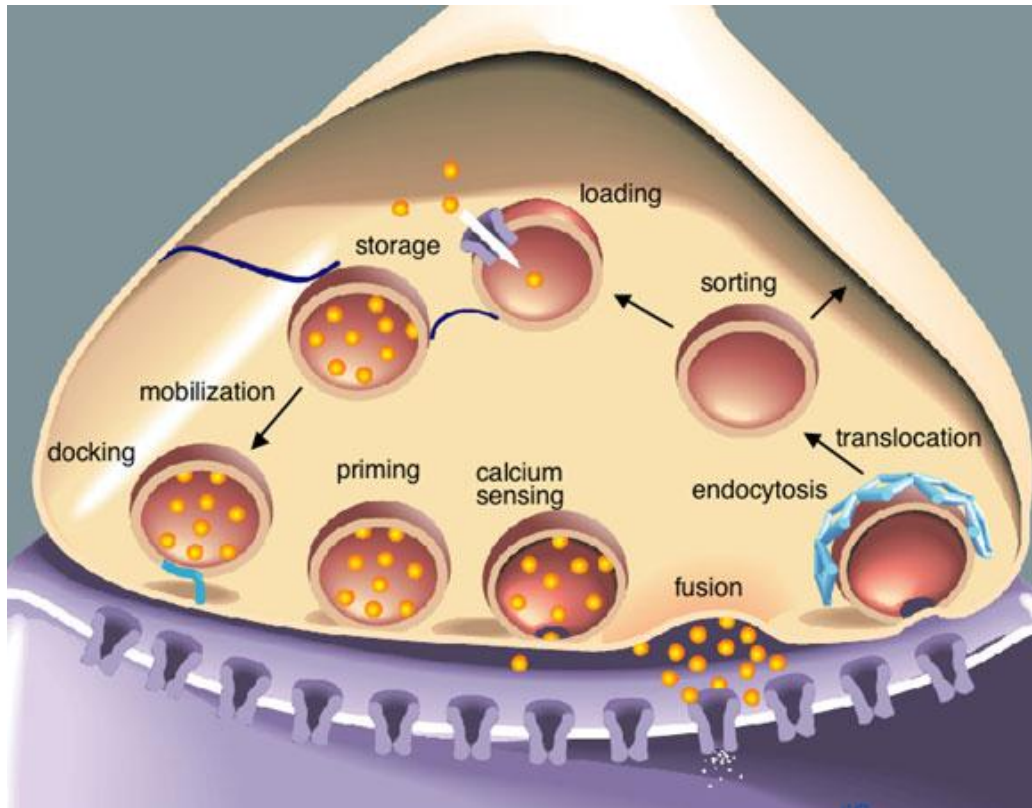
Fig 1.1 The classical view of the synaptic vesicle cycle. Synaptic vesicles contain neurotransmitter transporters that load the vesicles with neurotransmitters. Mobilized vesicles are translocated to the plasma membrane where they dock at the active zone. Docked vesicles then undergo priming steps. Docking and priming render the vesicle fusion-competent. A rise in intracellular calcium via influx through voltage-gated calcium channels results in binding of calcium to calcium sensors and triggering vesicle fusion which causes release of neurotransmitter into the synaptic cleft. Following full-fusion the vesicle membrane is retrieved endocytosis.
Richmond, J. Synaptic function (December 7, 2007)

The SM proteins interact with the SNARE complex to aid in fusion (26), however their exact mechanism of action is still under study. SM proteins are composed of an ~ 600 amino acid conserved sequence that forms a clasp like structure (30). The SM protein Munc18-1 "clasps" the SNARE protein syntaxin 1. Syntaxin 1 can exist in a "closed " confirmation where its own N-terminal folds back on its SNARE domain. In its closed form

syntaxin is unable to interact with the other SNARE binding partners. Munc 18-1 is known to bind to syntaxin and stabilize the "closed" conformation of syntaxin (31).The Rab proteins are GTP binding proteins and the Rab-effectors are complexes and their interaction with Rab proteins are GTP dependent. Both Rab proteins and Rab effectors are thought to be involved in the docking step of the synaptic vesicle cycle (32).

Two other families of proteins, Complexins and Synaptotagmins are also known to be essential in exocytosis. A single molecule of Complexin binds to a single assembled SNARE complex (33). Complexins consist of four (Complexin I- IV), 134-160 residue proteins, of which Complexin III and IV are the isoforms present in retinal ribbon synapses (34). The complexins are thought to act at a late step in exocytosis, just prior to calcium mediated fusion of vesicles (35). One suggested role is to clamp/stabilize assembled SNARE complexes and prevent fusion. This clamp is removed when calcium activates Synaptotagmin (a calcium binding protein) and interacts with the SNARE complex (36–38). In support of complexin's role in inhibiting fusion, glutametergic motor neurons of *Drosophila* complexin null mutants show increased spontaneous release (39). However a study from mouse complexin 1/2 and complexin 1/2/3 knockouts showed decreased spontaneous and evoked release in glutametergic hippocampal neurons and brainstem glycinergic/GABAergic neurons (40). These results suggest that complexins can act both as a facilitator and inhibitor of exocytosis. A series of recent studies suggest that a switch in Complexin's conformation may change its role from a inhibitor to a facilitator of fusion (41–43) .

Synaptotagmins (Syt) are calcium-binding proteins that have two C2 Ca^{2+}-binding - domains (44). Synaptotagmins are mostly present on synaptic vesicles (but can also be

found on the plasma membrane) and are the calcium sensors (Syt 1 , 2 and 9) for neuroexocytosis (26, 45–47) . However in hair cells, otoferlins are the calcium sensors (48, 49). Knocking out Synaptotagmin 1/2 in mice results is the loss of calcium-triggered exocytosis (50, 51) suggesting their role is synchronous release. Synaptotagmins have also been suggested to have a role in aligning releasable vesicles in proximity to calcium channels (52).

Types of synaptic release

Synaptic release triggered by calcium can be further classified into evoked release and spontaneous release. Evoked release commences within sub milliseconds of the calcium influx (53–56). This fast and synchronous release can be measured from post synaptic currents. These post synaptic currents have been fitted by a double exponential function, suggesting a fast phase followed by a slower phase of release (55, 57, 58). Evoked release may also have an asynchronous phase which sets in after a delay. While often thought to be negligible in excitatory synapses (however delayed asynchronous transmission has been reported in excitatory synapses (59, 60)) , asynchronous release may be the principal form of release during high frequency trains in some inhibitory synapses (61–63).

Spontaneous release is independent of membrane depolarizations such as action potentials. It represents fusion of single synaptic vesicles, giving rise to 'mini' post synaptic changes (64). Spontaneous release may be driven by stochastic calcium channel opening, basal intra-cellular calcium or spontaneous calcium transients from intra- cellular stores (65).

Synaptic vesicle pools

At the electron microscope level all synaptic vesicles look similar. However, vesicles may be found in different sub cellular spaces, such as docked to the plasma membrane or attached to a synaptic ribbon (see below, fig 1.2). The concept of vesicle pools comes from the finding that not all vesicles are functionally equal; some vesicles are released more easily than others (reviewed in Denker and Rizzoli, 2010). How readily a vesicle is released depends on many factors including its proximity to the plasma membrane and calcium channels, whether it is docked and whether it has undergone all the necessary priming steps. Therefore populations of vesicles may be located at different anatomical sub-cellular spaces and be biochemically distinct from each other. A recent study has suggested that vesicles which undergo spontaneous release are biochemically different from those that respond to evoked release. Specifically a synaptic vesicle protein VAMP7 was present in higher levels in the spontaneously releasing pool compared to the pool of vesicles undergoing evoked release (67)

The first hint that vesicles may be arranged in pools came from experiments in cat sympathetic ganglion (68). Birks and MacIntosh found that there were at least two fractions to the acetylcholine released from the cervical ganglia: a smaller 'readily releasable' fraction and a larger non-readily releasable fraction. The smaller fraction was also more rapidly depleted in response to high frequency stimulations. Based on these findings they proposed that there were different intracellular locations of these different fractions of acetylcholine and considered that there may be an interrelationship between the different fractions .

Vesicle pools have been studied in many neuronal preparations such as *Drosophila* neuromuscular junctions, hippocampal synapses, a giant synapse in the auditory pathway

called the calyx of Held and even in ribbon synapses such as salamander photoreceptors, goldfish bipolar cells and hair cells, reviewed in Rizzoli and Betz (69). For all these synapses, three major synaptic pools have been proposed. There is no consensus on the nomenclature for these pools in the literature and to avoid any confusion in this thesis, I will be referring to these three pools as the rapid pool (which has previously been referred to as the readily-releasing pool, rapidly releasing pool, immediately-releasing pool or the ultrafast pool); the releasable pool (has also been called as the recycling pool) and the reserve pool (has also been called the cytoplasmic pool).

The simplest interpretation of three functional pools is that their vesicles are localized to three different distances from the active zones or the vicinity of the calcium channels (69). The model assumes that the further away a cohort of vesicles is from an active zone the slower it is likely to release. While the rapid pool by definition must be able to undergo immediate release and therefore consists of vesicles docked at the active zones and primed for release, the vesicles in the releasable and reserve pools may be located at varying distances from the release sites and recruited to the active zone. Therefore higher levels of stimulation are required for the releasable and the reserve pool vesicles to undergo fusion. It is important to note that there may be intermixing of vesicles between the pools such that the pools are in dynamic equilibrium. Also, vesicles in one pool may be a subset of a larger pool. Some general characteristics of the three pools are listed below.

The Rapid Pool: These vesicles are generally thought to be anatomically closest to the plasma membrane, "docked" at the active zone and available for immediate release. The rapid pool is generally composed of ~1-2% of the total vesicles. These rapid pool vesicles can be released by 5-10 high frequency action potentials in conventional synapses such as

hippocampal neurons and the calyx of Held (70, 71) and 8- 30 milliseconds of depolarization in retinal ribbon style neurons (72–74). In the hippocampal neurons, calyx of Held and retinal bipolar neurons, the number of docked vesicles from anatomical studies has correlated well with the size of the rapid pool as estimated from physiological experiments (75–77).

The Releasable pool: The role of releasable pool vesicles is to maintain release once the rapid pool has been depleted. In the rat calyx of Held and drosophila neuromuscular junction, this pool is thought to be able to sustain release at physiological intensities of stimulation (78, 79). In the retinal bipolar neuron this pool has been defined as the cohort of vesicles which have already undergone all the ATP-dependent priming steps required for fusion (80, 81). The releasable pool contains ~ 10-20% of the synaptic vesicles, and in non-ribbon synapses are found scattered in the cytoplasm and are more mobile than the rapid and reserve pools (reviewed in Rizzoli and Betz, 2005). In ribbon synapses, the anatomical location of the releasable pool is contentious (82, 83).

The Reserve pool: The reserve pool serves as the depot for synaptic vesicles. It is composed of most of the vesicles (~80-90%) in the synapse. This pool serves to refill the other two pools and therefore participates in exocytosis during high stimulation protocols (78, 79, 84). These vesicles are found scattered in the cytoplasm (75, 76). They have low mobility in non-ribbon synapses, whereas in ribbon synapses they are highly mobile (85–87). Table 1.1 shows comparison of the characteristics of the three pools in four different neurons.

In non-ribbon synapses, synapsins (a family of neuron specific phosphoproteins) help to cluster synaptic vesicles by tethering them to each other and to the actin cytoskeletal meshwork (88). While it was originally thought that in non-ribbon synapses synapsins help

to cluster the reserve pool (88), experiments from synapsin knock-out animals have suggested that synapsins play a role in the size and exocytosis of the releasable pool (89, 90) and also in the formation of the rapid pool during neurodevelopment (91). Synapsins are absent in ribbon synapses (92–94). In ribbon synapses, electron micrographs have shown that a pool of vesicles is tethered to electron dense ribbon like structures (75, 95, 96).

The study of synaptic vesicle pools continues to be a very exciting field in neuroscience and several studies have suggested the existence of newer pools: 1) The "spontaneously releasing pool" is defined to be composed of vesicles that undergo spontaneous release (97–99). However another recent study has suggested that evoked and spontaneous release draws from the same vesicle pool (100). 2) The "surface pool" is a cohort of vesicles that are fused onto the plasma membrane and are ready for endocytosis. These vesicles are not a part of the rapid pool as they have already undergone exocytosis. These "stranded" vesicles are left on the plasma membrane till further stimulation can initiate their retrieval (101). The size of this surface pool has been quantified based on surface expression of vesicle associated proteins like synaptotagmin (102, 103). Finally 3) the "super pool" is composed of vesicles which can be exchanged between synaptic boutons (104–107). However the super pool may be a subset of the reserve pool as suggested by the finding that synaptic vesicle proteins associated with vesicles from the reserve pool in one synapse can be exchanged with vesicles at another synapse (107).

Table 1.1 A comparison of vesicle pool sizes and their properties in four different neuron systems.

	Frog NMJ *	Hippocampal bouton	Calyx of held	Mb1 neuron
Rapid pool	Depleted by 0.5s of 30Hz stimulation (108)	Depleted by 2s of 20Hz stimulation/ hypertonic saline (76, 109)	Depleted by 100Hz stimulations/ 10ms depolarization. Has two components: fast (3ms time constant of release) and slow (30ms time constant of release) (110–112)	Depleted by 8-30 ms depolarizations (72)
size (number)	~ 10,000 (113, 114)	~ 5-20 (76)	~ 1,500-4,000 (112, 115, 116)	~ 1,100 (72, 75)
Refilling-Rate	depends of refilling of releasable pool (114)	Time constant: 10-16s (117, 118)	Fast component: within seconds. Slow component: 100ms (112, 119)	Time constant : 4-12s. In the presence of high $(Ca^{2+})_i$: 400ms (72)
Refilled from	Releasable pool (114)	newly retrieved vesicles and from the releasable pool (120)	Possibly the recycling pool (112)	-
Releasable pool	Depleted by 10s of 30Hz stimulation. (114)	Undergoes fusion in response to high K^+ stimulation /400-600 repeated field stimulations (121, 122)	Can undergo release in response to 5-20Hz stimulation for minutes/ high K^+ stimulation (79)	Depleted by 250ms - 1s depolarizations (80, 123)
size (number)	~ 75,000 (108, 114)	~ 30-45 (121)	~ 7,000-10,000 (69, 79)	~ 5,500 (75, 123)
Refilling-rate	Can cycle continuously at 2Hz stimulation, (114)	Can continuously recycle with high K^+ depolarizations (121)	Slow refilling (79)	Refilling time constant of 8s. (80, 84, 124)
Refilled from	Recycled vesicles (114)	Can recycle from retrieved vesicles (121, 125, 126)	reserve vesicles (79)	Thought to be from reserve vesicles (84)

	Frog NMJ	**Hippocampal bouton**	**Calyx of held**	**Mb1 neuron**
Reserve pool	Recruited after 10-15s of high frequency stimulation (113)	Vesicles reluctant to fuse (121, 125)	Vesicles reluctant to fuse (79)	Undergoes fusion in response to trains of depolarizations (84)
size	~ 400,000 (69)	~ 170-200 (127)	~ 70,000 - 180,000 (79, 128)	~ 480,00- ~910,00 (75)
refilling	Time constant of recycling is several minutes (114)	Slow (121, 129)	-	-
Mixing between pools	Slow mixing between releasable and reserve pool over hours (113)	Mixing between rapid and releasable is fast. Mixing between releasable and reserve pools is slow (120, 121)	Mixing between rapid and releasable pools maybe fast. Mixing between releasable and reserve pools may be slow (79, 112)	Low mixing between releasable and reserve pools (87)

 *Note on pool sizes of NMJ : There are ~ 300 active zones at the frog NMJ and the active zones are ~ six times larger than other preparations. The number of docked vesicles per active zone at the NMJ is ~ 40 (69)

Ribbon Synapses

The ribbon synapses are named after "ribbon" like, electron-dense organelles found in the pre-synaptic neurons of these synapses. Ribbons come in various shapes and sizes. In the photoreceptor and bipolar cells they are more sheet like while in the inner hair cells in the cochlea they can be spherical , planar or oblong (130–132) . The exact molecular composition of the ribbon is not well understood. The only protein which exclusively localizes to the ribbon is RIBEYE (133–135). This is a 120 kDa protein which is a splice variant of a transcriptional repressor, CtBP2. Other proteins such as the GTPase Rab3 (136) ,scaffolding proteins Bassoon and Piccolo (135, 137–140), transcription factor CTBP1(135)

and calcium sensor protein GCAP2 (141) have been found to be a part of the ribbon complex.
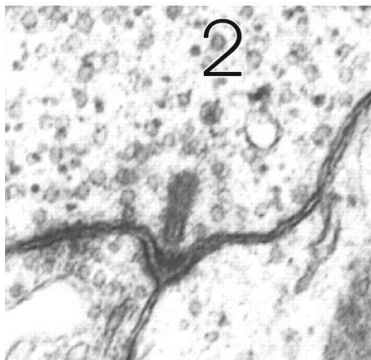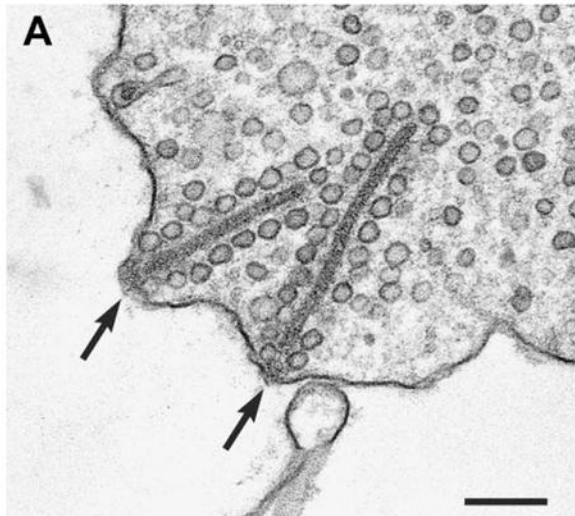
Fig 1.2 Ultrastructure of Retinal ribbon synapses Top - Electron Micrograph of the ultra structure of a the synaptic ribbon of a rod photoreceptor in an isolated cell. Magnification Bar = 200 nm (with permission from Thoreson, Rabl, Townes-Anderson, & Heidelberger, 2004). **Bottom** – Synaptic ribbon in a Mb1Goldfish bipolar neuron. Note the halo of vesicles around the synaptic ribbon (124).

Synaptic ribbons form the so called ribbon-style active zones. Electron micrographs show a pool of synaptic vesicles tethered via fine filament like structure to synaptic ribbons (96, 143–145). These vesicles have been shown to participate in evoked release (86, 87).

Calcium channels are found clustered near ribbons -immunocytochemical studies show that calcium channels co-localize with ribbon-associated proteins such as bassoon (146) and RIBEYE (135). Calcium imaging studies performed in retinal bipolar neurons and frog sacculus hair cells also show that the synaptic ribbons co-localize with the site of calcium entry and therefore form "ribbon-style" active zones (85, 134, 147).

There are several differences between ribbon style active zones and conventional active zones. Conventional synapses release neurotransmitter in response to action potentials. By comparison ribbon synapses in general release neurotransmitters responding to graded changes in membrane depolarization, or in a manner that is proportional to the level of depolarization of the neuron. However exceptions do exists in conventional synapses: in the mammalian mossy fiber and the neocortical layer 5 pyramidal cell axons, graded changes in membrane potential can propagate over 1 mm distances and modulate action potential dependent neurotransmitter release (148). Certain proteins regulating exocytosis also differ between ribbon and conventional synapses. For example in ribbon synapses, synapsins are absent (92), syntaxin 3 is present in the SNARE complex in place of syntaxin 1 (149–151), otoferlin has been proposed to be the calcium sensor instead of synaptotagmin in hair cell ribbon synapse (48, 49) and complexins 3 and 4 are unique to retinal ribbon synapses (34, 152, 153).

How does the synaptic ribbon support rapid and sustained neurotransmitter release over long periods of time? Several theories have been suggested which include 1) The ribbon itself may act as a conveyer belt to bring the vesicles to the release sites (154). In support of this idea, KIF3A, a subunit of the kinesin II motor protein has been found at ribbon synapse (155). 2) Ribbons may function as a large surface area for vesicle capture

and thus permit fast reloading, and may play a role in tonic release in these synapses (132). Compared to conventional chemical synapses such as those found in the hippocampus where an active zone has ~ 10 docked vesicles (127), in ribbon synapses, each ribbon tethers a much larger number of vesicles at the active zone. For example, in the goldfish retinal bipolar neuron, each ribbon tethers ~ 110 vesicles (75) (however only ~22 of these tethered vesicles are actually docked to the plasma membrane). 3) Another possible function of the ribbons may be to tether vesicles, keeping spontaneous fusion low. 4) Ribbon have also been proposed as sites of vesicle priming (80). In support of this, photo bleaching the synaptic ribbon at a mammalian bipolar cells leads to a decreased synaptic transmission (156). After photo bleaching, only one round of release was observed with subsequent rounds being inhibited. Examination of the ultra structure shows vesicles are localized to the ribbon, no different from control synapses. These findings suggest that after acute photo destruction of the synaptic ribbon only those vesicles which were already primed are capable of fusing. Photo bleaching impairs the ribbon's ability to prime vesicles resulting in inhibition of subsequent rounds of release. 4) The synaptic ribbon has also been proposed to be a site of compound fusion (96, 131, 157) - where vesicles attached to the ribbon may fuse with each other before or after the vesicle at the base of the ribbon fuses with the plasma membrane. This sort of fusion allows for reuse of the same release site.

The number of vesicles associated with SNARE complexes, among other factors, regulates how quickly and reliably a nerve cell can transmit a signal. In conventional synapses, ~10-60 vesicles are found clustered near the plasma membrane at active zones (76, 77). Only the docked vesicles (closest to the plasma membrane) are thought to be associated with SNARE complexes. The number of vesicles and the identity of the pool of

vesicles in SNARE complex in ribbon synapses is unknown. Interestingly, a recent study has suggested that vesicle fusion not requiring neuronal SNAREs occur at hair cells (158). Therefore the role of neuronal SNAREs at ribbon synapses is contentious.

The mechanism underlying continuous release at ribbon synapses remains an active field of study. *We hypothesize that a serial organization in the vesicle pools and a large pool of vesicles in SNARE complex aid in the continuous neurotransmission at retinal ribbon style synapses.*

CHAPTER II

GENERAL METHODS

1. *Animals:* Goldfish (*Carassius auratus*) 4-5 " in size were maintained on a 12 hr light/dark cycle. All animal procedures conformed to the National Institute of Health (NIH) guidelines and were approved by the Animal Welfare Committee of the University of Texas Medical School at Houston.

2. *Acute Dissociation of Bipolar cell terminals:* The procedure for acute dissociation of bipolar cell terminals was similar to that described in Heidelberger & Matthews 1992. The protocol we used is as follows. Goldfish were dark-adapted for 20 minutes. The animals were then decapitated and the eyeballs enucleated. Retinae were dissected free in oxygenated low calcium ringers containing in mM, NaCl 120, KCl 2.6, MgCl$_2$ 1.0, CaCl$_2$ 0.5, Hepes 10, Glucose 10 pH 7.3, and ~ 260mosm. Each retina was cut into 8-10 pieces that were incubated for 30 minutes at 20°C in a digestion solution containing NaCl 115, KCl 2.5, MgCl$_2$ 1.0, CaCl$_2$ 0.5, Pipes 10, Glucose 10, cysteine 2.7 and papain (varying concentrations were used depending on lot and vendor: see below), pH 7.25-7.3, ~ 260mosm. After digestion, the pieces were rinsed several times in low calcium ringers and stored at 10°C for up to 6-8 hours. 1- 2 pieces of retinae were mechanically triturated with a fire polished pipette and plated onto a 25 mm glass cover slip which was bathed in external solution. The external solution had the same composition as the calcium ringers solution above except the calcium concentration was increased to 2.5mM.

Note on Papain: Experiments were done with either papain from Fluka (MW= 23000) or from Calbiochem (MW=21000). We used 8mg of the papain from Fluka. The activity of the Fluka papain was 3.1U/mg - 3.6U/mg (depending on lot number) where 1U defined by the vendor corresponds to the amount of enzyme which hydrolyzes 1micoM N-benzoyl-L-arginine ethyl ester (BAEE, Fluka No. 12880) per minute at pH 6.2 and 25 C.

For the papain from Calbiochem, we used 5 mg. The activity of the Calbiochem papain was 30,000 USP units /mg where 30 USP units was defined by the vendor as 1 MCU (milk clotting unit) = 9 HDU (hemoglobin digestion units)= 6 GU (gelatin units).
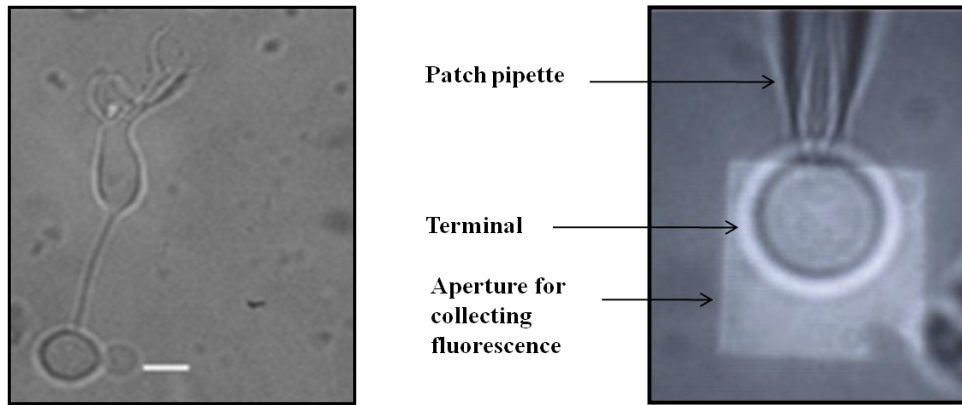
Fig 2.1 Isolated Mb1 neuron and terminal Left - A single Mb1 neuron (scale bar = 10 μm). **Right-** A single Mb1 terminal under voltage clamp. Patch pipette and aperture used for collecting florescent measurements are marked.

3. *Electrophysiology:* Goldfish terminals were identified mainly by their characteristic round shape, large size (diameter of 8-12 μm) and lack of an obvious nucleus. A 10 μm scale bar was used to confirm the size of the terminals. Some terminals had a short axon stub attached. During recordings the identity of the terminal was also verified by the presence of long-lasting voltage gated calcium channels and the lack of sodium currents (159, 160). The extracellular recording solution was identical to the low calcium ringers solution, except the calcium concentration was increased to 2.5mM. The standard internal solution contained in mM: Cs Gluconate 100, TEA 10, $MgCl_2$ 3.0, EGTA 5, $CaCl_2$ 2.5, Hepes 35, Na_2ATP 2, and GTP 0.5, pH 7.25-7.3, 265-275 mOsm. This solution was calculated to buffer the intracellular calcium concentration to 150 nM (Maxchelator; http://maxchelator.stanford.edu). The buffering ability of this solution was also verified

experimentally – please refer to values of basal calcium in each set of experiments and a list of the calibration constants used in appendix A. (80, 161).

In experiments where ATPγS was used to block functional refilling, 2mM of ATPγS replaced the 2mM ATP. In experiments where high mM EGTA was required, the calcium concentration was 2.5 mM and the EGTA concentration was increased to 7.5 mM. This solution was calculated to buffer the intracellular calcium to 73 nM and yield 4.7mM of free EGTA (Maxchelator; http://maxchelator.stanford.edu). A detailed note on the solutions containing peptides is given below.

For whole-cell recordings, 5-7 MΩ pipettes were made from unfilamented 8250 borosilicate glass (1.5 O.D, 0.86 I.D., A-M systems) and coated with sylgard to decrease their capacitance. A computer-controlled EPC-9 patch clamp amplifier was used for recordings, and capacitance measurements were made with "Pulse" software (version 8.53, HEKA Electronik, Lambrecht, Germany). For capacitance measurements, a sine wave voltage command (805 Hz, 30 mV peak to peak) was applied about a holding potential of -60mV. The Lindau-Neher technique (162, 163) was used to give estimates of the membrane capacitance (C_m), series conductance (G_s) and membrane conductance (G_m). For depolarizing pulses, the membrane was depolarized from the holding potential of -60mV to 0mV. ΔC_m changes less than 1 SD of the average baseline C_m were considered null responses. Recordings from terminals with $G_s < 50$ nS or current at holding potential > 40 pA were excluded from analysis.

Wash-out of exocytotic responses:

Generally in our experiments, the first exocytotic response is the largest. This is observed even under conditions where complete pool refilling might be expected, such as in

the presence of 5mM ATP. This phenomenon of decreased exocytosis over the time period of the recording can be attributed to wash out of exocytotic response. Wash out or run-down of exocytosis has been previously reported in Mb1 terminals (123) and also in other secretory cells (164). The slow run down may be due to loss or diffusion of soluble factors and small molecules aiding in pool refilling such as α-SNAP and GTP binding proteins during whole cell dialysis. The extent of rundown of neuronal responses is proportional on the resistance of the pipettes used (164–166). In our experiments we tried our best to minimize wash out of exocytosis by using high resistance pipettes (5-7 MΩ), loaded with a high concentration of the peptide. In addition we probed the terminal within the first 60-200s following break-in (164).

4. *SNARE complex-inhibiting peptides*: Three different SNARE complex inhibiting peptides were used. The peptides were synthesized by Biosynthesis (Lewisville, TX).The syntaxin 3B peptide was derived from the N-terminal part of the SNARE domain of syntaxin 3B (sequence - NH2- RHKDIMRLESSIKELHDMFVDVA-OH), while a scrambled peptide (sequence- NH2- RIALKDDVIHMRESVDHKSFMEL-OH) was used as a control (151). Both these peptides were tagged with FITC (fluorescein isothiocyanate) at the N terminal using a AHX linker. A previously designed scrambled peptide (sequence-NH2-SMKIRFSVHARVELHMEDLDIDK-OH) was not used as it did not dissolve in the internal solution at the concentration of 0.5mM.

The SNAP peptide (sequence - NH2-IMEKADSNKTRIDEANQRATKMLGSG-OH) was derived from the C terminal of the SNARE binding domain. A scramble SNAP 25 peptide (sequence -NH2- KNKGTSDEGSDIMQKAILNEARMTRA-OH) was used as a control. The Synaptobrevin peptide (sequence - NH2-RLQQTQAQVDEVVDIMRVN-OH)

was derived from the N terminal of the SNARE binding domain of Synaptobrevin. The SNAP peptide, the scrambled SNAP peptide and the Synaptobrevin peptide were not fluorescently tagged.

For each peptide solution the lyophilized peptide was dissolved in internal solution that was similar to the standard internal solution expect the ATP concentration was increased to 5 mM (in place of 2mM ATP) and $MgCl_2$ to 6mM (in place of 3mM $MgCl_2$) to provide 1mM free Mg^{2+}. Once the peptide dissolved, we filtered the internal solution using 0.2 μm PES filters (Nalgene 25 mm Cat# 194-2520). These filters are known to be low peptide binding filters. Effects of osmolarity on vesicle dynamics (161) were taken into consideration and the final osmolarity of the peptide containing solution was adjusted to ~270 - 274 mosm by the addition of 2-4 μl of Millipore water.

Note on peptide concentration: The concentration of the peptide in solution by weight was 500mM. The calculated final concentration of the peptide used on the day of each experiment was lowered to 0.25 mM by diluting with equal volume of peptide - free internal solution. In previous experiments where short peptides have been dialyzed into CNS terminals, similar concentration of peptides have been found to have an effect. In the calyx of held, an N terminal syntaxin1 peptide blocks neurotransmitter release at 0.25- 1 mM concentrations in a dose dependent manner (167).To estimate the actual concentration of peptide in the internal solution our collaborator Dr. Roger Janz performed spectroscopy measurements on peptide internal solution samples. The scrambled peptide sample (original concentration 0.5 mM) was diluted 1:20 (10 μL in 200μL) and the syntaxin peptide sample (original concentration 0.25 mM) was diluted 1:40 (5 μL in 200μL). A wavelength of 494nm was used to measure the optical density using spectroscopy. Internal solution with

no added peptide was used as a blank/control. The final concentrations using this method was 0.127 mM for the scrambled peptide and 0.165 mM for the syntaxin peptide. The samples used had been stored for a duration of more than one year at - 80 ºC. Possible photo bleaching of the fluorescent peptide was not taken into consideration while making the above calculations.

5. *Fluorescence measurements of tagged peptides:* In experiments with the FITC tagged peptides, we were able to establish that the peptides were dialyzed into the terminal. A computer controlled photometry system (ASI/TILL Photonics) was used to record fluorescence. The excitation wavelength for fluorescein was 475 nm and emission wavelength was 505 nm. To test whether the Syntaxin 3B peptide and the scrambled peptide dialyzed into the terminal at the same rate, we fit the fluorescent loading trace with a exponential function. The τ (time constant) of loading was not different in terminals dialyzed with either peptide. [Syntaxin $\tau = 89.1 \pm 10.5$ (n=6), Scrambled peptide $\tau = 87 \pm 12.17$ (n=5), p = 0.9 for experiments where pulse trains were used]. A τ of ~ 90 suggests that plateau in the fluorescence was typically reached within ~ 270 s or 4-5 minutes, after achieving the whole-terminal recording configuration.

6. *Intracellular calcium measurements:* Spatially averaged intracellular calcium concentrations were made with the fluorescent calcium indicator dye bis fura2 in all experiments except those with the tagged syntaxin and synaptobrevin peptides. The Kd of bis fura2 binding to calcium is ~ 370nM (molecular probes catalogue). 0.1mM of Bis fura2 was added to the internal solution. Alternating excitation at 360 and 388 nm was provided by a computer-controlled monochromator based system (ASI/T.I.L.L. Photonics, (168) and the emitted fluorescence (f1&f2) at 505 nm was recorded. An adjustable aperture is used to

position the collection field for the emitted fluorescence selectively over a single bipolar cell terminal. Intracellular calcium was calculated from the formula $[Ca]_i = k_{eff} *(ratio-ratio_{min}) / (ratio_{max} - ratio)$, (169), where ratio = f1/f2 after the subtraction of background florescence from each trace. Calibration constants k_{eff}, $ratio_{min}$, and $ratio_{max}$ were determined by in-vitro calibrations with solutions containing highly buffered known concentrations of calcium. For calibration constants used see appendix A.

6. *In-vitro protein assay:* Experiments were performed by collaborators in Roger Janz laboratory. Goldfish retina was homogenized in a buffer containing 1% Triton-X-100 and centrifuged. The supernatant was mixed with the peptide derived from syntaxin 3B or the scrambled control peptide (final peptide concentration 0.5 μM) and incubated for 2 hrs. at room temperature. The samples were then mixed with SDS-sample buffer, separated by SDS-PAGE without boiling of the samples and analyzed by western blot with a syntaxin 3 antibody.

7. *Analysis:* Data analysis was performed in Igor Pro (Wavemetrics Inc.) or Microsoft Excel. Data are expressed as mean ± s.e.m. Statistical analysis was done using Student's unpaired t-test. P value < 0.05 is marked with * and <0.005 with **.

Analysis of the train pulse was done using programs written in Igor (see Appendix B). The programs were written with help from Ian Gemp, a summer student from Northwestern University. The data was then entered into either an Igor Pro or Excel spreadsheet for further analysis.

CHAPTER III

RELATIONSHIP BETWEEN VESICLE POOLS

INTRODUCTION

Synaptic vesicle pools have been studied in several model systems. Examples of ribbon style synapses in sensory systems where vesicle pools have been identified and characterized include the salamander photoreceptors, rodent bipolar neurons, goldfish bipolar neurons and rodent hair cells (131, 132, 170–173). The retinal bipolar neuron in the goldfish has served as a great model for the study of vesicle pool dynamics and is the model cell used in all the experiments described in this thesis. In this section I will provide a background regarding the 1) Basic physiology of the bipolar neuron 2) Organization of vesicle pools in the goldfish bipolar neuron and 3) endocytosis in the goldfish bipolar neuron .

Basic physiology of the bipolar neuron

In the retina, a single output cell –a ganglion cell is able to reliably transmit information in response to the absorption of a single photon of light by a single input cell – a photoreceptor (174). Retinal bipolar cells are interneurons which play a crucial role in the retinal circuitry. Bipolar cells are second-order neurons, which transmit information from photoreceptors to third order neurons the amacrine cells or output neurons - ganglion cells. In the primate retina golgi staining has revealed at least nine types of bipolar cells, of which eight are cone bipolar cells and there is a single rod-bipolar cell type (175).

Physiologically bipolar neurons can be broadly divided into ON and OFF bipolar cells depending on their response to light. The photoreceptors are depolarized and release glutamate (176) in the dark (177). The two types of bipolar cells respond differently to glutamate release. The ON bipolar cell hyperpolarizes in response to glutamate (thus it

depolarizes to a light response) and the OFF bipolar cell depolarizes to glutamate ,thus hyperpolarizing to light (178). This difference in response to glutamate is due to the different glutamate receptors on the two types of bipolar cells. The ON bipolar cells expresses metabotropic(mGluR) , specifically mGluR6 (179, 180) while the OFF bipolar cells express ionotropic glutamate receptors (iGluR), specifically of the AMPA and Kainate type (181).The rod contacting bipolar cells are unique in that there is only one type (ON) whereas cone-bipolar cells may be ON or OFF. Also, irrespective of species the Rod bipolar cell is highly immunoreactive to Protein kinase C (PKC), which has been used as a marker for this neuron (182–184). ON and OFF bipolar cells also arborize to different layers in the retina. In general the ON bipolar cells stratify to sublamina b in the inner plexiform layer (IPL) where it makes synapses with the ON ganglion cell or amacrine cell. The OFF bipolar cell stratifies to sublamina a of the IPL where is forms synapses with the OFF ganglion cells. In the mammalian retina the rod bipolar cell (ON) stratifies to the sublamina b where it synapses with the AII amacrine cell. This pattern of stratification is relatively consistent in all vertebrate retina examined, specifically in mammals (185–188).

The bipolar cells have ribbon style active zones and release glutamate (189). Exocytosis is driven via the activation of voltage gated calcium channels - L-type calcium channels in fish (159, 190). In mammals the presence of both L and T type calcium channels have been suggested (191–194). In the Mb1 goldfish bipolar neuron the L-type channel has been identified as $Ca_v 1.3$ (195). The slow rate of calcium-dependent inactivation of this channel may help to main graded exocytosis in the bipolar neurons (159, 195, 196).

Bipolar cell responses to membrane depolarization as measured from post synaptic

cells show both transient and sustained components (58, 197–199).The bipolar cells were originally considered non-spiking neurons, since they do not fire Na$^+$ dependent action potentials, however spontaneous calcium spikes (200), light flash induced calcium spikes (201) and evoked calcium spikes (202) have been reported.

Organization of vesicle pools in the goldfish bipolar neuron

The fish rod-dominant bipolar cell, the counterpart of the mammalian rod bipolar cell, is a part of the fish scotopic pathway and receives inputs predominantly from rods (203). The Mb1(mixed bipolar) neuron in the goldfish is an ON type bipolar cell and usually synapses onto a postsynaptic dyad of two amacrine cells and rarely onto ganglion cells (204, 205). The Mb1 neuron has a large synaptic terminal which is 8-12μm in size (206). This large size of the synaptic terminal makes it amenable to patch clamp techniques and membrane capacitance techniques to study exocytosis. Membrane capacitance (C_m) measurements track membrane surface area and therefore indicate membrane addition, during exocytosis and its retrieval, during endocytosis (163). It is an excellent tool to study exo/endocytosis of populations of vesicles. The bipolar cell terminal has been well characterized using this technique and has yielded much information about its vesicle pools (132, 207)

The diameter of a single vesicle in the Mb1 cell is ~ 29nm (75). Therefore, fusion of a single vesicle should increase the C_m by ~26 aF (assuming the vesicle membrane has a specific capacitance of 1μF/cm^2, the same as the plasma membrane). The sizes of the different vesicle pools in the sections below are based on these calculations and correlated with ultrastructural findings. EM reconstruction of two Mb1 bipolar terminals has suggested

that a bipolar terminal has ~ 45-60 synaptic ribbons (75), each of which tether ~ 110 vesicles. The vesicles on the ribbon are arranged in~4- 5 rows, with each row containing ~11 vesicles. Therefore a single ribbon may tether 55 vesicles on each side (fig3.1)

The rapid pool

The pool of vesicles closest to the plasma membrane and the calcium channels constitute the rapid pool. This pool was discovered by examining exocytosis response to brief depolarizing pulses 10-30 ms (72, 73, 208). Capacitance measurements show this pool to be ~30 fF in size. This 30 fF size corresponds to ~ 1100 vesicles. From correlations with EM reconstructions, 1100 vesicles match the number of vesicles which form the bottom most row of vesicles attached to the ribbon; each ribbon tether ~ 22 vesicles (75).

The idea that the bottom most row of vesicles on the ribbon form the rapid pool is strengthened by two other findings -1)The rate of fusion of this pool is limited only by the activation kinetics of the calcium channel and 2) the rapid pool is also resistant to milli molar levels of intracellular EGTA, a slow calcium buffer, but is blocked by BAPTA, which has the same calcium binding affinity to EGTA but is 100 times faster (72). The rapid pool can be depleted with an 8-30 ms depolarization from -60to 0mV. The time constant of refilling (τ_{refill}) of this pool, as measured from paired-pulse depletion experiments, has been reported to be ~4s when 8ms pulses were used to probe for the rapid pool (72). When a 20 ms pulse was used to deplete the rapid pool, 30% of the pool refilled with a time constant of 0.64s and the remainder had a τ_{refill} of 31s (208). Calcium aids in refilling of this pool (72, 208). In the presence of high calcium (during on-going release, open calcium channel) the τ_{refill} is ~400ms, which is almost 10 times faster as compared to 4 s (72). It is not known
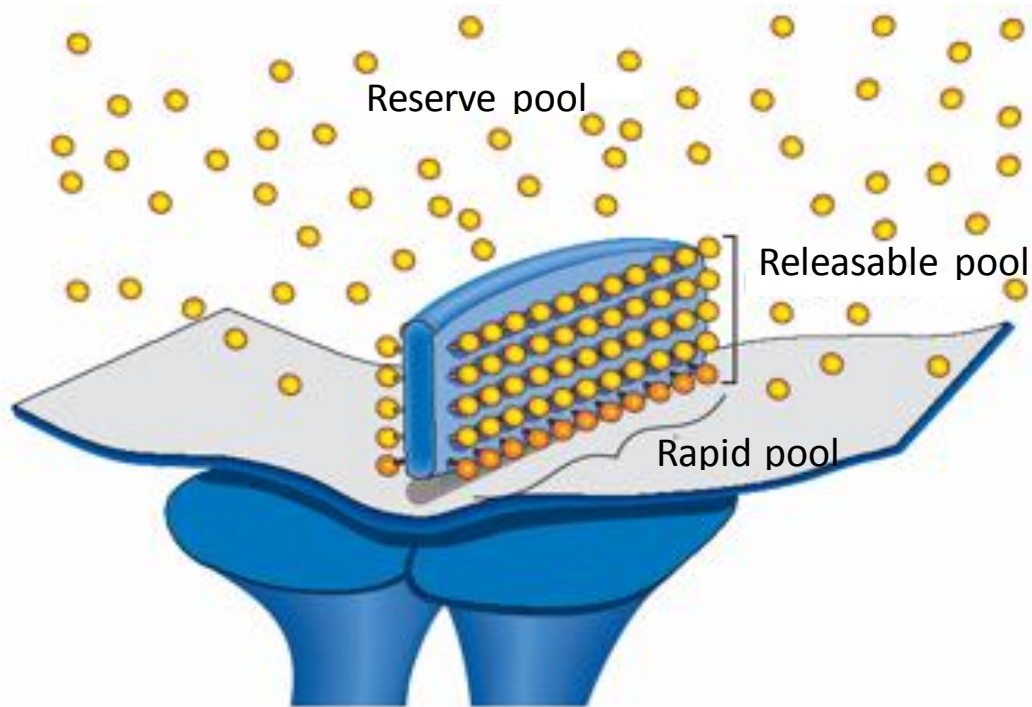
Vesicle pool	ΔC_m (fF)	No. of vesicles
Rapid Pool	~ 30 -50	~1100
Releasable Pool	~100 -150	~5500
Reserve Pool	-	~480,00- ~910,00

Fig 3.1 : Location and size of vesicle pools of the goldfish bipolar cell
The top cartoon (adapted from original source) denotes the *hypothesized* arrangements of vesicles at 1 of the ~45-60 pre synaptic ribbons of the bipolar cell onto a post synaptic dyad (two post synaptic processes). The table gives estimates of the size in fF and vesicle number of each pool (72, 75, 132, 171).

whether vesicles which are tethered higher up on the ribbon, or vesicles from the cytoplasm or recently endocytosed vesicles refill this pool. It is also not known whether vesicles from multiple sources can be recruited to this pool in the presence of high calcium.

The releasable pool

The Mb1 terminal contains a finite set of vesicles which have undergone all the ATP dependent steps required for fusion (80, 81). This fusion competent pool is known as the releasable pool (RP). A 250 ms to 1 s depolarization from -60mV to 0 mV is sufficient to deplete this pool. Capacitance measurements show the size of this pool to be 80-150fF (75, 80, 209) which corresponds well to the ~5000-6000 ribbon-tethered vesicles.

The time constant of refilling for the releasable pool has been reported to be 6.5- 8 s as measured from paired pulse depletion experiments (80, 84). One study which looked at diurnal variation in the refilling of the releasable pool (124) found that recovery from paired pulse depletion could be fit with a double exponential function, and was not significantly altered between night and day (day: 67 % of the pool recovered with a τ_{fast} =359 ms, remainder recovered with a τ_{slow}= 2.9s; night: 64 % of the pool recovered with a τ_{fast} =421 ms, remainder recovered with a τ_{slow}= 7s). The source of these vesicles is assumed to be from the reserve pool (87). ATP is required for the functional refilling of this vesicle pool rather than physical refilling - ATP hydrolysis does not seem to be required for the movement of the vesicle to a ribbon and attachment to the ribbon. ATP hydrolysis does seem to be required in order for a newly arrived vesicle to attain fusion competence (80).

Based on the correlation between the size of rapid and releasable pool from capacitance measurements and the anatomical number of vesicles on the ribbon it has been postulated that 1) the ribbon associated pool forms the releasable pool and 2) the rapid pool

is a subset of this releasable pool. These two assumptions have not been specifically tested. The above model also assumes that all release occurs at the ribbon. However, vesicle fusion at non-ribbon associated sites or extra-ribbon release has been reported in bipolar neurons (82, 83, 134). The magnitude of extra-ribbon release compared to ribbon associated release is contentious (82, 83). While Midorikawa et al., 2007 (82) suggest that the magnitude of extra-ribbon release is significant, occurs at discrete locations and may contribute to the sustained component of release, Zenisek 2008 (83) shows the extra-ribbon release does not show clustering to discrete sites and seem to occur with only a slightly more frequency that that would be expected from a completely random distribution .Synaptic ribbons have been shown to detach from active zones during night (124) suggesting that synaptic ribbons are not stationary organelles. It is possible that extra-ribbon sites may be sites where a ribbon was previously present.

The reserve pool

At the EM level the synaptic terminal of the bipolar cell has thousands of vesicles scattered in the cytoplasm (75). The size of this pool is estimated to be between 480,000-910,00.This reserve pool of vesicles are more mobile compared to cytoplasmic vesicles in conventional synapses (85–87), possibly due to the lack of synapsin at ribbon synapses (92). Experiments where styryl dyes were used to track vesicle movement in mice bipolar cells (87) have shown that vesicles attached to the ribbon are non-mobile and do not freely exchange with the reserve cytoplasmic vesicles. However following depolarization the vesicles on the ribbon undergo exocytosis and are replaced by vesicles from the cytoplasm. This suggests that the reserve pool plays a role in refilling the ribbon-tethered pool of

vesicles. The high mobility of the reserve vesicles may also aid in rapid refilling of the ribbon-tethered pool as may be required during sustained release.

Anatomically there is no difference between reserve pool vesicles. However, a cohort of the reserve pool vesicles may function to reload the releasable pool, at least one time during high frequency trains of depolarizations (84) . This is based on the finding that when synaptic terminals were stimulated with a train of depolarizations each 250 ms in duration, a plateau was reached at ~ 300 fF. Since the size of the releasable pool is ~150 fF, it suggests that at least one round of refilling was possible before the synapse was depressed. However, it is possible that the plateau in release could be due to depletion of pool-refilling factors, inhibition by some factor or that the extra vesicles came from extra-ribbon sites (these vesicles may be mobilized or undergo fusion due to high intra-cellular calcium during pulse trains).

Endocytosis in goldfish bipolar neuron

After exocytosis synaptic vesicles are retrieved by endocytosis. In the goldfish bipolar neuron vesicles two types of endocytosis after exocytosis have been described. A fast mode of endocytosis that has a time constant of 1-2 s is seen in response to brief depolarizations while a slower mode of endocytosis that has a time constant of 10-20 s is seen in response to larger depolarizations (73, 123, 161). The slow mode, but not the fast mode of endocytosis is affected by proteins regulating clathrin-dependent endocytosis such as AP2 adaptor protein, amphiphysin and clathrin (210). Elevated hydrostatic pressure also selectively affects the slow phase of endocytosis (161). Elevated basal calcium, above 20 µM (211) or spatially averaged calcium above 500nM (209) inhibits endocytosis. High basal

calcium, as would be seen after a strong depolarization also delays the onset of endocytosis (73, 209, 212). GTP hydrolysis is required for both modes of endocytosis (210), suggesting a role for dynamin, a GTPase known for its role in membrane scission (213–216). However, retrieval after a releasable pool depleting stimulus has been shown to be unaffected in the presence of non-hydrolysable GTP analogs but not non-hydrolysable ATP analogs (212). The non-requirement of GTP and therefore possibly dynamin after a large (releasable pool depleting) stimulus may be similar to that seen in the calyx of Held where GTP-independent endocytosis is activated after intense stimulus after the saturation of GTP dependent mode of endocytosis (217).

In this chapter I will use the Mb1 neuron to 1) design a paradigm in which all three components of the release can be captured 2) test the hypothesis that the rapid pool vesicles are a subset of the ribbon- tethered releasable pool of vesicles

RESULTS

1. A stimulus train reveals exocytosis that draws from multiple vesicle pools

EXPERIMENT 1:To determine whether fusion from multiple vesicle pools can be captured using a pulse train

We designed a stimulation paradigm that allowed us to resolve multiple components of neurotransmitter release from an individual, isolated Mb1 bipolar cell synaptic terminal using membrane capacitance measurements. This paradigm consisted of a train of 136 depolarizing voltage steps (-60 to 0 mV, 20 ms duration) separated by 50 ms, during which time membrane capacitance, C_m, was measured. Protocol is shown in Fig 3.2.
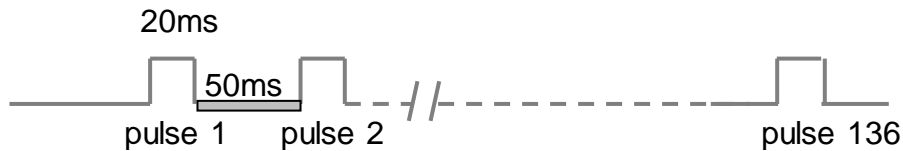
Fig 3.2 Protocol used for the train stimulus
Each depolarization pulse was 20 ms long. 136 such pulses were given with an inter-pulse interval of 50ms, during which membrane capacitance was measured.

A representative C_m trace in response to the paradigm from a single terminal is shown in fig 3.2. $\Delta C_{m,1}$ was defined as the magnitude of the capacitance change evoked by the first pulse in the train and $\Delta C_{m,total}$ was defined as the total cumulative capacitance increase at the end of the pulse train (fig 3.2). The inset shows a representative ΔC_m response and the corresponding calcium current, I_{Ca}, evoked by a single pulse in the train at higher resolution. No correlated changes were noted in the conductance traces G_s and G_m (inset), although a brief spike (< 20 ms duration) was observed in G_m To avoid possible contribution of this transient to ΔC_m, the first 20 ms of the capacitance record was excluded

from analysis (218, 219). The presented calcium currents (I_{ca}) amplitudes were calculated from the average amplitude over the last 5 ms of each 20ms pulse. To measure the calcium influx corresponding to $\Delta C_{m,1}$, we defined I_{ca1} as the calcium current the first pulse. To measure the calcium influx at the end of the pulse train we defined $I_{ca\,total}$ as the average current of the last five pulses in the train.
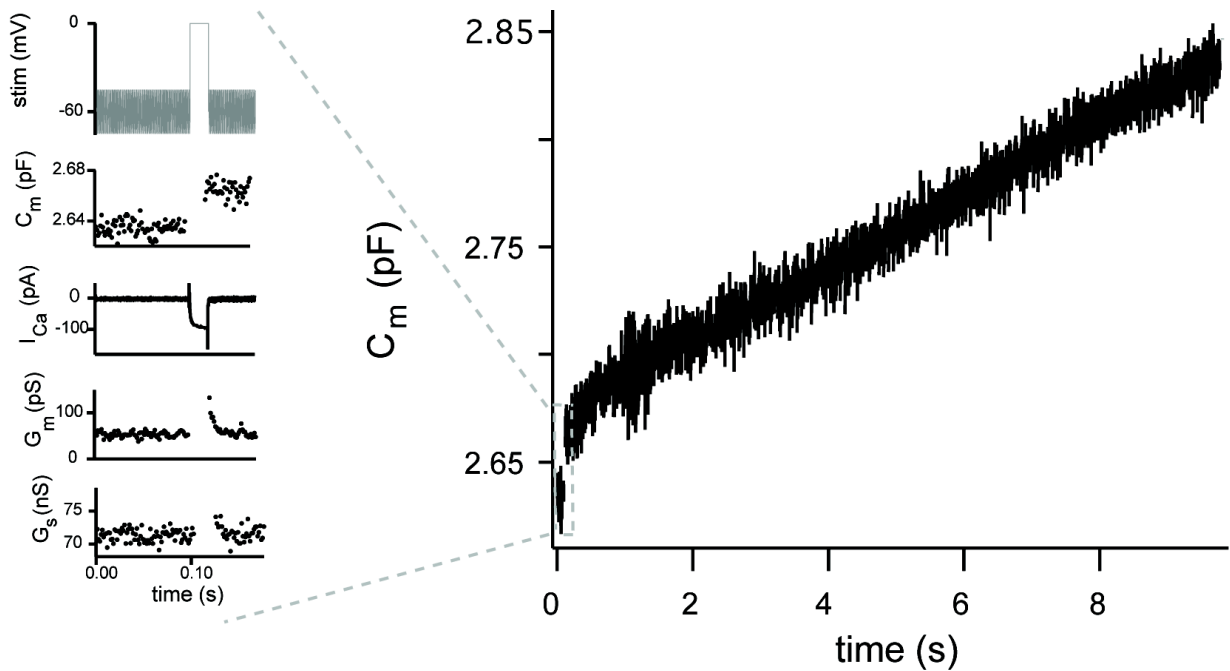
Figure 3.3. Sample capacitance (C_m) trace from a terminal stimulated with a pulse train.
A representative C_m trace in response to a pulse train is shown on the right. The inset marked by the grey dashed line shown on the left shows high-resolution measurements of the stimulus (topmost panel), membrane capacitance C_m, calcium current (I_{Ca}), series conductance (G_s) and membrane conductance (G_m, bottom most panel) in response to the first pulse in the train.
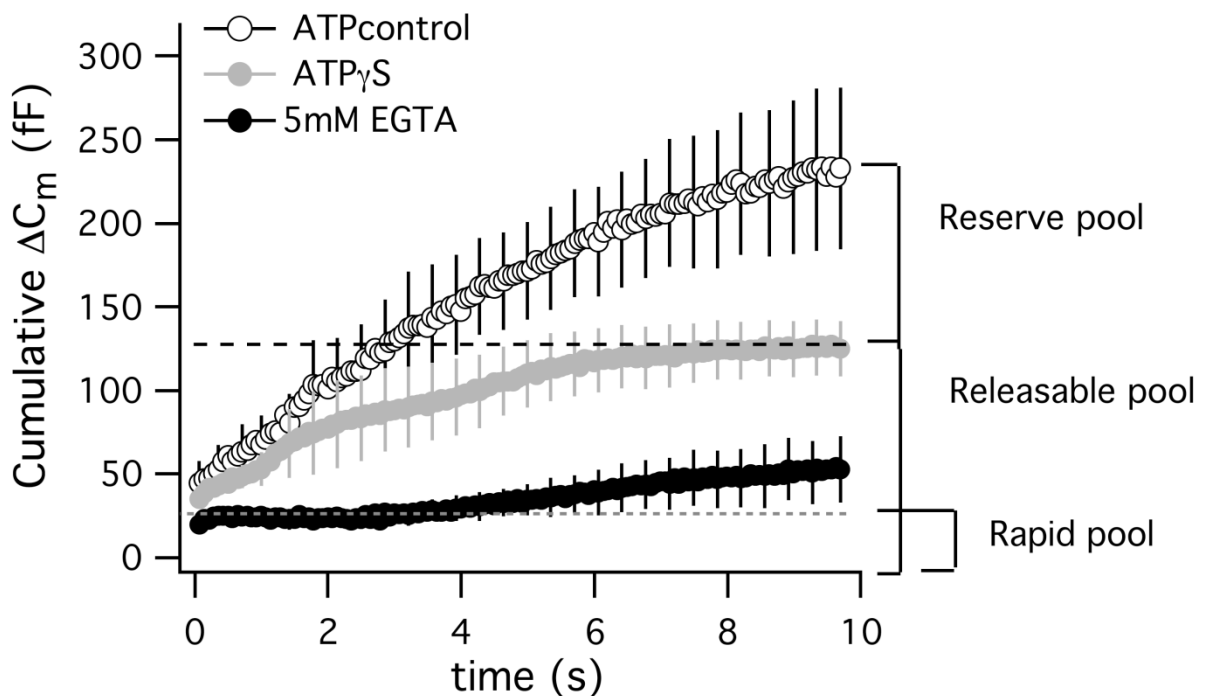
Figure 3.4. **A pulse train stimuli reveals fusion of multiple vesicle pools**. In response to a pulse train given 1min after attaining whole-cell configuration terminals dialyzed with control internal solution (ATP, open circles, n= 6) showed a cumulative capacitance change that could be attributed to multiple components of release. 5mM EGTA blocked all but the first component of release, with some amount of recruitment from the second component seen after 4s. (rapid pool, block circles, n=4) With ATPγS the third component of release was blocked.(gray circles, n = 7)

The rapid pool: A rapid component of release, attributable to the fusion of vesicles docked at plasma membrane active zones (131, 132), is evoked by a brief depolarization from -60 to 0 mV (72). The first 20 ms depolarization of our stimulation paradigm would be expected to tap this pool. Accordingly, in response to the first pulse, $\Delta C_{m,1}$, there was an average capacitance increase of 45 ± 13 fF (n = 6; Fig 3.4 open circles), which is in the reported range of the rapid pool (72). The average calcium current $I_{ca1} = 171.6 \pm 31.8$ pA (n = 6).

The stimulus-evoked increase in membrane capacitance in response to the first 20 ms depolarization was not significantly inhibited when the patch pipette contained 5 mM EGTA ($\Delta C_{m\,1:EGTA} = 22.3 \pm 3.3$. fF, n= 5, black circles, p value $= 0.16$ compared to ATP control), a perturbation commonly used to isolate the rapid pool (72, 208), and there was no effect on the calcium current, $I_{ca1:EGTA} = 167 \pm 33.5$ pA (n=5, p value $= 0.92$, compared to ATP control). These results are consistent with the interpretation the first pulse in the train triggers the fusion of the rapid pool of vesicles, and therefore we used $\Delta C_{m\,1}$ as a proxy for the rapid pool.

Reserve and Releasable pool: The average cumulative increase in membrane capacitance at the end of the pulse train, $\Delta C_{m,total,} = 233 \pm 48$ fF (n $= 6$; fig 3.4 open circles). This value is larger than expected for the Mb1 bipolar cell releasable pool and most likely includes the fusion of additional vesicles that were recruited from the reserve pool during the pulse train (58, 80, 84, 208). In 3/6 cells , a secretory plateau was reached at the end of the pulse train – the magnitude of this plateau ($\Delta C_{m,total,} = 197 \pm 12$ fF). To explore the possibility that our stimulation paradigm tapped reserve vesicles, we blocked the functional refilling of the releasable pool by replacing ATP in the internal recording solution with ATPγS. ATPγS has been shown to block functional refilling the releasable pool (presumably) from reserve pools vesicles (80, 96). There was no significant difference in the resting calcium between terminals dialyzed with ATP or ATPγS, (ATP: $[Ca]_i: = 174.3 \pm 48.6$ nM, n $= 6$; ATPγS: $[Ca]_i: = 186.2 \pm 60.9$ nM, n $= 7$, p value $= 0.8$). The average calcium current $I_{ca\,total}$ was also not significantly different between terminals dialyzed with ATP and ATPγS (ATP: $I_{ca\,total} = 107.8 \pm 14.8$ pA, n $=6$; ATPγS: $I_{ca\,total} = 83.2 \pm 31.8$ pA , n $= 7$, p value $= 0.12$)

The total secretory response, in $\Delta C_{m,total}$ evoked by the pulse train was decreased by $\approx 46.4\%$ in terminals dialyzed with ATPγS when compared with controls (Figure 3.4). Moreover, the value of $\Delta C_{m,total}$ in ATPγS terminals was 125 ± 16 fF, n=7 consistent with the magnitude of the releasable pool (75, 80). These data suggest that ≈ 108 fF's of membrane capacitance (~ 4000 vesicles) did not initially reside in the releasable pool and were recruited during the pulse train when ATP hydrolysis was not inhibited. ATPγS did not have an effect on the fusion of vesicles in the rapid pool. In terminals dialyzed with ATPγS, $\Delta C_{m1} = 35 \pm 5.5$ fF, $I_{ca1} = 138.5 \pm 16$ pA, n = 7, not significantly different from control terminals , p value = 0.5 and 0.14 respectively.

The releasable pool of vesicles hypothesized to be located at a distance from the calcium entry sites is expected to be affected by mM levels of EGTA. In terminals dialyzed with 5mM EGTA, the $\Delta C_{m\,total} = 52.5 \pm 20$ fF , n= 4, significantly smaller than control terminals, p value =0.02. The $I_{ca\,total}$ was not significantly different between terminals dialyzed with 5mM EGTA compared to controls (ATP: $I_{ca\,total} = 107.8 \pm 14.8$ pA, n =6; EGTA: $I_{ca\,total} = 112.6 \pm 17.7$ pA , n = 4, p value = 0.8)

Together, the data indicate that the pulse train is able to capture multiple components of release. Experiments with ATPγS and high EGTA provide an estimate for the expected magnitude of the rapid and releasable pools.

To determine the rate of endocytosis after a train stimulation, we fitted the time course of endocytosis with a double exponential function which revealed the following averages (only the response after the first train was used and not all responses could be fit with a double exponential function): ATP controls $\tau_{fast} = 3.6$s in 5/7 terminals, ATPγS terminals- $\tau_{fast} = 3.8$s in 2/5 (p value = 0.9). ATP controls $\tau_{slow} = 42.6$s in 5/7 terminals;

ATPγS terminals- $\tau_{slow} = 55.3$ in 5/5 terminals (p value = 0.5), 3/5 terminals showed only a single slow component.
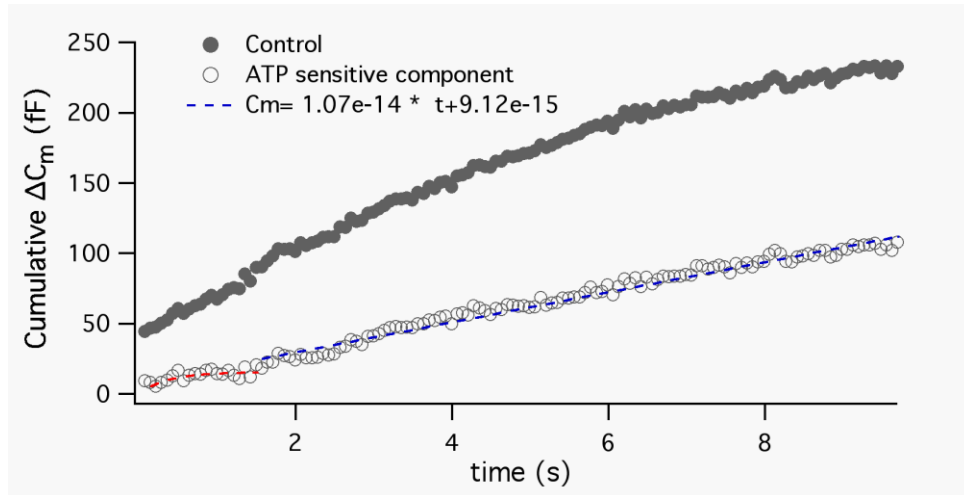
Fig 3.5 The ATP sensitive component.
The component of release requiring ATP hydrolysis (ATP train - ATPγS train from fig 3.4) is plotted (open circles) along with the original ATP control from fig 3.4 (filled circles). After the first 1.49s the ATP sensitive component was fit with a line (slope = 1.07e-^{14}, y intercept = 9.12e-^{15}).

To get an estimate of the rate of recruitment and fusion of the component of release which requires ATP hydrolysis, we subtracted the mean cumulative ΔC_m (gray trace in fig 3.4) from the mean cumulative ΔC_m ATP control (open circles trace in fig 3.4). The resultant is shown in fig 3.5 (open circles). The data from the first 1.49 s seconds was not a good fit suggesting a possible non-linear rate of recruitment. The ATP sensitive component after 1.49 s was fit with a line function. The slope of the line was 10.7 fF/s (or ~366 vesicles /s), which gives us the rate of recruitment and fusion of the vesicles (possibly from the reserve pool) which require ATP hydrolysis, or in other words fusion of vesicles that are not

already in the releasable pool. The 1.49 s delay in start of the linear component may suggest that ATP priming is initiated only after a certain number of vesicles have already fused.

2. The rapid pool is a subset of the releasable pool

EXPERIMENT 2: To determine if depletion of the releasable pool also depletes the rapid pool, using a pulse train

To test whether depletion of the releasable pool would also deplete the rapid pool we performed the following experiment. ATPγS was included in the internal solution in place of ATP in order to block functional refilling of the releasable pool (control experiments). A pulse train was given every 60 s after attaining the whole cell configuration. To account for the variability in the size of the releasable pool we normalized the magnitudes of ΔC_{m1} and cumulative ΔC_{mtotal} to their respective magnitudes obtained in the first pulse train (e.g. Normalized ΔC_{m1} of train 3 = ΔC_{m1} of train 3/ ΔC_{m1} of train 1).

In control terminals n=6, the cumulative $\Delta C_{m\,total}$ decreased by 42.5% (133.4 ± 25fF), 58.9% (108 ± 31fF) and 67% (96.06 ± 43fF) in the second, third and fourth trains (numbers in parenthesis refer to the cumulative ΔC_m 136 for each train, fig 3.6). This rundown of release has been previously reported (123). By comparison, there was a dramatic decrease in the refilling of the releasable pool in the presence of ATPγS. The cumulative $\Delta C_{m\,total}$ in ATPγS terminals, n=5, was decreased by 73.1% (26.7 ± 6.7fF) $p < 0.0001$, 94.4% (6.08 ± 3.6fF), $p < 0.001$ and 98.9% (1.04 ± 2.08fF), $p<0.01$, in the second, third and fourth pulse trains respectively (numbers in parenthesis refer to the cumulative $\Delta C_{m\,total}$ for each train, p value compared to controls, fig 3.6). This agrees with previously published findings that in the presence of ATPγS only one round of release from the releasable pool can be elicited (80, 81).
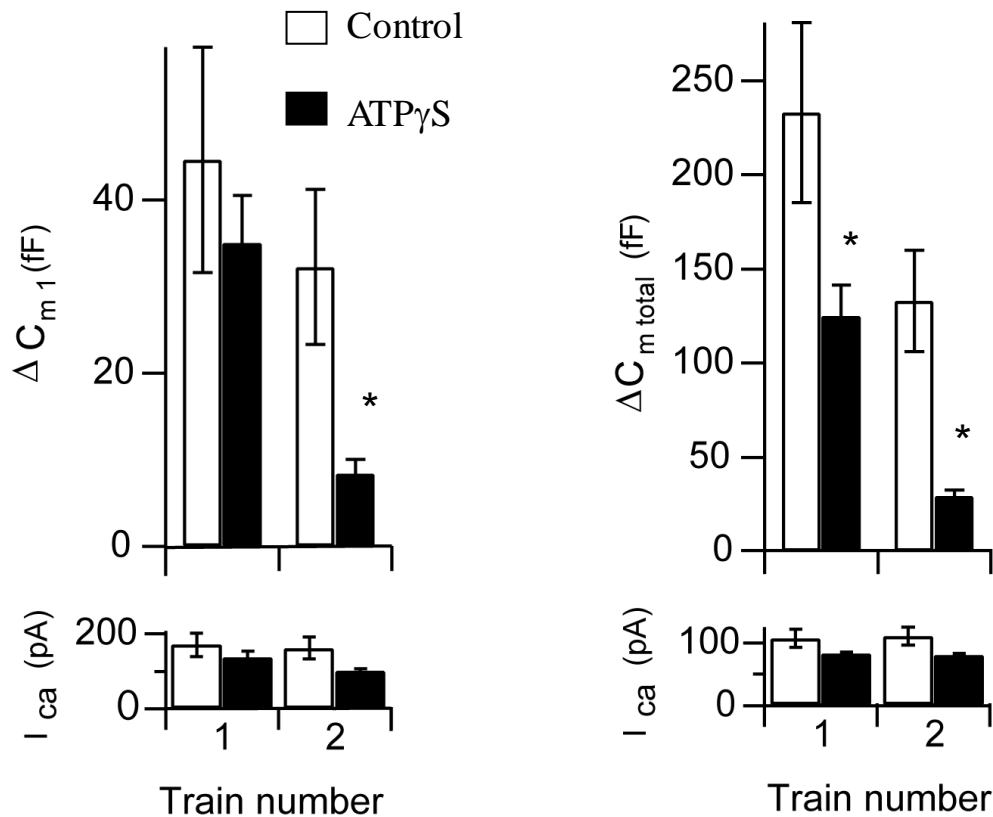
Fig 3.6 ATP is required for the refilling of the releasable and rapid pool.
Left – The capacitance change in response to the first 20 ms pulse (ΔC_{m1}) of train 1 and 2 (top panel) in ATP and ATPγS terminal shows decreased refilling of ΔC_{m1} or the rapid pool in train 2. This decrease is not due to significant decrease in calcium influx (bottom panel).
Right – The cumulative capacitance change at the end of the pulse train ($\Delta C_{m\ total}$) of train 1 and 2 (top panel) in ATP and ATPγS terminal shows decreased refilling of ΔC_m total or the releasable pool in train 2. This decrease is not due to significant decrease in calcium influx (bottom panel)

Next we examined the state of the rapid pool under conditions where the refilling of the releasable pool was blocked. We compared the $\Delta C_{m\ 1}$ of the trains 1 to 4 between controls and ATPγS terminals. In control terminals n=6, ΔC_{m1} was only decreased by 22% (32.3 ± 8.3fF), 39% (24.2 ± 8.3fF) and 46% (20.4 ± 5fF) in response to the second, third and fourth trains respectively. In ATPγS terminals, n=5, by the second train the rapid pool, ΔC_{m1}

was decreased by 61% (8.68 $\pm$ 2fF), p<0.05 (numbers in parenthesis refer to the ΔC_{m1} for each train, p value compared to controls, fig 3.6). The rapid pool could not be refilled in the third and fourth trains in ATPγS terminals (ΔC_{m1} values were not higher than 1 SD of the baseline). The effect of ATPγS was not due to a decreased calcium influx (as shown in fig 3.6) or differences in basal calcium. The basal intra-cellular calcium in these experiments were buffered to ~150 nM calcium, the same as in experiment 1. (ATP: $[Ca]_i$: = 174.3 $\pm$ 48.6 nM, n = 6 ; ATPγS: $[Ca]_i$: = 186.2 $\pm$ 60.9 nM, n = 7, p value = 0.8)

In ATPγS terminals, the second, third and fourth trains probe a state where the releasable pool has been depleted (in the first train) and its refilling has been blocked. These data suggest that 1) when the releasable pool is not functionally refilled, the rapid pool is also not functionally refilled or 2) the rapid pool is being refilled from the reserve pool by an ATP-sensitive step. However at ribbon synapses, vesicles once tethered to the ribbon show low exchange with vesicles from the cytoplasm (presumed to be the reserve pool) until the tethered pool is released (presumed to be the rapid and releasable pool) (87). Therefore we support the first conclusion that the rapid pool refills vesicles from the releasable pool.

EXPERIMENT 3: To determine if depletion of the releasable pool also depletes the rapid pool, using single depolarizations

We sought to investigate whether depletion of the releasable pool depletes the rapid pool using a second paradigm. In this second paradigm we used traditional single pulses (rather than a train of pulses) known to deplete the specific pool of vesicles : a 1s depolarization to deplete the releasable pool of vesicles (123, 132, 151) and a 20ms depolarization to probe the rapid pool of vesicles (72, 208). The paradigm was as follows - ATPγS was dialyzed into terminals and a 1s pulse (80, 81, 84) was given every 30 s till the

releasable pool was depleted. Then, a 20 ms pulse was given to probe the state of the rapid pool. The 30 s inter-pulse interval was chosen to allow for refilling of the releasable pool which takes about ~ 20 s under control conditions ($\tau = 8$ s, (80, 84)). Once the releasable pool depleted by > 86%, a 20 ms pulse was given to probe the state of the rapid pool. A sample trace is shown in fig 3.7.

The amplitude of the exocytotic response evoked by the first 1s depolarization was not significantly different between the two groups (ATP: $\Delta C_m = 124.2 \pm 48$ fF, n=5; ATPγS: $\Delta C_m = 156.5 \pm 25.5$ fF, n = 5, p value = 0.57), consistent with the interpretation that the releasable pool is intact prior to stimulation in the presence of ATPγS (80, 96). In ATPγS terminals, depletion of the releasable pool was associated with a profound depletion of the rapidly-releasing pool (Fig. 3.8 ; n= 5). By contrast, the rapid pool remained relatively intact in ATP terminals following depletion of the releasable pool ($\Delta C_m = 20.9 \pm 5.7$ fF, n= 5;p value = 0.01 fig 3.8). There was no significant difference between the calcium influx during the 20 ms depolarization as assayed by the peak I_{ca} between ATP and ATPγS terminals (fig 3.8, ATP: $I_{ca} = 139.2 \pm 24.8$ pA, n= 5; ATPγS: $I_{ca} = 127.4 \pm 22.7$ pA, n= 5). The spatially averaged resting calcium, before the first depolarization in both group of terminals were not significantly different (ATP: $[Ca]_i = 133.9 \pm 34$ nM, n = 5 ; ATPγS: $[Ca]_i = 135.5 \pm 20.6$ nM, n = 5). There was also no significant difference in the spatially averaged basal calcium, between the two groups before the 20ms pulse (ATP: $[Ca]_i = 175 \pm 47.2$ nM, n = 5 ; ATPγS: $[Ca]_i = 157.6 \pm 23.5$ nM, n = 5).
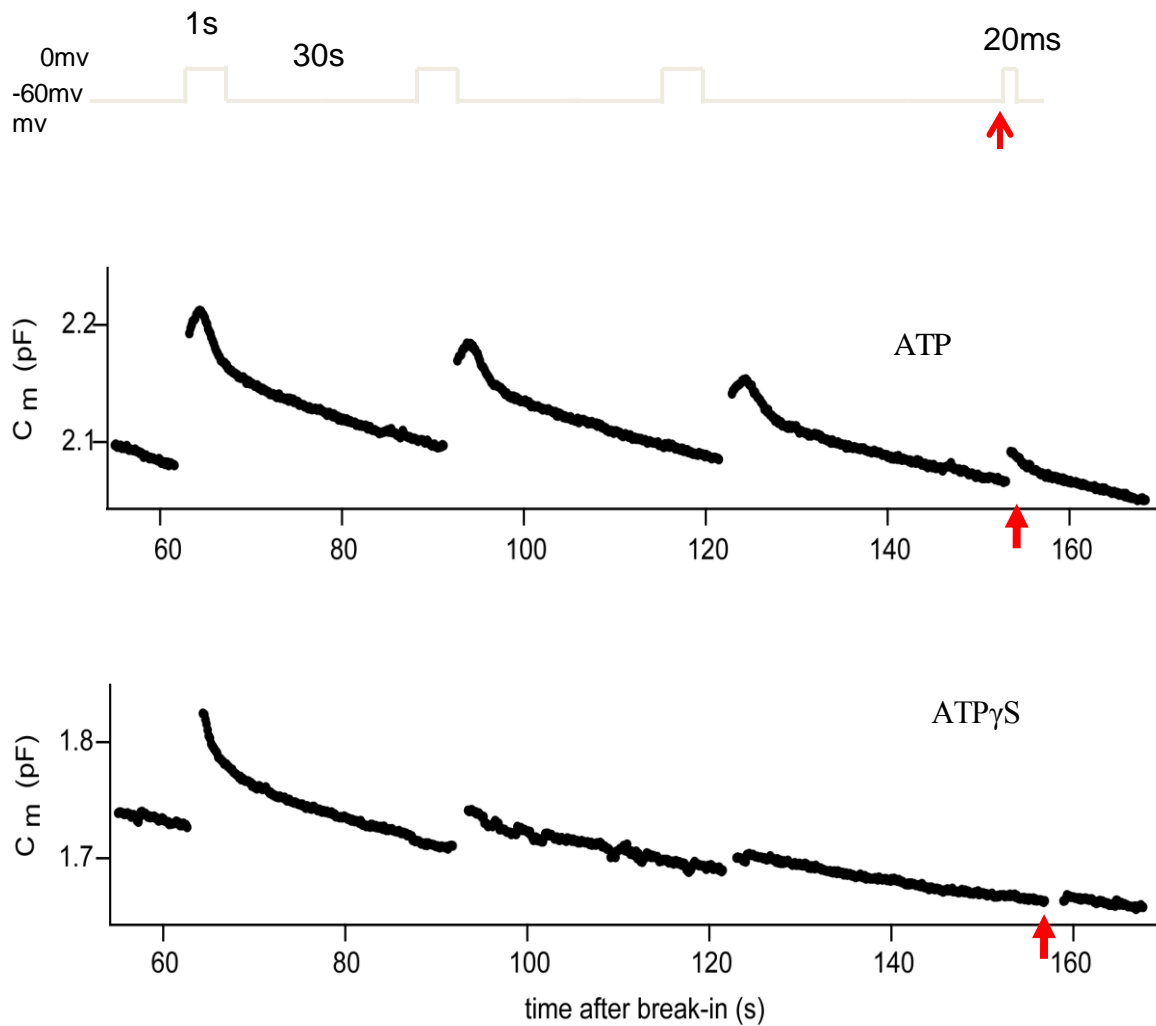
Fig 3.7: Depletion of the releasable pool also depletes the rapid pool
Top panel: Protocol. In terminals dialyzed with ATPγS, a1s depolarization was given every 30 s till the releasable pool was depleted >86%, then, a 20 ms depolarization (red arrow) was given to probe the state of the rapid pool. A representative trace is shown in the **bottom** panel (ATPγS). A similar number and length of depolarizations were given to ATP control terminals, a representative trace is shown in the **middle** (ATP) panel. The capacitance change in response to the 20ms pulse was decreased in ATPγS terminal compared to control terminal (red arrows). In both capacitance traces (middle and bottom) the return of the membrane capacitance to baseline between the 1 s pulses is suggestive of endocytosis.
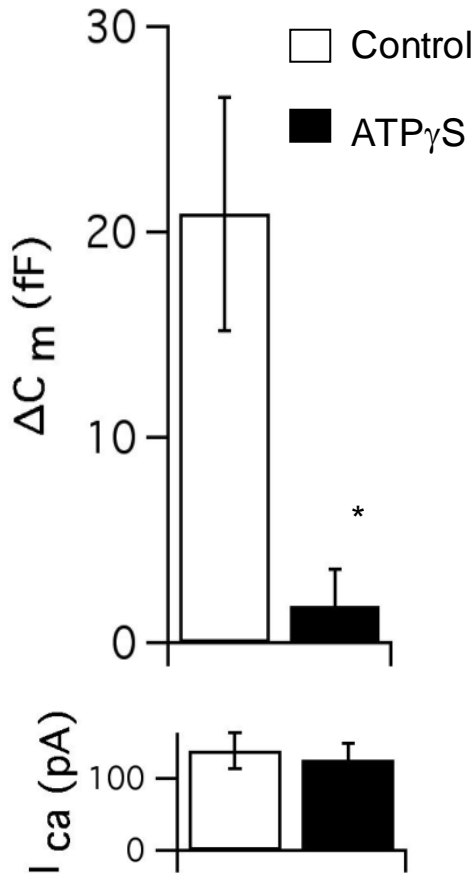
Fig 3.8 : Depletion of the releasable pool also depletes the rapid pool
Terminal dialyzed with ATPγS were stimulated with 1s depolarizations every 30secs until the releasable pool could no longer be refilled (ΔC_m < 86% of the ΔC_m seen in response to the first pulse). We then probed the rapid pool with a 20ms pulse. Control (ATP) terminals were stimulated with similar number and length of depolarizations. The capacitance change in response to the 20ms pulse was significantly decreased in terminals dialyzed with ATPγS (black bar, n = 5) compared to those dialyzed with a control ATP solution (white bar, n= 5). This effect was not due to a decreased calcium influx as evidenced by the I_{ca} (bottom panel).

EXPERIMENT : To determine if depletion of the rapid pool also depletes the releasable pool, using single depolarizations

We sought to investigate whether the rapid pool was a subset of the ribbon tethered releasable pool such that fusion of the rapid pool would also deplete vesicles from the releasable pool. Four to five 20 ms pulses were given with an inter pulse interval of 30 s. Each 20ms pulse is sufficient to deplete the rapid pool (72). The last pulse in the series was immediately followed by 1s pulse to probe the state of the releasable pool. Terminals were dialyzed with ATP (control) or with ATPγS in order to block any functional refilling of the releasable pool. The size of the initial rapid pool (first pulse) was not significantly different between ATPγS and control terminals (ATP: $\Delta C_m = 23.3 \pm 4$ fF, n = 6; ATPγS: $\Delta C_m = 33.2 \pm 6.4$fF, n = 8; p value = 0.25)

In control terminals the rapid pool was refilled multiple times (sample trace fig 3.9). In ATPγS terminals, the rapid pool was refilled only 4 to 5 times and with decreasing amounts each time (fig 3.9 sample trace). In addition, the magnitude of the capacitance increase evoked by the 1 s depolarization was reduced by more than 80% in ATPγS terminals relative to controls (ATPγS: 14.1 ± 3.3 fF, n= 8; ATP: 76.8 ± 28.2fF, n= 6 ,p value =0.024). As an upper estimate of the size of the total releasable pool remaining after four 20 ms depolarizations, we combined the magnitudes of capacitance increases from the last 20 ms depolarization and the 1 s depolarization. ATP: combined $\Delta C_m = 90.6 \pm 26.5$fF, n = 6; ATP$\gamma$S: combined $\Delta C_m = 16.7 \pm 3.8$ fF, n = 8; p value = 0.007 (fig 3.10 bottom panel labeled releasable pool). The total amount of membrane added by the four or five 20 ms pulses was also similar between the two groups (Fig 3.10, ATP: total membrane added = 74

± 10.5 fF, n= 6; ATPγS: total amount of membrane added= 73.9± 13.2 fF, n = 8, p value = 0.99)

The difference in the exocytotic response to the 1 s depolarization between terminals dialyzed with ATP and ATPγS were not due to differences in calcium influx (ATP: I_{ca} = 141.3 ± 16.1 pA, n= 6; ATPγS: I_{ca} = 125.4 ± 10 pA, n= 8, p value = 0.4, fig 3.10 middle panel). To control for changes in basal calcium in the presence of ATPγS, we used a Ca-EGTA buffered internal solution (see methods). The spatially averaged resting calcium, before the first 20 ms depolarization in both group of terminals were not significantly different (ATP: $[Ca]_i$ = 93.9 ± 20.6 nM, n= 6; ATPγS: $[Ca]_i$ = 112.7± 19.5 nM, n= 8, p value = 0.53). There was also no significant difference in the spatially averaged basal calcium, between the two groups before the last 1s pulse (ATP :$[Ca]_i$ = 101.2 ± 16.3 nM, n= 6; ATPγS : $[Ca]_i$ = 114.5 ± 18.3 nM, n = 8, p value = 0.61). The change in calcium, ΔCa in response to the 1s depolarization was not significantly different between terminals dialyzed with ATP and ATPγS (ATP: ΔCa =538.7 ± 117 nM ,n = 5; ATPγS: Δ Ca = 465.6 ± 109 nM, n = 8, p value = 0.67).

The above findings suggest that under conditions where the functional refilling of the releasable pool is blocked the rapid pool can be refilled only 4-5 times. After 4-5 rounds of release the releasable pool is also depleted. Decreasing size of the rapid pool in terminals dialyzed with ATPγS may suggest incomplete functional refilling of the rapid pool from releasable pool vesicles in the absence of ATP hydrolysis.
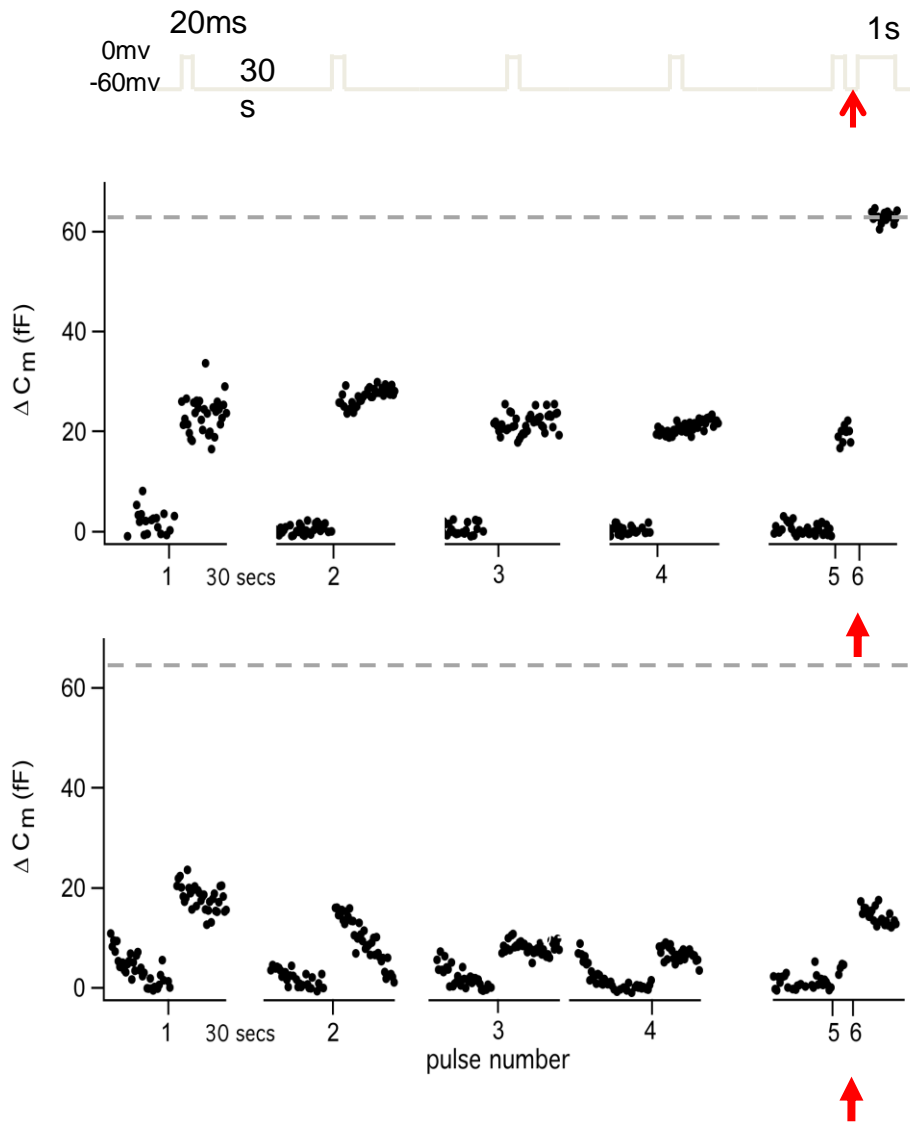
Fig 3.9 The rapid pool is a subset of the releasable pool
Top panel : protocol -The rapid pool was depleted with 4-5, 20ms pulses followed by a 1s pulse (arrow) to probe the state of the releasable pool. Representative traces with ATP (middle) and ATPγS (bottom) are shown. Dashed line shows expected size of the releasable pool in the terminal dialyzed with ATP control solution.
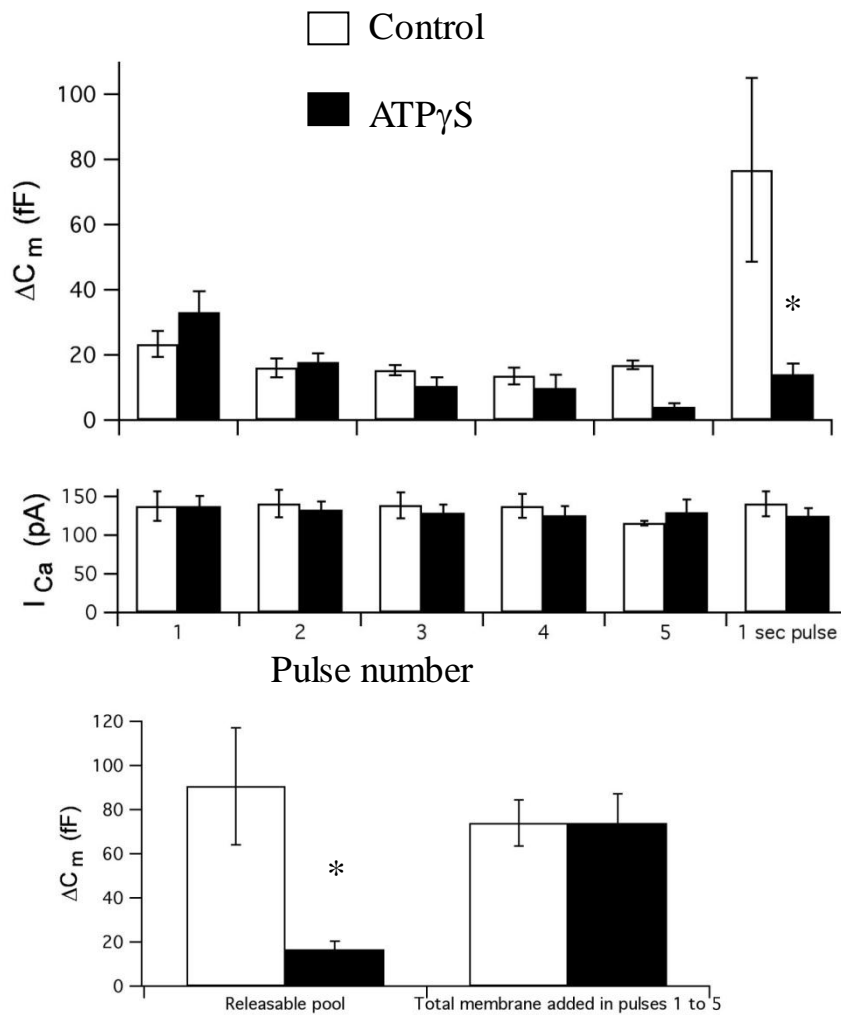
Fig 3.10 The rapid pool is a subset of and draws from the releasable pool
Top panel: Mean capacitance change in response to five 20 ms depolarizations followed by the 1 sec depolarization shows that after 4-5 rounds of release of the rapid pool the releasable pool is also depleted in the presence of ATPγS. **Middle panel:** The depletion is not due to decreased calcium influx. **Bottom panel:** Mean estimate of the size of the total releasable pool remaining after four 20 ms depolarizations, (combined magnitudes of capacitance increases from the last 20 ms depolarization and the 1 s depolarization) and total membrane added in ATP (n=6) and ATPγS terminals (n=8).

Intracellular calcium measurement

In bipolar terminals, the plasma membrane Ca-ATPase are the main regulator of the intra terminal calcium (220). Therefore in terminals dialyzed with ATPγS (a non-hydrolysable analogue of ATP) , the Ca-ATPases, may be inhibited allowing for a larger calcium micro domain width and increase in basal calcium during the recording time and also with multiple depolarizations. To control for increases in basal calcium, we used calcium-EGTA buffered internal solutions (buffered to a free calcium of 150nM, see also methods) in all our experiments. To further verify whether terminals dialyzed with ATPγS had higher basal calcium before or during the several depolarizations, we measured the basal $[Ca]_i$ and the average $[Ca]_i$ during the 5 ms before each 20ms depolarization. The basal $[Ca]_i$ and the $[Ca]_i$ before each pulse was not significantly different between terminals dialyzed with either ATP or ATPγ (fig 3.11). The trend was for higher spatially averaged calcium with ATPγS (possibly due to inhibition of Ca-ATPase in the absence of ATP hydrolysis), indicative of a possibly larger microdomain, but fusion of a fewer vesicles with multiple depolarizations (fig 3.10).

We wanted to resolve whether the increase in $[Ca]_i$ and its subsequent recovery to baseline was different in terminals dialyzed with ATPγS compared to control solution. I was not able to measure a detectable rise in the spatially average intra cellular calcium $[Ca]_i$ after each 20ms pulse. However I could measure the increase in calcium after a 1 s pulse and measure the time course of the decay of the calcium transient. The spatially averaged increase in $[Ca]_I$ was 538 ±117nM in ATP (n= 5) and 465.6 ±102 nM in ATPγS terminals (n= 8) (p value =0.7). The time course of recovery after a 1 s depolarization was 5. 8 ± 1.54 in ATP terminals (n=6) and 7.1 ± 0.7 in ATPγS terminals (n=8) and was not statistically

different between the two groups (p value = 0.4). The time course of recovery of the calcium

transient would be faster in response to a 20 ms pulse. Therefore it is reasonable to assume

that in terminals dialyzed with ATPγS, 20 ms depolarizations cause similar intracellular

calcium changes as controls.
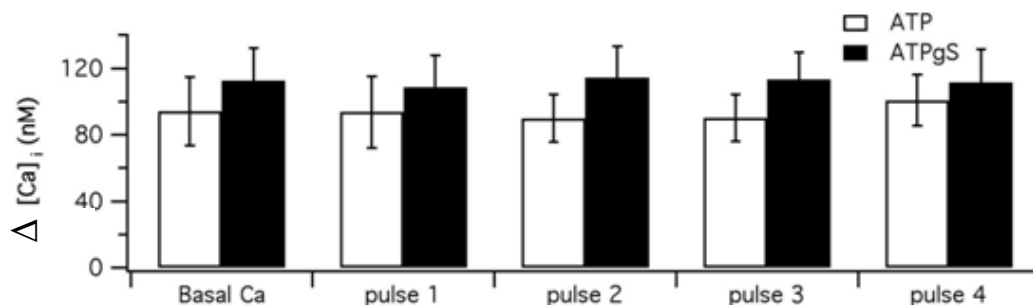
Fig 3.11 Changes in intracellular calcium during experiment 4: Mean spatially averaged intra-cellular calcium ($[Ca]_i$) before the terminal is depolarized (basal) and specifically 5 s before each 20 ms depolarization's (given four times, denoted on the x axis as pulse 1- pulse 4) in terminals dialyzed with internal solution containing either ATP or ATPγS

DISCUSSION

The main findings are: 1) A stimulus train reveals exocytosis that draws from

multiple vesicle pools 2) Inhibition of functional refilling of the releasable pool also blocks

fusion of the rapid pool. This suggests that the rapid pool is a subset and draws from the

releasable pool.

Using a pulse train we were able to study fusion from three distinct vesicle pools (fig

3.4). Our findings correlate well with the known sizes, and ATP and EGTA sensitivities of

the previously characterized vesicle pools in synaptic terminals of Mb1 bipolar cells (72,

80, 132, 208) . In our paradigm the capacitance change after the first pulse represents fusion

of the rapid pool which is predicted to be ~ 20-40 fF or ~1000- 1500 vesicles. Using ATPγS

to block functional refilling we were able to capture the releasable pool which is predicted to be 100-150fF or ~3800- 5800 vesicles. Under control conditions the magnitude of the cumulative capacitance change at the end of the pulse train suggested recruitment of reserve pool vesicles. While the number of reserve pool vesicles, from EM studies show >400,00 vesicles scattered throughout the cytoplasm (75), it has been suggested that a small cohort of this population (~ 6000 vesicles) maybe available for immediate refilling of the releasable pool during repetitive stimulations (84). Our results suggest this pool to be ~108 fF or ~ 4200 vesicles suggesting that our train may not have captured all the reserve vesicles available for immediate refilling. Also in our experiments under control conditions, by the end of the stimulus train (after 136 pulses) the rapid pool was refilled at least 5.29 times (cumulative $\Delta C_{m\ total}/\Delta C_{m\ 1}$), half of what would expected if the releasable pool was refilled completely (cumulative $\Delta C_{m\ total}/\Delta C_{m}\ 1$ would be closer to 10). The lack of a complete refilling/turnover of the releasable pool could be due to depletion of factors required for refilling (due to dialysis) or perhaps adaptation of exocytosis machinery such as the calcium sensor. Recording using perforated patch clamp techniques may help to prevent wash-out. A longer pulse train might be required to turn over the entire pool of releasable vesicles. Therefore a train with a more pulses (e.g. 150 instead of 136) or longer pulses (50 ms-250ms) could be used to test this hypothesis and address the second issue.

Under conditions where functional refilling was blocked with ATPγS, the rapid pool was refilled 3.57 times suggesting decreased pool refilling, as would be expected for ATPγS. We calculate the refilling and fusion rate of the ATP sensitive component (or reserve pool vesicles which refill the releasable pool) to ~10.9fF /s or 366vesicle/s (fig 3.5). Interestingly, we were able to fit the ATP sensitive component with a linear function. This

suggests that during the pulse train there appears to be a steady rate of recruitment of vesicles, even while the vesicles in the releasable pool are not completely depleted. Whether this continuous recruitment of vesicles require high levels of intracellular calcium, known to aid in pool refilling (208, 211), that is seen during the pulse train, would be an interesting hypothesis to test.

Capacitance measurements track changes in surface area. Therefore a flat capacitance trace, as seen in capacitance measurements in between the pulses of the train may represent a balance of exo- (addition of membrane) and endocytosis (removal of membrane). However two lines of evidence suggest that the C_m measurements during the train are most likely due to exocytosis. 1) An increase in intracellular calcium has been suggested to block endocytosis in several types of nerve terminals (216, 221, 222) including the retinal bipolar cell terminal (73, 209, 211). Specifically, an increase in spatially averaged calcium above 500 nM has been shown to suppress endocytosis (209). During a pulse train the basal calcium in the terminal reached values more than 500nM by the 20th pulse (time = 1.43 s) and more than 1μM by the 30th pulse (time =2.14 s) [The $[Ca]_i$ by the 20th pulse was 679 ± 272 nM (n=6) in ATP terminals and 872 ± 319 nM in ATPγS terminals (n= 7), p value =0.67. The $[Ca]_i$ the 30th pulse was 2.37 ± 1.6μM (n=6) in ATP terminals and 1.39 ± 0.5μM in ATPγS terminals (n= 7), p value = 0.57]. 2) The 50 ms inter-pulse interval during the train is too short for even the fast mode of endocytosis, which has a τ of 1-3 s (73, 123, 161). Also long stimulus durations (as used in our pulse train) decreases the fraction of membrane recovered by the fast mode of endocytosis in bipolar cells (73).Therefore we suggest that the membrane capacitance changes during the train are most likely entirely due to exocytosis.

The magnitude of the rapid pool from capacitance measurements is ~1/5th the magnitude of the releasable pool. The rapid pool of vesicles can undergo immediate release while longer depolarizations are required for the fusion of the releasable pool. Therefore based on the relative sizes and kinetics of the releasable and rapid pools, an obvious assumption is that the rapid pool is a subset of the releasable pool. Here we show that this correlation is not just coincidental. Depletion of the larger releasable pool depletes the rapid pool (fig3.6, 3.7) and vice versa (fig 3.8, 3.9), suggesting that not only is the rapid pool a subset of the larger releasable pool but the rapid pool is also refilled from the releasable pool vesicles. Based on correlation between the size of the vesicle pools from capacitance measurements and a matching number of vesicles tethered to the ribbon from EM analysis it has been assumed that the releasable pool of vesicles is composed of vesicles tethered to the ribbon, with the rapid pool forming the docked row of vesicles. In the next section we attempt to prove that this finding is also not merely co-incidental.

The rapid and releasable pool undergo fusion at ribbon style active zone

In Mb1 bipolar cells, synaptic ribbons co-localize with calcium entry sites at ribbon-style active zones (82, 85). The distance between a ribbon and the nearest calcium entry site is 122 ± 10nm (82). In TIRFM experiments an active zone is defined to be where two or more vesicles fuse within 300nm of each other (83, 85). Two definitions have been proposed for the area of the ribbon-associated active zones :1) within 700nm of the ribbon, (83) or 2) within 300 nm of the center of the ribbons (82). However the length of the longest axis of the ribbon is ~500 nm (75) and two vesicles fusing at the ends of a ribbon may not be considered to be a part of the same ribbon- associated zone according to the second definition. Also Zenisek 2008 (83) noted that fusion event that were within 300 nm of each

other were also with in 700 nm of the ribbon. Therefore, we will be using the first definition of a ribbon associated active zone (within 700nm) as our definition.

Beumont et al., 2005 measured the width of calcium micro domains using TIRFM and calcium indicator dyes. In the presence of 10mM EGTA a 20-40 ms depolarization spreads the calcium micro domain over 580 ± 40nm while in the presence of 0.1mM EGTA the micro domain spread wider to 930 ± 110nm. Using perforated patch clamp conditions they measured the calcium micro domain in the presence of endogenous buffering in response to a 20-40ms depolarization to be 770 ± 60nm. The endogenous buffering present in Mb1 terminals is equivalent to ~1.2mM BAPTA or 0.9mM EGTA (223). In our experiments calcium handling in terminals dialyzed with ATP or ATPγS were not significantly different (fig 3.11).The internal solution contained 2.5mM free EGTA (as calculated by maxchelator, http://maxchelator.stanford.edu) . Therefore we can expect that in our experiments the calcium micro domain in response to a 20 ms depolarization is between 580 nm and 770 nm. The width of this calcium micro domain is similar to the size of the ribbon associated zone. Therefore under our experimental buffering conditions, a 20ms depolarization can be expected to elicit fusion of ribbon associated vesicles, most likely the bottommost docked row of vesicles or the rapid pool.

In the ATPγS terminals from experiment 4 we find that in the absence of the functional refilling, multiple 20ms pulses can deplete the releasable pool (evidenced by the decrease in response to a 1s depolarization after a series of 20 ms pulses). This suggests that the releasable pool is largely located at ribbon-style active zones. Four to five 20 ms pulses were needed to deplete the releasable pool (in the absence of functional refilling). This suggests that the releasable pool may be composed of 4-5 rows of vesicles which also fuse at

ribbon style active zones. This co-relates nicely with EM reconstruction of the ribbon associated active zone (75)

In experiment 4 , after 4-5 20 ms depolarizations the terminals were stimulated with a 1s depolarization. Compared to a 20 ms depolarization a 1 s depolarization should result in a larger spread of the calcium signal. This global elevation in $[Ca]_i$ may elicit fusion of vesicles both at ribbon and non-ribbon sites (more than 700 nm from the ribbon). In experiment 4, in terminals that were dialyzed with ATPγS there is a remaining 14 ± 3 fF of exocytotic response measured after the depletion of the releasable and rapid pools (fig 3.9). This may reflect either incomplete block of refilling by ATPγS (due to competing endogenous ATP) or fusion of vesicles docked at non ribbon sites. If this remainder were indicative of release from sites more than > 700 nm from the synaptic ribbons, we can estimate the number of this vesicles population to be $\sim 542 \pm 126$ vesicles per terminal (assuming all vesicles to be of equal size , 29 nm (75)).

CHAPTER IV

VESISCLE POOLS ASSOCIATED WITH SNARE COMPLEXES IN A RETINAL

BIPOLAR NEURON

INTRODUCTION

The ability of a neuron to respond to repetitive stimulation depends on many factors including number of synaptic vesicles available for release, mobilization of vesicles into the fusion-competent vesicle pool and recycling of the exocytosed vesicles. For a vesicle to be fusion -competent or available for release it must be docked, primed and associated with SNARE complexes. These vesicles form the rapid pool of vesicles. The size of the rapid pool determines the release probability and synaptic strength of the neuron.

At conventional synapses, an action potential drives a burst of neurotransmitter release. Ribbon style synapses can release neurotransmitters continuously (tonically) where graded changes in the pre synaptic membrane potential modulate the release rate. The Mb1 bipolar neuron can also releases neurotransmitter in response to calcium-dependent action potentials (200–202). How does the bipolar neuron sustain this high demand for exocytosis which can be mediated via both graded and calcium-dependent action potentials? One possibility might be via the availability of a large number of vesicles at active zones. In support of this hypothesis, cerebellar mossy fiber terminals which are capable of sustained release at more than 200Hz have been shown to have 300 vesicles/active zones (224). Analysis of EM micrographs of goldfish bipolar neuron suggest ~ 5500 vesicles at ribbon style active zones (75). For a terminal with 50 ribbon, this translates to ~ 110 per ribbon-style active zone. However, the number of docked vesicles which are thought to be available for immediate release is not different between conventional synapses and the bipolar neuron: ~10-40 docked vesicles from EM analysis of single boutons from rodent hippocampal neurons (76, 127) ,~ 5 vesicles within 20 nm of active zone for the calyx of Held (128, 225) and ~ 22 vesicles/ ribbon-style active zone for the bipolar neuron (75). In conventional

synapses such as CA3 hippocampal neurons of rodent, the size of the fusion-competent pool of vesicles is set by the number of vesicles associated with fully assembled SNARE core complexes (226). The size of the vesicle pool associated with SNARE complexes in ribbon synapses is not known.

The aim of this chapter is to determine the size of the vesicle pool associated with SNARE complexes and therefore the size of the vesicles available for immediate fast release in retinal ribbon synapses. We hypothesize that similar to conventional synapses in ribbon synapses the rapid pool of vesicles will be associated with SNARE complexes.

In this section I will first discuss SNARE proteins in general and in ribbon synapses and docking and priming of synaptic vesicles

SNARE proteins

SNARE proteins are ubiquitously found and orchestrate vesicle fusion in organisms from yeast to humans (25, 227). The order of SNARE complex formation is thought to be as follows: an intermediate binary complex is formed at the plasma membrane between Syntaxin and SNAP 25 where the SNARE domains of these two proteins are oriented in parallel. The stable ternary SNARE complex is formed when Synaptobrevin, on the synaptic vesicle, interacts with the binary structure. Biochemically the ternary SNARE complex is very stable and resistant to high temperature (228) and denaturation by SDS. The SNARE complex is assembled via a "zippering" action starting at the N terminal towards the C terminal (229, 230). As the zippering progresses towards the C terminal, the vesicle is pulled closer to the plasma membrane rendering the vesicle ready for calcium dependent fusion with the plasma membrane. After the fusion of the synaptic vesicle SNAPs and NSF

help in the regeneration of the SNARE proteins. NSF is a ATPase and it is thought that the energy requirement for the disruption of the SNARE complex is provided by the hydrolysis of ATP by NSF (231).

SNARE proteins in Ribbon synapses

The three core proteins required for the formation of the neuronal SNARE complex are present in ribbon synapses. Syntaxin 1 is found in hair cell ribbon synapses and pinealocytes (94, 232, 233). Retinal ribbon synapses however express syntaxin 3B (149–151). SNAP 25 and Synaptobrevin are also found in ribbon synapses (94, 149, 232–237). However a functional role for SNARE proteins at ribbon synapses is controversial. Only two studies have looked at the physiological role of SNARE proteins at ribbon synapses (151, 158). In 2010 we published data showing that in the Mb1 bipolar neuron, a peptide derived from Syntaxin 3B, when introduced into the bipolar terminal, affects exocytosis (151). Data from Curtis et al.,2010 will be presented in the results section. Nouvian et al., 2011 provide physiological experiments where, in spite of the presence of SNARE mRNAs, neuroexocytosis in rodent inner hair cells seem to operate independently of neuronal SNAREs. In their study, Nouvian et al ., 2011 show that exocytosis in the inner hair cell of rodents are not affected by neurotoxins known to cleave neuronal SNARE proteins. They also show that in mice lacking certain SNARE proteins (SNAP 25 or Synaptobrevin 2/3-double knock out) exocytosis is maintained. Nouvian et al., 2011 suggest that it is possible that retinal ribbon synapses are different from hair cell ribbon synapses (probably due to different developmental origins- retinal cells being neuronal and hair cells being epithelial).

Therefore the role of neuronal SNAREs in ribbon synapses is controversial and further studies are required.

Docking and Priming of synaptic vesicles

Before a vesicle fuses with the plasma membrane it undergoes several preparatory steps that include docking and priming. Docked vesicles have been defined as those which are apposed to the plasma membrane. Under an electron microscope, docked vesicles are those that are within 30 nm of the plasma membrane (238, 239) or a vesicle whose membrane directly touches the presynaptic membrane with no cytoplasmic space between the two membranes (76, 240). In the traditional view, docking precedes priming. While docking functions to physically bring a vesicle in proximity to the fusion site, priming consists of maturation steps which render the vesicle "fusion competent" in response to calcium. In conventional synapses docked pool of vesicles contains both primed and non-primed vesicles (239, 240).

In hippocampal neurons the size of the docked pool is thought to be the anatomical correlate of the physiological rapid pool (76). Therefore, proteins that regulate the size of the docked pool may also effect the release properties of the neuron. Two presynaptic proteins, Munc18-1 (an SM protein) and Syntaxin (a SNARE protein,) have been established as docking factors (18, 19, 23, 241). However in *Drosophila,* synaptic vesicles are able to dock even in the absence of syntaxin(238). The vesicles are also undergo fusion evoked via hyperosmotic saline, suggesting a role downstream from docking for syntaxin, at least in *Drosophila.*

The definition of priming is less concrete compared to docking. It is dependent on the technique used to study this step, suggesting that there may be several forms of priming.

Traditionally, it was defined as the Mg-ATP and calcium dependent step that render a vesicle fusion-competent (80, 81, 242, 243) but other molecules such as Phosphatidylinositol-4,5-biphosphate (PIP$_2$) (244, 245), Munc 13-1 (an SM protein) and RIM1 (a Rab effector protein) (22, 246) have been suggested to be involved in priming. A newer definition of priming includes the opening of syntaxin and the beginning of the formation of the SNARE core complex (27, 247, 248). Syntaxin can exist in two conformations, open or closed. In the closed conformation the N-terminal folds back on the SNARE domain. In its closed form syntaxin is unable to interact with the other SNARE binding partners. The open syntaxin however is able to bind to SNAP 25. Munc 18-1 is known to bind to syntaxin and stabilize the "closed" conformation of syntaxin and block its interaction with other SNARE partners (31). In conventional synapses Munc 13-1 has been shown to prime vesicles for release via its interaction with Syntaxin. Munc 13-1 hastens the opening of syntaxin and the binding of other SNARE proteins to the SNARE domain of syntaxin and thus the formation of the core complex (249).

The role of SNARE proteins other than syntaxin in docking and priming is an active field of research. The absence of Synaptobrevin in *Drosophila* does not affect docking of s vesicles (238). A similar result has been shown in the squid, where disruption of Synaptobrevin function by neurotoxin or competing peptides also does not affect the docking step of vesicles.(250).

Docking and Priming in Retinal Bipolar Ribbon synapses

Unlike conventional synapses (76), in ribbon synapse the docked pool is not necessarily a correlate of the rapid pool. In ribbon synapses, EM micrographs of goldfish

bipolar neuron show docked vesicles at both the ribbon and at varying distances away from the ribbon style active zones (75, 82). Docked vesicles away from the ribbon style active zone are not thought to be the anatomical correlate of the physiological rapid pool since they are at a large distance from the calcium channel clusters (72, 82). TIRFM (Total internal reflectance fluorescence microscopy), which allows for tracking of vesicle mobility and fusion events at the plasma membrane has also been used to study docked vesicles. Vesicles with restricted mobility and those that remain continually visible for more than 500ms are considered docked (83, 251). Results from TIRFM studies show that ribbons (specifically within 700 nm from the center of a ribbon) are the preferred site for docking and once docked the vesicles do not undock but undergo evoked release. Compared to ribbon-associated sites, un-docking of a docked vesicles is more common at extra-ribbon sites which are defined to be > 700nm from a ribbon center (83). Calculations based on EM reconstructions for Mb1 terminals suggest that the number of docked vesicles at the ribbon is ~22 per ribbon, i.e. 1100 for a terminal with 50 ribbons (75). These vesicle are not only docked to the plasma membrane but are also tethered to the ribbon via filaments that are 25 nm long.

The primed pool of vesicles in the Mb1 terminals is also called the releasable pool of vesicles. These vesicles have undergone all ATP-dependent priming steps and are release ready (80, 81). From correlation between EM studies and capacitance measurements (132) and the results of chapter 3, we and others have suggested that the majority of the releasable pool is also ribbon associated. Two presynaptic proteins Munc 13-1 and RIM1, known for their role in priming in conventional synapses, have been found to be a part of the ribbon

and active zone complex (135, 246). A role of the ribbon as a site for priming of vesicles has been suggested (80, 156).

In this chapter we sought to determine which synaptic vesicle pool was associated with SNARE complexes in retinal ribbon synapses using the Mb1 goldfish bipolar neuron as a model neuron.

Three methods have been commonly used to study the function of SNAREs and identify which vesicle pool is associated with them. 1) Tetanus and Botulinum toxins: The tetanus toxin cleaves Synaptobrevin while Botulinum toxin A cleaves SNAP25 and Botulinum toxin C cleaves SNAP 25 and syntaxin (252). 2) Knock out animals lacking specific SNARE proteins and 3) SNARE inhibiting peptides.

For our purpose we used peptides derived from SNARE proteins instead of toxins or knock-out animals for the following reasons: Neurotoxins typically require a long (10-30 minutes) incubation period at mammalian body temperature (239, 250) and are thus not a viable option for experiments on acutely dissociated neurons from a cold-blooded vertebrate such as goldfish. Zebra fish, where SNARE proteins have been genetically ablated may provide an exciting model for our study but magnitude and properties of specific vesicle pool have not yet been defined in the zebra fish.

RESULTS

1. A peptide based on the SNARE domain of syntaxin 3B interferes with SNARE complex formation in-vitro

EXPERIMENT 1: To determine the effect of a short SNARE domain peptide on SNARE complex formation in-vitro

Note: *Experiment 1 was performed by the Roger Janz laboratory and has been included in this thesis for completeness.*
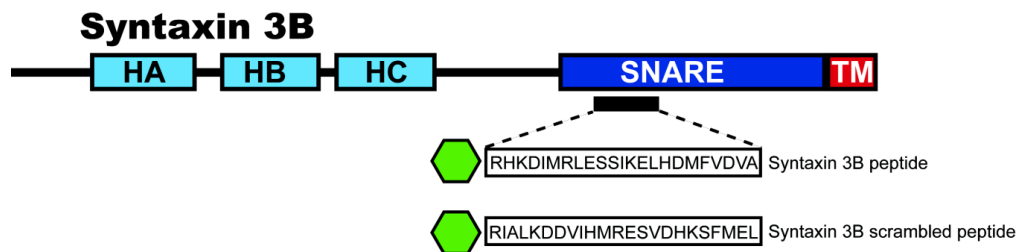
Fig4.1 Syntaxin 3 and scrambled peptides. Location and sequence of the SNARE competing peptide derived from syntaxin3B and the control scrambled peptide. Both peptides were tagged with fluorescein at the N terminal.

We first wanted to confirm whether a short peptide based on a SNARE protein could disrupt SNARE complex formation in-vitro. Dr. Roger Janz designed a peptide (fig 4.1) based upon the SNARE binding domain of syntaxin 3B, the specific syntaxin isoform found in the retinal ribbon synapses (150, 151). Another peptide (fig 4.1) with the same amino acid residues but in a randomly ordered/scrambled order, served as the control.
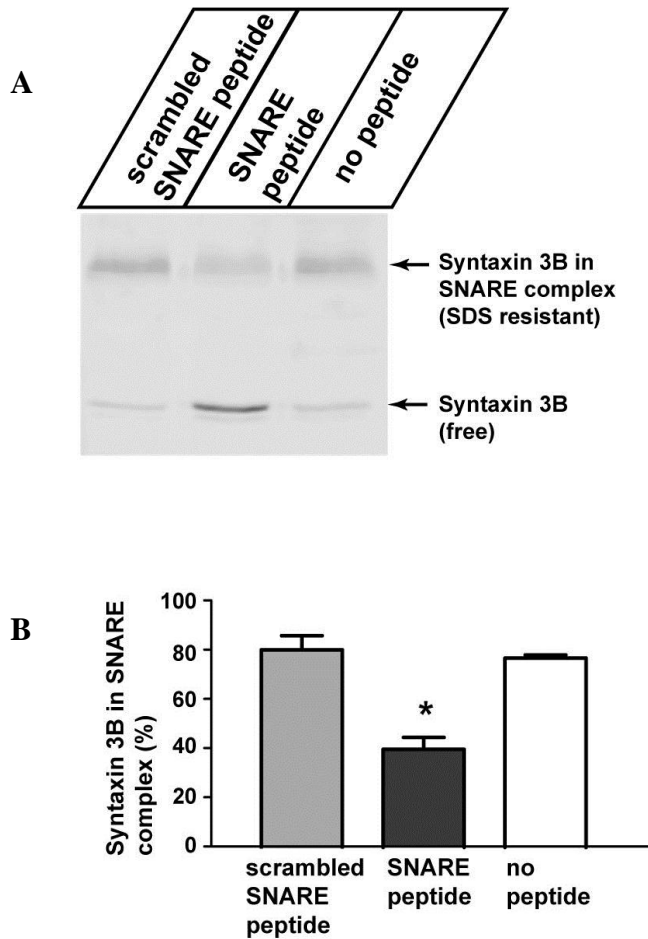
Fig 4.2 Syntaxin 3 peptide prevents formation of the SNARE complex

A. Under the experimental conditions (see methods) the majority of syntaxin 3B is found in a high molecular weight SDS-resistant SNARE complex (top arrow). The SNARE peptide (syntaxin 3B peptide) inhibits the formation of new SNARE complexes as apparent by the presence of the free syntaxin 3B (bottom arrow). The remaining SNARE complexes (top arrow) is likely already assembled in the tissue and is not affected by the SNARE peptide. **B.** Quantification of three different experiments. The amount of Syntaxin 3B present in the higher molecular weight SNARE complex relative to the total syntaxin 3B is given (mean +/- SEM).The SNARE peptide caused a significant reduction in the amount of syntaxin 3B that is in the high molecular SNARE complex (p=0.0331).

Retinal extracts were incubated with syntaxin or the scrambled-peptide for two hours at room temperature. Under these conditions, the majority of syntaxin 3 was found in a high molecular SDS resistant SNARE complex (Figure 4.2, top arrow). However, only the SNARE peptide (syntaxin3B peptide) caused a significant reduction in the percent of total syntaxin 3B found in the high molecular SNARE complexes (Figure 4.2). In addition, it was only in the presence of the SNARE peptide that free syntaxin 3B was seen (Figure 4.2, lower arrow). These results suggest that the SNARE peptide interfered with the formation of new SNARE complexes without greatly affecting already-formed SNARE complexes. These results suggest that the SNARE peptide interfered with the formation of new SNARE complexes without greatly affecting already-formed SNARE complexes.

EXPERIMENT 2: To determine the effect of the Syntaxin peptide on fusion from multiple vesicle pools

2. A Syntaxin 3B peptide does not initially affect the rapid and releasable pools

Our aim was to determine which of the many vesicles pools in the retinal bipolar cell exist in preformed SNARE complexes. Based on the results of experiment 1, we used the Syntaxin 3B peptide as a tool to block the formation of new SNARE complexes and therefore determine the size of the vesicle pool associated with formed SNARE complexes. The pulse train protocol described in chapter 3- experiment 1 provides a paradigm where all three vesicle pools can be visualized. In response to the train stimulus, the change in capacitance after the first pulse or ΔC_{m1} gives us an estimate of the rapid pool where as the cumulative ΔC_m at the end of the train or $\Delta C_{m\,total}$ gives us an estimate of the releasable pool and its refilling (chapter 3). Isolated bipolar terminals were dialyzed with the Syntaxin

3B peptide or the scrambled control. Bothe peptides were tagged with FITC and loading of

the terminal with either peptide was verified by an increase in fluorescence in the terminal

over time (fig 4.3)
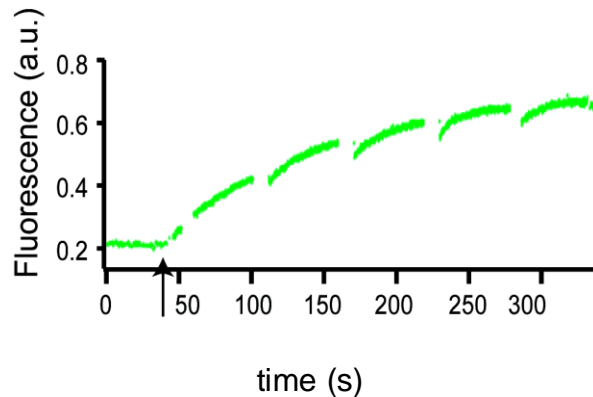
Fig 4.3 Dialysis of the FITC tagged peptides were verified by an increase in fluorescence : In order to visually confirm the diffusion of the specific peptides into bipolar cell terminals, the peptides were tagged with FITC (Fluorescein iso-thiocyanate) at the N-terminus. After achieving whole-cell voltage clamp (marked by arrow), increase in the spatially averaged fluorescence was observed over time. A steady state is reached in 3-4 minutes. (The gaps in the trace denote time points where fluorescent measurement was stopped for real-time adjustment of the visual scaling of the trace or when the terminal was stimulated with a pulse train.)

Effect of syntaxin 3B on the fusion of the releasable pool vesicles:

Terminals were stimulated after 1 minute of dialysis with either the syntaxin 3B

peptide or the scrambled peptide. In response to the train stimulus, terminals dialyzed with

the syntaxin peptide showed an overall smaller exocytotic response compared to terminals

dialyzed with the scrambled peptide (fig 4.4). To study this finding in detail we first looked

at $\Delta C_{m\,total}$ as a measure of the releasable pool and recruitment from reserve vesicles. We

compared the total cumulative capacitance response, $\Delta C_{m\,total}$, between terminals dialyzed

with either peptide. In terminals dialyzed with scrambled peptide, $\Delta C_{m\,total}$ was not

significantly different from that seen with standard recording solution from chapter 3 experiment 1 (scrambled: $\Delta C_{m\,total} = 276 \pm 53$ fF, n=5; ATP control: $\Delta C_{m\,total} = 233 \pm 48$ fF ,n = 6;, p value = 0.56). By contrast, $\Delta C_{m\,total}$ was significantly reduced by nearly half in terminals dialyzed with the syntaxin 3B peptide (Syntaxin 3B: $\Delta C_{m\,total} = 91 \pm 16$ fF; n= 6; p value = 0.006) relative to scrambled. The magnitude of $\Delta C_{m\,total}$ in the presence of the syntaxin peptide was comparable to that seen when functional refilling was blocked with ATPγS (i.e., fig 3.4), suggesting that in the presence of the syntaxin peptide recruitment of reserve pool vesicles may be blocked. This finding also suggests that the syntaxin peptide does not appreciably block fusion of vesicles in the releasable pool.

To determine whether the effect of the decreased $\Delta C_{m\,total}$ was due to a decreased influx of calcium we looked at the average Ica of the last five pulses of the train, $I_{ca\,total}$. The $I_{ca\,total}$ in terminals dialyzed with the syntaxin peptide compared to the scrambled peptide was smaller, and close to being significantly different (scrambled: $I_{ca\,total} = 124 \pm 19$ pA, n =5; Syntaxin: $I_{ca\,total} = 74 \pm 12.5$ pA ,n = 6, p value = 0.052). The $I_{ca\,total}$ in terminals dialyzed with syntaxin 3B and in terminals dialyzed with the scrambled peptide was decreased relative to the $I_{ca\,1}$. This could be due to i) a difference in calcium accumulation between terminals dialyzed with syntaxin 3B and the scrambled peptide during the train and calcium-dependent calcium channel inactivation (253) or a activity -dependent effect of Syntaxin 3B on the calcium channel (254). To bypass these two issues we used an alternate protocol which consisted of a single 1s depolarization to verify if the releasable pool was indeed spared in the presence of the syntaxin peptide. The effect of the syntaxin 3B peptide on the calcium channel is further addressed in the discussion section of this chapter.
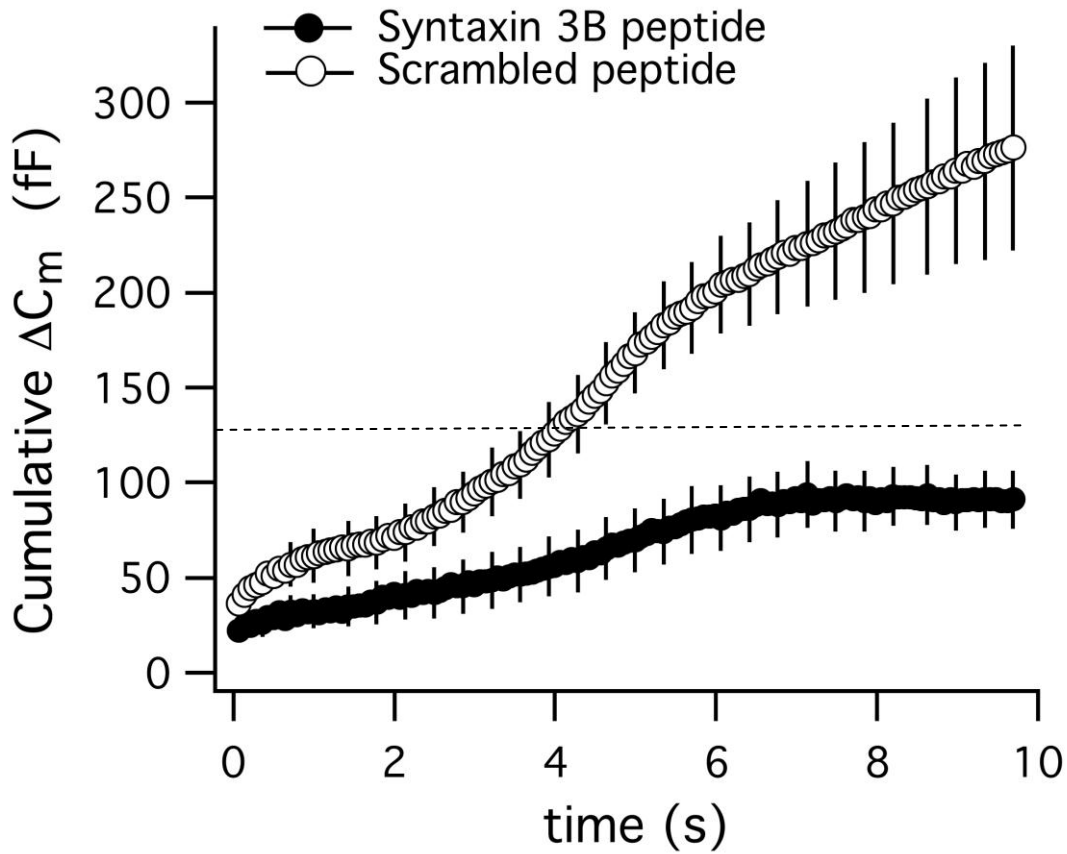
Fig 4.4 . A SNARE complex inhibiting peptide blocks fusion of the reserve vesicles but not the releasable pool vesicles.

In response to a pulse train given 1 min after achieving whole cell configuration, terminals dialyzed with a SNARE complex inhibiting peptide (syntaxin, black circles, n = 6) showed a decrease in the cumulative capacitance compared terminals dialyzed with a scrambled peptide (open circles, n = 5). The dotted line marks the magnitude of the total cumulative capacitance seen in terminals dialyzed with ATPγS (from fig 3.4). The release component attributed to refilling from reserve pool vesicles is inhibited in the presence of the syntaxin peptide but not the scrambled peptide.
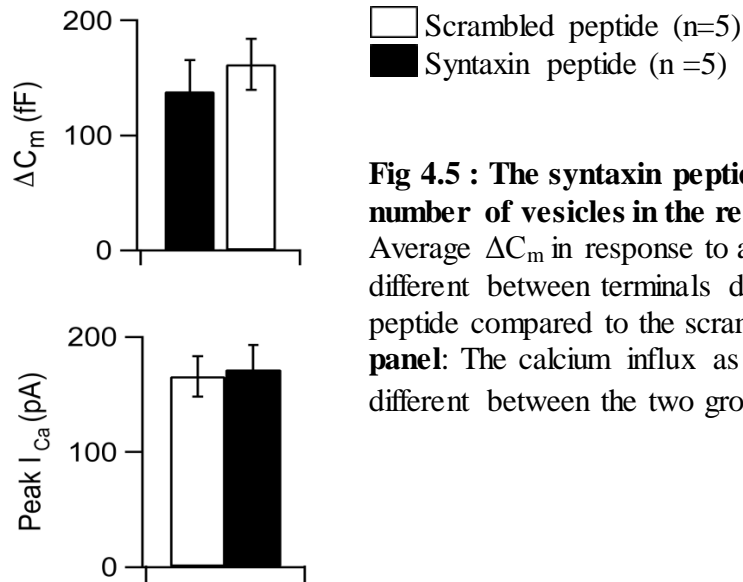
Fig 4.5 : The syntaxin peptide does not affect the number of vesicles in the releasable pool Top panel: Average ΔC_m in response to a 1 s depolarization is not different between terminals dialyzed with the syntaxin peptide compared to the scrambled peptide. **Lower panel**: The calcium influx as measures by peak I_{ca} is not different between the two groups.

In Mb1 terminals, a 1s depolarization (-60 mV to 0mV) has been traditionally used to study the releasable pool (75, 80). Therefore we used a 1s depolarization to probe the releasable pool (fig 4.5). The magnitude of the capacitance change in response a 1 s pulse was not significantly different between terminals dialyzed with the syntaxin peptide; $\Delta C_m = 138 \pm 27.4$, n= 5, and the scrambled peptide, $\Delta C_m = 162 \pm 22.2$, n=5; p value = 0.52. This magnitude of response is also consistent with previously reported values of the releasable pool (75, 80, 132). The calcium influx due to the 1 s pulse was not different between terminal dialyzed with either peptide (scrambled: $I_{ca} = 165.9 \pm 17.6$ pA, n =5; syntaxin: $I_{ca} = 172 \pm 21$ pA, n = 5, p value = 0.8).

Effect of syntaxin 3B on the fusion of the rapid pool vesicles:

Next we sought to examine whether the syntaxin 3B peptide inhibited fusion of the rapid pool vesicles. By definition the vesicles of the rapid pool are thought to be docked. The SNARE proteins on the vesicles in this pool are thought to form trans-SNARE complexes with the plasma membrane SNARE proteins. To test whether the rapid pool was associated with SNARE complexes we compared the capacitance change in response to the first 20 ms pulse (ΔC_{m1}) in the train as a measure of the rapid pool. In terminals dialyzed with the scrambled-peptide (Fig 4.4 and 4.6), the mean ΔC_{m1} was similar to that obtained using standard internal solutions (scrambled: $\Delta C_{m1} = 36.4 \pm 6.4$ fF; n=5). In terminals dialyzed with the syntaxin peptide, the mean ΔC_{m1} was 22 ± 7 fF, n=6. These values were not significantly different from each other (p value $= 0.2$). The magnitude of the ΔC_{m1} in the presence of syntaxin is similar to what is seen in the presence of 5 mM EGTA, known to block fusion of all vesicles pools except the rapid pool (72, 208), (fig 3.4, 5mM EGTA:ΔC_{m1} $_{=} 22.3 \pm 3.3$ fF). Analysis of I_{ca} in response to the first pulse ($I_{ca}1$) revealed that neither peptide had a significant effect on stimulus-evoked calcium entry (scrambled: $I_{ca\,1} = 203.5 \pm 23$ pA, n =5; syntaxin: $I_{ca\,1} = 127.5 \pm 30$ pA, n = 6, p value $= 0.09$). The $I_{ca\,1}$ in terminals dialyzed with either peptide was not significantly different from control experiments (terminals dialyzed with peptide-free solution, ANOVA-NS). From these data, we conclude that after one minute of dialysis, the rapid pool is largely intact in the presence of syntaxin peptide.
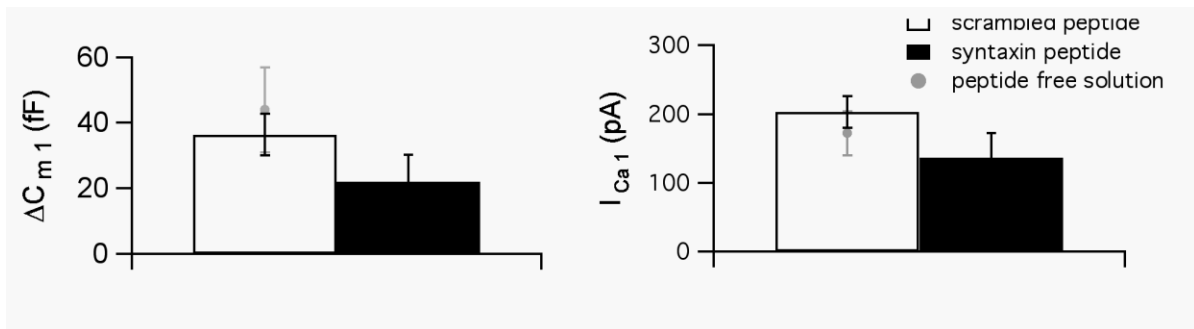
Figure 4.6 : The Syntaxin peptide does not affect fusion from the rapid pool :
Left: In response to the first 20ms pulse of the train the ΔC_{m1} was not significantly different between terminals dialyzed with the syntaxin peptide (n= 6), scrambled peptide (n=5)
Right: The calcium influx measured by the calcium current was also not different between terminals dialyzed with the syntaxin peptide (n= 6), scrambled peptide (n=5). Magnitude of ΔCm_l and calcium current in terminals dialyzed with peptide free control is shown in gray for visual comparison (from chapter 3-experiment 1).

EXPERIMENT 3: To determine the effect of the syntaxin peptide on refilling of the vesicle pools

3. The Syntaxin 3B peptide blocks refilling of the releasable and rapid pools

Given that the syntaxin 3B peptide inhibited SNARE complex formation in vitro (Fig 4.2), but the rapid and releasable pools were initially intact, we next asked whether SNARE complex formation was required for subsequent rounds of release. To test whether the formation of new SNARE complexes were required for fusion of the rapid and releasable pools that occur following pool refilling, synaptic terminals were stimulated with four pulse trains given one minute apart. Refilling of the releasable pool under standard conditions has been shown to have a time constant of ~7- 8 seconds and therefore

completed within ~20 seconds (80, 84). The 60 s inter train interval should therefore be sufficient to refill the releasable pool under control conditions.

Refilling of the Releasable pool:

Results above (fig 4.4) show that recruitment of reserve vesicles is blocked in the presence of syntaxin 3B suggesting that the syntaxin peptide compromises refilling of the releasable pool. As further proof we measured the $\Delta C_{m\,total}$ of each train (train 1 to 4) in terminals dialyzed with either peptide. To quantify percentage refilling we normalized the $\Delta C_{m\,total}$ of each train to that of the first train (fig 4.7 right panel). Terminals dialyzed with the scrambled peptide showed some run down, as seen in standard control experiments (Gray bars shown for comparison, fig 4.7). By contrast, the releasable pool dramatically decreased with each pulse train in terminals dialyzed with syntaxin 3B (to right panel fig 4.7). By the second train, $\Delta C_{m\,total}$ was dramatically reduced in syntaxin terminals to 37 ± 10.6 fF (n=5), reflecting a 64% decrease from the initial value (Fig 4.7). By contrast, $\Delta C_{m\,total}$ with scrambled peptide was 197 ± 47 fF (n=5), reflecting a decrease of 31% from the initial value (Fig 4.7). To determine whether the effect of the syntaxin could be attributed to a change in calcium entry, we examined the average peak I_{Ca} for the last 5 pulses ($I_{ca\,total}$) of each pulse train. The $I_{ca\,total}$ in terminals dialyzed with the syntaxin peptide was smaller than that measured in terminals dialyzed with the scrambled peptide and the difference was close to significance (scrambled: $I_{ca\,total\_}3 = 130 \pm 17.6$ pA, n =5; syntaxin: $I_{ca\,total\_}3 = 80.6 \pm 16$ pA, n = 5, p value $= 0.07$ Fig. 4.7). As seen before this may suggest a decreased calcium influx over time, during the pulse train, and that the syntaxin peptide could affect refilling or refilling rates of the releasable pool via an effect on calcium channels. This is specifically important as calcium aids refilling of the releasable pool in bipolar cells (208) .

We also employed an alternate protocol using a 1s depolarization, which would avoid any calcium-dependent or any syntaxin-dependent inhibition of calcium channels to measure if refilling is blocked in the presence of the syntaxin peptide. Bipolar terminals were stimulated with four depolarizations each of 1 s duration (from -60mV to 0mV) . The first pulse was given 1 min after attaining whole-cell configuration and the inter pulse stimulus was 60 s.

As shown in fig 4.8 and earlier in fig 4.5, after 1 min of dialysis with the syntaxin peptide , the initial size of the releasable pool is not affected. Upon subsequent stimulation synaptic terminals dialyzed with the syntaxin peptide showed pronounced, progressive decrease in the size of the releasable pool. To quantify percentage refilling we normalized the ΔC_m in response to each 1 s pulse to that of the first pulse. By the fourth pulse, the response was reduced to 89% in syntaxin terminals compared to 45% in terminals dialyzed with the scrambled peptide (fig 4.8). These data suggest that refilling of the releasable pool was greatly affected by the syntaxin peptide.

In this experiment the syntaxin peptide did not have an inhibitory effect on the calcium current. The amplitude of the peak I ca in response to each pulse was not significantly different between terminals dialyzed with the syntaxin peptide and those dialyzed with scrambled peptide. By the fourth pulse scrambled: $I_{ca} = 153 \pm 18.3$ pA, n =5; syntaxin: $I_{ca} = 135 \pm 19.7$ pA, n = 5, p value = 0.5. Thus, we can rule out the possibility that changes in calcium entry and cytosolic calcium underlie the effect of the syntaxin 3B peptide on refilling.
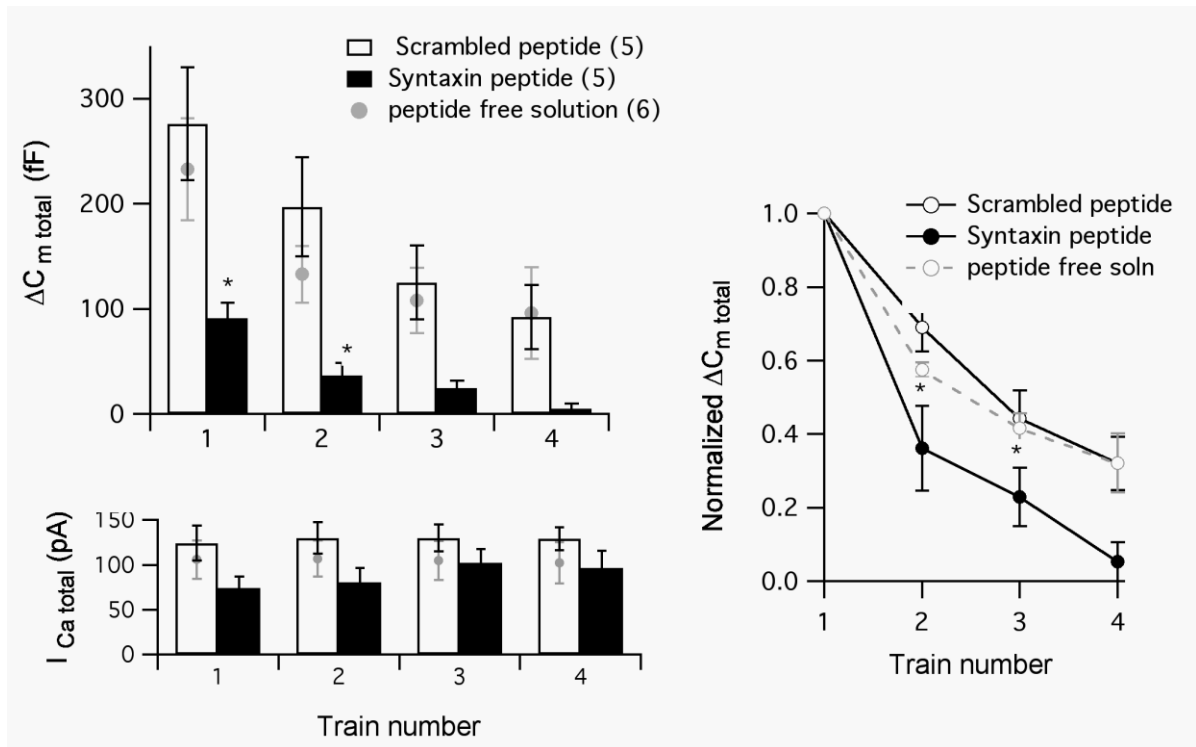
Fig 4. 7 A SNARE complex inhibiting peptide blocks refilling the releasable pool of vesicles. Left top. Mean cumulative capacitance ($\Delta C_{m\,total}$) in response to a pulse train given every min (train number is indicated on the x axis) in terminals dialyzed with syntaxin (black), scrambled peptide (white) is shown. $\Delta C_{m\,total}$ in terminals dialyzed with the syntaxin peptide is significantly smaller compared to terminals dialyzed with scrambled peptide. **Right;** Normalizing to the $\Delta C_{m\,total}$ of the first train shows a progressive block of refilling in syntaxin peptide terminals compared to scrambled peptide **. Left bottom**: The effect of the syntaxin peptide was not due to a decreased calcium influx. There was no significant difference between the I_{Ca} in terminals dialyzed the syntaxin peptide versus the scrambled peptide. Magnitude of $\Delta C_{m\,total}$ and calcium current in terminals dialyzed with peptide free control is shown in gray for visual comparison (from chapter 3).
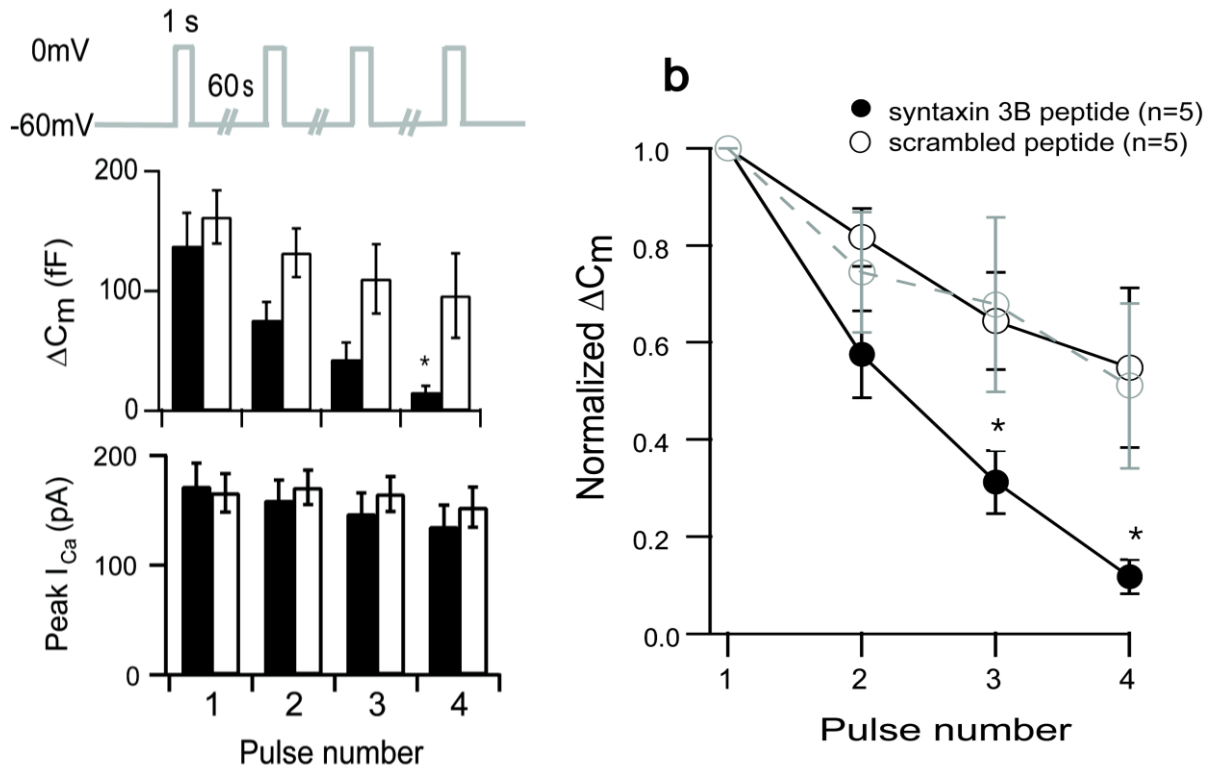
Fig 4. 8 A SNARE complex inhibiting peptide blocks refilling the releasable pool of vesicles. Left top: The stimulation paradigm used: A 1 s depolarization was given every 60s. **Left middle**: average ΔC_m in response to each 1 s pulse shows that in terminals dialyzed with the syntaxin peptide showed a progressive decrease in the exocytotic response compared to scrambled peptide. **Left bottom**: There was no significant difference in the mean peak amplitudes of the calcium current between the two groups. **Right**: The ΔC_m was normalized to the magnitude of the response of the first pulse. Syntaxin terminals showed a successive decrease in the refilling of the releasable pool. The grey dotted line shows normalized data from ATP controls (n=3).

Refilling of the Rapid pool:

      Next we sought to examine the effect of the syntaxin peptide on refilling of the rapid pool. Isolated terminals were stimulated with four pulse trains given one minute apart. As before ΔC_{m1} was used as a measure of the releasable pool. By the second train, the rapid pool in terminals dialyzed with the syntaxin peptide was significantly diminished relative to scrambled peptide (scrambled: $\Delta C_{m1}\_2 = 31 \pm 6$ fF, n = 5; syntaxin: $\Delta C_{m1}\_2 = 8.3 \pm 3.5$ fF, n = 5; p=0.012). This represents a 66% decrease in the rapid pool in terminals dialyzed with the syntaxin peptide compared with a 14% decrease in terminals dialyzed with the scrambled peptide (fig 4.9). This effect was not due to a decreased calcium influx as the I_{Ca} of the first pulse of each train was not significantly different between the two groups (e.g. scrambled: $I_{ca\,1}\_2 = 194.4 \pm 21.5$ pA, n =5; SCIP: $I_{ca\,1}\_2 = 127 \pm 32.7$ pA, n = 5, p value =0.123, fig 4.9). Our results suggest that the syntaxin 3B peptide affects refilling of the rapid pool.

Data from the above experiments have been compiled in table 4.1-4.4.
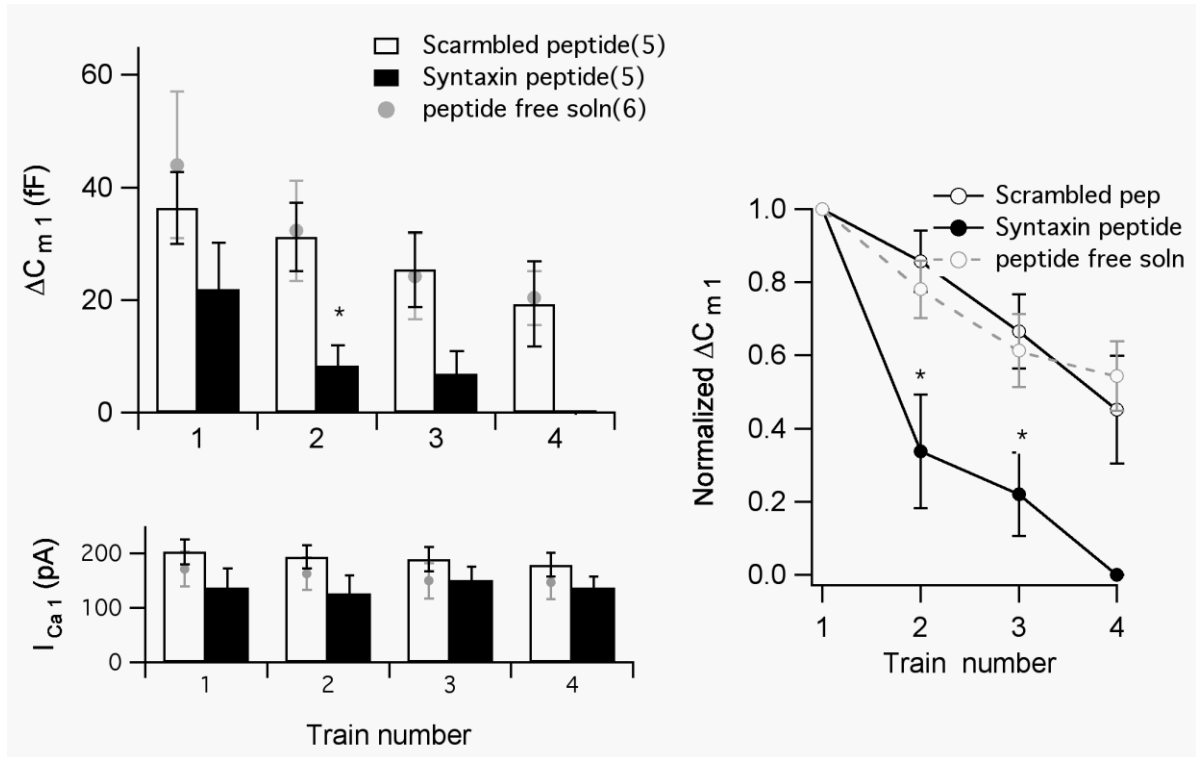
Fig 4. 9 A SNARE complex inhibiting peptide blocks refilling the rapid pool of vesicles.
Left top: Mean cumulative capacitance (ΔC_{m1}) in response to a pulse train given every min (train number is indicated on the y axis) in terminals dialyzed with syntaxin (black), scrambled peptide (white) solutions is shown. After the first train ΔC_{m1} in terminals dialyzed with the syntaxin peptide is significantly smaller compared to terminals dialyzed with scrambled peptide. **Right:** Normalizing to the ΔC_{m1} of the first train shows a progressive block of refilling in terminals dialyzed with the syntaxin peptide compared to the scrambled peptide **. Left bottom**: The effect of the syntaxin peptide was not due to a decreased calcium influx. There was no significant difference between the I_{Ca1} in terminals dialyzed with the syntaxin peptide versus scrambled peptide. Magnitude of ΔCm_1 and calcium current in terminals dialyzed with peptide free control is shown in gray for visual comparison (from chapter 3).

Table 4.1: The size of the rapid pool and its refilling in response to multiple trains

| Internal Solution	Train 1	Train 2	Train 3	Train 4
Scrambled peptide	36.4 ± 6.3	31.2 ± 6 (85.7%)	25.4 ± 6.6 (66.5%)	19.3 ± 7.6 (45.1%)
Syntaxin 3B	21.5 ± 7	8.3 ± 3.3 (33.8%)	6.9 ± 4 (22%)	0 (0)
p-value (Scrambled vs. Syntaxin)	0.148	0.01 (0.012)	0.09 (0.03)	0.1 (0.06)
Peptide free solution	44.6 ± 13	32.33 ± 9 (78.1%)	24.2 ± 7.6 (61.3%)	20.4 ± 5 (54.4%)

The capacitance response to the first pulse in the train, ΔC_{m1} (an estimate for the rapid pool) in response to train1 -4 for the different internal solutions is tabulated. All values are in fF and expressed as mean $\pm$ s.e.m. Values in bracket for trains 2-4 show the percentage refilling calculated by (ΔC_{m1} for train x/ ΔC_{m1} for train 1)* 100. P value in brackets are for percentage refilling in the terminals dialyzed with syntaxin peptide versus scrambled peptide. Values from experiments where no peptides were added are shown in grey below the table.

Table 4.2 Calcium currents in response to the first 20ms depolarization (I_{ca1}) in multiple trains

Internal Solution	Train 1	Train 2	Train 3	Train 4
Scrambled peptide	203 ± 22.9	194 ± 21.5	189 ± 22.6	178 ± 22
Syntaxin 3B	127 ± 30.4	127 ± 32.7	151 ± 24.7	138 ± 19.6
p-value (Scrambled vs. Syntaxin)	0.09	0.12	0.31	0.27
Peptide free solution	172 ± 31.8	163 ± 29.6	155 ± 32.4	147 ± 30.3

The calcium current in response to the first pulse in the train or I_{ca1} in response to train1- 4 for the different internal solutions is tabulated. All values are in pA and expressed as mean $\pm$ s.e.m. Values from experiments where no peptides were added are shown in grey below the table.

Table 4.3: The size of the releasable pool and its refilling in response to multiple trains

Internal Solution	Train 1	Train 2	Train 3	Train 4
Scrambled peptide	276 ± 53.7	197 ± 47.2 (69.1%)	125 ± 35 (44.2%)	92.2 ± 30 (32.1%)
Syntaxin 3B	91.2 ± 17	36.9 ± 11 (36.2%)	24.9 ± 7 (22.9%)	4.8 ± 4.8 (5.2%)
p-value (Scrambled vs. Syntaxin)	0.006	0.01 (0.02)	0.07 (0.01)	0.07 (0.04)
Peptide free solution	233 ± 48.4	133 ± 27 (57.5%)	108 ± 31 (41.7%)	96.1 ± 43 (32.2%)

The total amount of exocytosis evoked by the train - cumulative capacitance $\Delta C_{m\,total}$ (an estimate for the releasable pool and recruitment of reserve vesicles) in response to train1 -4 for the different internal solutions is tabulated. All values are in fF and expressed as mean ± s.e.m. Values in bracket for trains 2-4 show the percentage refilling calculated by ($\Delta C_{m\,total}$ for train x/ $\Delta C_{m\,total}$ for train 1)* 100. P value in brackets are for percentage refilling in the terminals dialyzed with syntaxin peptide versus scrambled peptide. Values from experiments where no peptides were added are shown in grey below the table.

Table 4.4 Calcium currents ($I_{ca\,total}$) in response to multiple trains

Internal Solution	Train 1	Train 2	Train 3	Train 4
Scrambled peptide	124 ± 19.4	130 ± 17.6	129 ± 14.9	129 ± 12.9
Syntaxin 3B	74.2 ± 12.5	80.6 ± 16	102.3 ± 15	96.5 ± 19
p-value (Scrambled vs. Syntaxin)	0.05	0.07	0.27	0.24
Peptide free solution	108 ± 14.8	111 ± 14.5	110 ± 15.4	106 ± 15.4

The average calcium current of the last five pulses of the train or $I_{ca\,total}$ in response to train1- 4 for the different internal solutions is tabulated. All values are in pA and expressed as mean ± s.e.m. Values from experiments where no peptides were added are shown in grey below the table.

EXPERIMENT 4: To determine whether the effect of the syntaxin peptide was time dependent or activity dependent

In the above experiments the inhibitory effect of the peptide on the reserve pool vesicles was seen after dialysis with the Syntaxin 3B peptide for 1minute and the inhibitory effect on the releasable and rapid pool vesicles was seen after dialysis for 2minutes and 1 round of stimulation with the pulse train. We wanted to know whether the effect of the syntaxin peptide on exocytosis was dependent on dialysis time or whether it required vesicle turnover (activity dependent) . To answer this question, we stimulated terminals with the pulse train similar as described above except that we gave the first pulse train three minutes after achieving the whole-terminal configuration, a time point at which there was a significant inhibition of the fusion of all three vesicle pools. In terminals dialyzed with the syntaxin 3B peptide, the cumulative $\Delta C_{m\,total}$ in response to the first train given at 3 min showed an amplitude indicating the loss of the component attributed to recruitment of reserve pool vesicles. The secretory component attributed to the releasable pool was intact. This was similar to $\Delta C_{m\,total}$ in response to the first train given at 1 min Fig 4.10 (3min: $\Delta C_{m\,total} = 105 \pm 43$ fF ,n=2, 1 min: $\Delta C_{m\,total} = \Delta C_{m\,total} = 91 \pm 16$ fF; n= 6). The calcium current at the end of the first train given at 3 min was $I_{ca\,total} = 95.2 \pm 20$ pA, n = 2. For comparison the $I_{ca\,total}$ at the end of the first train given at 1 min, $I_{ca\,total} = 74 \pm 12.5$ pA ,n = 6, fig 4.10.

In terminals stimulated with the train pulse at 3 min , the rapid pool was also intact, similar to that see with terminals stimulated after 1 min of peptide dialysis (3min:ΔC_{m1}: Syntaxin $= 29.1 \pm 9$ fF, n= 2; 1 min: $\Delta C_{m1} = 22 \pm 7$ fF , n=6). The calcium influx measured by $I_{ca\,1}$ was similar between terminals probed at 1 min and 3 minutes (3min: $I_{ca\,1} = 139 \pm 2$

pA, n = 2; 1min:$I_{ca\ 1}$ = 127.5 ± 30 pA, n = 6). This suggests that vesicle turnover is required for the inhibitory effect of the syntaxin 3B peptide on the vesicles of the rapid and releasable pools.

Fig 4.10 shows a comparison of the responses seen after 1min to that seen after 3 min of peptide dialysis.
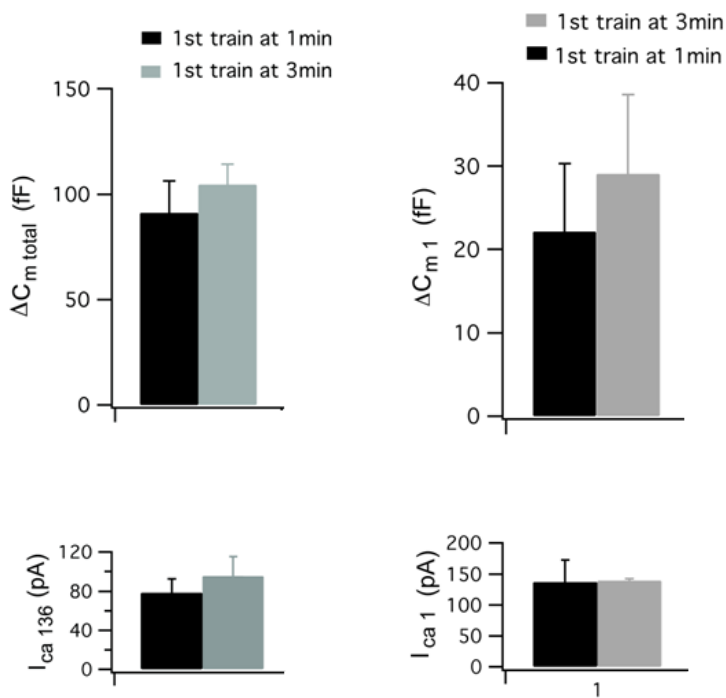
Fig 4.10 Increase in dialysis time does not change the effect of the syntaxin 3B peptide on the rapid and releasable pool
Left Top: Average cumulative $\Delta C_{m\ total}$ in response to the first train pulse given after 3min of dialysis (grey bar, n=2) was not different from that seen after 1 min of dialysis (black bar , n= 6). **Right top**: Average cumulative $\Delta C_{m\ 1}$ in response to a train pulse given after 3min of dialysis (grey bar, n=2) was not different from that seen after 1 min of dialysis (black bar , n= 6). **Left and right bottom**: The calcium influx at the end of the train ($I_{ca\ total}$,left bottom) and the calcium influx in response to the first pulse in the train ($I_{ca\ 1}$,right bottom) was also not different between terminals dialyzed with the syntaxin peptide for 1 min (black bars, n= 6) versus 3 min (grey bars, n= 2).

5. A SNAP 25 peptide blocked recruitment of reserve pool vesicles while a Synaptobrevin competing peptide did not have an inhibiting effect on exocytosis

EXPERIMENT 5: To determine which vesicle pools were associated with SNARE complexes using short peptides based on other SNARE proteins

We used two other short SNARE competing peptides: one based on the other t-SNARE, SNAP25, and another based on the v-SNARE Synaptobrevin to study which vesicle pool/s is associated with SNARE complexes. The SNAP 25 peptide was 26 amino acids long and was based on the C-terminal of the SNARE domain. A matching scrambled SNAP 25 served as control. In a first set of experiments, we dialyzed terminals with the SNAP 25 peptide or the SNAP 25-scrambled peptide and stimulated with the pulse train. We waited 3 minutes before stimulating the terminals with the pulse train. In the experiments with the syntaxin 3B peptide, the inhibitory effect of the peptide did not seem to depend on the duration of dialysis (similar results were seen in response to a first pulse train given 1 min or 3 minutes after break-in, fig 4.10) .

In response to the first train, terminals dialyzed with SNAP 25 showed $\Delta C_{m1} = 29.6 \pm 5.3$ fF and the $\Delta C_{m\,total} = 153 \pm 30$ fF (n = 4). This suggests that the effect of the SNAP 25 peptide was similar to that seen with the syntaxin peptide. Recruitment and fusion of the reserve pool vesicles was blocked but the fusion of rapid and releasable pool vesicles remained intact (fig 4.11). The effect of the SNAP peptide on exocytosis of reserve vesicles was not due to a difference in calcium influx as measured by calcium current (SNAP: $I_{ca\,total} = 99.8 \pm 10$ pA, n =4; scrambled SNAP: $I_{ca\,total} = 91.9 \pm 4$ pA, n = 2).

In terminals dialyzed with the SNAP scrambled peptide, the size of the rapid pool was unusually large. ($\Delta C_{m1} = 60 \pm 0.5$ fF, p value 0.02 compared to SNAP). This could be

due to a larger calcium influx in the terminals dialyzed with the scrambled SNAP peptide compared to the SNAP peptide (SNAP: $I_{ca1} = 115 \pm 14$ pA, n = 4 ; scrambled SNAP: $I_{ca1} = 146 \pm 4$ pA, n = 2). However more experiments and a larger n would be needed to prove this possibility. In terminals dialyzed with the SNAP scrambled peptide the exocytotic component attributed to the releasable pool and recruitment of reserve vesicles was comparable to ATP controls (SNAP-scrambled: $\Delta C_{m\,total} = 255 \pm 23$ fF , n = 2, compared with fig 3.4).

Refilling of the rapid and releasable pool as measured by ΔC_{m1} and $\Delta C_{m\,total}$ was decreased in response to subsequent trains (fig 4.12). The calcium influx did not decrease with subsequent pulses (fig 4.12). The basal calcium was not different between the terminals dialyzed with SNAP 25 and the scrambled SNAP peptide (SNAP:$[Ca]_i = 150 \pm 11.8$nM, n = 5; scrambled SNAP: $:[Ca]_i = 190 \pm 5.3$nM, n = 2, p value = 0.1

In a second set of experiments we tested a19 amino acid peptide based on the N-terminal of the SNARE domain of Synaptobrevin. The Synaptobrevin peptide did not have any inhibitory effect on fusion of any vesicle pool. After the first train the $\Delta C_{m1} = 38.2 \pm 6$ fF and the $\Delta C_{m\,total} = 278 \pm 53$ fF (n=3). The calcium current in terminals dialyzed with Synaptobrevin were: $I_{ca1} = 174 \pm 15$ pA, n = 3, $I_{ca\,total} = 113 \pm 29$ pA, n = 3.

A SNAP 25

B Synaptobrevin/VAMP2
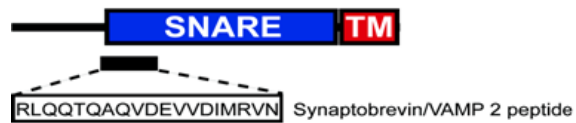
Fig 4.11 : Location and sequence of SNAP 25 and Synaptobrevin peptides
A The SNAP 25 peptide was based on the C terminal of the SNARE binding domain. A scrambled SNAP 25 peptide served as control. **B**. The Synaptobrevin peptide was based on the N-terminal domain of the SNARE binding domain. These peptides were not tagged with fluorescent proteins.
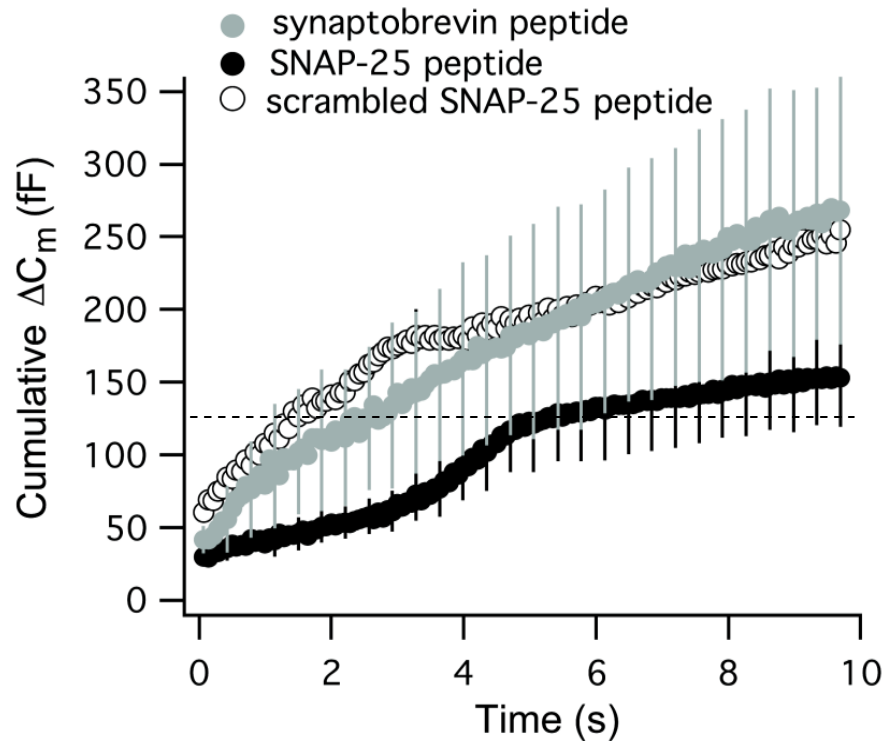
Figure 4.12 : The SNAP 25 peptide blocked recruitment of reserve pool vesicles while the Synaptobrevin peptide did not inhibit exocytosis of any pool.

In response to a pulse train given 3 min after achieving whole cell configuration, terminals dialyzed with a SNARE complex inhibiting peptide (SNAP25, black circles, n = 4) showed a decrease in the cumulative ΔC_m compared terminals dialyzed with a scrambled SNAP peptide (open circles, n = 2). The dotted line marks the magnitude of the total cumulative capacitance seen in terminals dialyzed with ATPγS (from fig 3.4). Terminals dialyzed with SNAP 25 showed a loss of fusion from the reserve pool. Terminals dialyzed with Synaptobrevin (grey circles , n=3) did not block exocytosis of any vesicle pool.
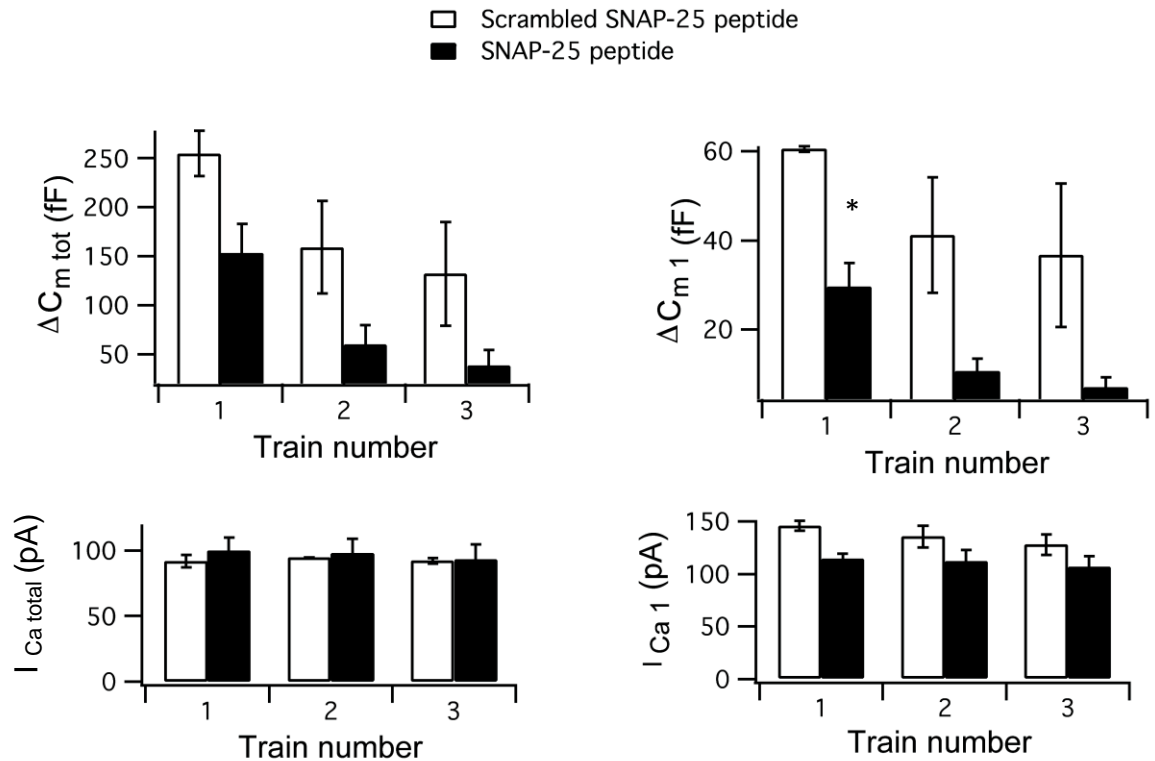
Fig 4.13 A SNAP 25 peptide blocks refilling of the releasable and rapid pool

Left top Mean cumulative capacitance ($\Delta C_{m\,total}$) in response to a pulse train given every min (train number is indicated on the y axis) in terminals dialyzed with SNAP 25 (black), scrambled SNAP peptide (white) solutions is shown. The $\Delta C_{m\,total}$ is smaller in terminals dialyzed with the SNAP 25 peptide (n= 4) in every train compared to the scrambled SNAP peptide (n =2). **Right top**: The mean capacitance in response to the first pulse in the train ($\Delta C_{m\,1}$) in terminals dialyzed with the scrambled peptide (white bars, n= 2) was abnormally large and significantly different from $\Delta C_{m\,1}$ seen in terminals dialyzed with the SNAP 25 peptide (black bars , n= 4). An activity-dependent inhibition in the magnitude of $\Delta C_{m\,1}$ is also seen with multiple trains (decreased $\Delta C_{m\,1}$ in train 2,3) in terminals dialyzed with SNAP 25 compared to the scrambled peptide. **Bottom left and right:** Mean calcium influx in response to the first pulse (I_{ca1}) and the average of the last 5 pulses ($I_{ca\,total}$) suggest that the difference in the capacitance response between the SNAP peptide and the scrambled peptide was not due to a decreased calcium influx.

We noted that the mean calcium currents in terminals dialyzed with the syntaxin peptide was smaller and close to being significantly different from those dialyzed with the scrambled peptide in our pulse train experiments. This suggests that the syntaxin 3B peptide may have a mild inhibitory effect on the calcium channel. To study the effect of the magnitude of capacitance change on the calcium influx we plotted the capacitance response, ΔC_{m1} versus the calcium current I_{ca1} in response to the first 20 ms depolarization the train pulse. Fig 4.14 shows that irrespective of which internal solution was dialyzed , terminals which had a larger I_{ca} also had a larger $\Delta C_{m..}$ This is consistent with the idea that a larger calcium current would allow influx of more calcium and therefore result in fusion of more vesicles. However it is possible that increasing the number of experiments (n) may reveal a more specific effect of syntaxin 3B on the calcium current.
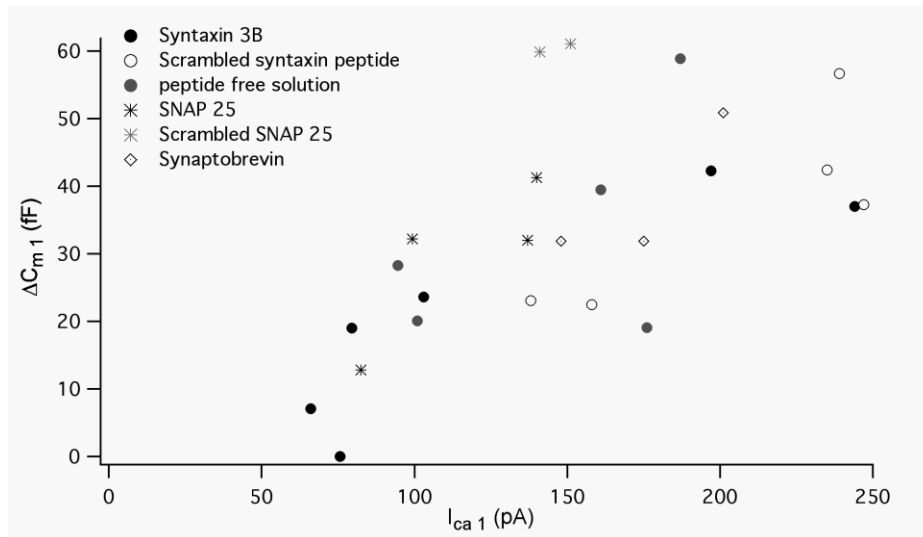
Figure 4.14 Larger Calcium currents were associated with a larger initial capacitance change (ΔC_{m1}): Irrespective of the internal solution dialyzed into the terminal, those which had larger calcium current (I_{ca1}) also had a larger initial exocytosis response (ΔC_{m1}).

DISCUSSION

The results show 1) a syntaxin3B peptide is able to perturb SNARE complex formation in dissociated neurons. 2)The syntaxin peptide initially blocks the fusion of the exocytotic component attributed to the recruitment of reserve pool vesicles while leaving vesicles in the rapid and releasable pools intact. 3) With multiple stimulations, the syntaxin 3B peptide blocks refilling of both the rapid and releasable pool. 4) A SNAP 25 peptide blocks recruitment of the reserve pool vesicles leaving the rapid and releasable pools intact. 5)A Synaptobrevin peptide does not block fusion from any vesicle pool.

1. A syntaxin3B peptide is able to perturb SNARE complex formation in-vivo

Results from fig 4.2 show that the syntaxin 3B decreases the amount of SNARE complex in a retinal extract, as detectable by a syntaxin 3 antibody. Since the peptide is based on the N-terminal part of the SNARE domain it is likely that it competes with the endogenous syntaxin in the formation of SNARE complexes. The decreased amount (compared to controls) of SNARE complex detectable is possibly the complexes that were already formed. Therefore, a reasonable interpretation is that the syntaxin peptide inhibits formations of new SNARE complexes but does not disrupt already formed complexes. Previous in-vivo studies have shown that SNARE complexes formation in the presence of a competing SNARE domain peptide are decreased or more unstable (255, 256).

2. Syntaxin 3 B blocks the component of release attributed to the reserve pool

Fig 4.4 shows that in response to the train pulse, syntaxin 3B inhibits the recruitment of the reserve pool vesicles as measured by loss of the release component attributed to fusion of reserve vesicles. The syntaxin 3B peptide might block recruitment either via 1) blocking formation of new SNARE complexes, thus blocking fusion ability of the reserve

vesicles, 2) via decreased calcium influx, thus blocking exocytosis drive, or 3) inhibition of translocation of vesicles to ribbon style active zones. We can rule out any differences in calcium buffering as we used the same base solution to make up the syntaxin 3B and the scrambled peptide containing internal solution and have monitored for possible changes in pH upon peptide addition that might additionally affect calcium buffering. The possible role of syntaxin on the calcium current is discussed in detail, later in this section.

Our results show that in the presence of the syntaxin peptide these reserve vesicles are unable to refill the releasable pool as detected by capacitance measurements. EM micrographs of Mb1 terminals show more than 400,000 vesicles in the cytoplasm considered to be the reserve pool which can refill the releasable pool. Recruitment of these reserve vesicles may be blocked either by blocking the actual translocation of the vesicle to the ribbon style active zone or block of actual fusion of vesicles. The molecular mechanisms underlying the translocation of the reserve vesicles to ribbon sites is not known. In experiments where ATPγS was dialyzed into the terminal, EM studies show that even after a confirmation of block of refilling of the releasable pool from capacitance measurements, synaptic ribbons were populated with tethered vesicles no different from control experiments (80). Based on the known function of the syntaxin protein in fusion, it is more likely that the syntaxin peptide affects the fusion of the reserve vesicles which may be recruited to the ribbon style active zones rather than translocation of vesicles. However experiments where terminals are dialyzed with the syntaxin peptide and then stimulated followed by a quick fixation technique and EM analysis would be required to answer this question.

Taking into consideration results from fig 4.2 it is likely that the syntaxin peptide effects exocytosis by competing with the endogenous syntaxin protein in the formation of SNARE complexes. Based on this, our results suggests that vesicles that are in the reserve pool must form new SNARE complexes before they can be functionally recruited into the releasable pool and fuse. To estimate the rate of recruitment which is dependent on SNARE complex formation we subtracted the mean cumulative ΔC_m over time as seen in the presence of the syntaxin 3B peptide from the mean cumulative ΔC_m over time as seen in response to the scrambled peptide. The result is shown in fig 4.15 below. The syntaxin sensitive component was fit with a straight line. For the syntaxin sensitive component, data for the first 2 s was not a good fit suggesting a non linear rate of recruitment in the first 2 seconds. The slope of the linear component was 18.7 fF/s (or ~628 vesicles /s). This rate is almost twice the rate of recruitment that is mediated by the ATP dependent priming step (~366 vesicles/s from fig 3.5) . Considering results from this section, results from fig 3.5 and previous published work (80, 81), we suggest that along with other possible steps, reserve vesicles must undergo ATP-priming and from new SNARE complexes to attain fusion-competence/ be recruited to the releasable pool of vesicles. However based on the slower rate (slope) of the ATP sensitive component compared to the syntaxin3B sensitive component, I suggest that for reserve vesicles, the recruitment step dependent on ATP-priming is slower than the recruitment step dependent on Syntaxin 3B dependent SNARE complex formation. This implies that the ATP priming step may be a series of molecular steps while the SNARE complex formation may be a quicker single biochemical step. Inability to fit the syntaxin sensitive component with a single line at time < 2s also suggests

that formation of new SNARE complexes may be a delayed till a certain number of SNARE complexed-vesicles have already fused.
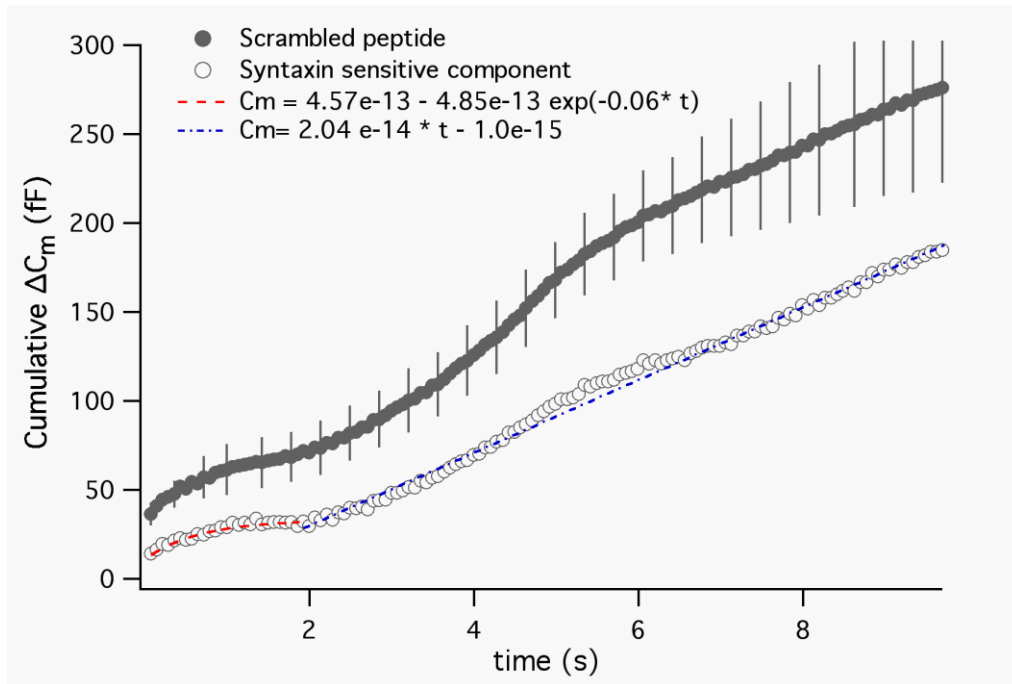
fig 4.15 The syntaxin 3B sensitive component
The component of release requiring SNARE complex formations and thus sensitive to the syntaxin 3B peptide (Scrambled peptide train- Syntaxin peptide train from fig 4.4) is plotted (open circles) along with the original response to the train pulse seen in terminals dialyzed with scrambled peptide. The syntaxin sensitive component was fit with a line function after the first 2 s (blue dashed line, slope = $2.04e^{-14}$, y-intercept = $-1.0e^{-15}$).

3. **The fusion of vesicles of the rapid and releasable pool are resistant to the syntaxin 3B peptide**

Results from fig 4.4-4.6 show that the dialysis of the syntaxin 3B peptide does not initially block the component of release attributed to the rapid and releasable pool. The rapid and releasable pools are preserved whether the terminal is probed after 1 min of

dialysis of the peptide or after 3 minutes of dialysis (fig 4.10). This suggests that irrespective of dialysis time fusion of reserve pool vesicles are blocked in the presence of the syntaxin 3B peptide. A longer dialysis time does not change the effect of the syntaxin peptide on the rapid and releasable pools, but rather activity dependent turnover is required to inhibit fusion of vesicles from the releasable and rapid pools.

The in-vivo experiment suggests that only those vesicles that are in SNARE complex are resistant to the syntaxin peptide. Our finding suggests that not only the rapid pool but also the releasable pool is associated with SNARE complexes. Results from chapter 3 suggest that the rapid pool is a subset and draws its vesicles from the releasable pool. Thus one interpretation is the following: The releasable pool of vesicles is associated with SNARE complexes. The traditional SNARE complex is formed between Synaptobrevin on the vesicles and SNAP25 and syntaxin on the plasma membrane. The releasable pool of vesicles contains vesicles that are both docked and tethered to the ribbon and also tethered at higher rows on the ribbon and therefore not docked at the plasma membrane. This raises two questions. 1)How might the releasable pool vesicles form SNARE complexes and 2) how might the releasable pool vesicles fuse with the plasma membrane?

In response to the first question of how might the releasable pool vesicles form SNARE complexes, one possibility may be a limited number of vesicle-occupied docking and fusion sites. The ribbon style active zones may consist of a number of docking sites which are already occupied by vesicles. The syntaxin peptide may form non-functional SNARE complexes at all fusion sites except for those already occupied by a vesicle associated with a functional SNARE complex. In support of this hypothesis most of the syntaxin 3 B seems to be at the plasma membrane from analysis of images of

immunostaining of a single Mb1 cell (151). The number of fusion sites must at least be ~1100; the number of the rapid pool vesicles; since these vesicles can fuse with kinetics that are limited by the opening of the calcium channels (72). However, for the releasable pool of vesicles to be associated with SNARE complexes , the entire pool of releasable vesicles must occupy fusion sites. This would suggest that the number of occupied fusion sites is ~ 5500, to match the number of the releasable pool vesicles. A possible location for these sites may be along the flank/ side of the ribbon (an area of~$150 * 350 \ \mu m^{2}$, on each side of the ribbon (75)). In support of this idea in rod spherules EM micrographs showed that after a couple of minutes of exposure to darkness there was an increase in fused synaptic vesicles not only at the base of the ribbon but all along the sides of the ribbon (257). However in another study, EM micrographs of lizard cones showed a 3.7 fold decrease in vesicles at the base of the ribbon between dark adapted and light adapted cones. This suggests that vesicles fuse at the base of the ribbon (258). EM micrographs of bipolar cells suggest that the flank of the ribbon is not near the plasma membrane (96, 124, 145) and dynamic changes in the structure of the ribbon-style active zone of the bipolar cells, where the plasma membrane invaginates at the ribbon during prolong stimulations have yet to be shown. Therefore a large number of fusion sites supporting the fusion of the releasable pool seems an unlikely possibility.

A second possible explanation is that these vesicles may have both v and t SNAREs on them. In support of this idea previous studies from conventional synapses have reported the presence of t-SNAREs on vesicles, a possible result of improper sorting (259, 260). Protein stoichiometry of synaptic vesicles show that there are 69.8 copies of Synaptobrevin, 6.2 copies of syntaxin and 1.8 copies of SNAP 25 on each vesicle (261). A recent study has

suggested that only two SNARE complexes maybe sufficient for vesicle fusion (262). Therefore if the protein stoichiometry of vesicles in the bipolar terminal is similar to that of conventional neurons SNARE proteins of two adjacent vesicles may be complexed.. It may also be possible that the SNARE proteins on the vesicles may also participate in the formation of homotypic SNARE complexes. If the releasable pool vesicles do indeed form SNARE complexes, the ribbon may help by tethering vesicles and bringing the vesicles membrane attached proteins in close to each other. The proteins forming the ribbon organelle do not seem to participate in SNARE complex formation as SNARE proteins seem to be entirely absent from the structure of the synaptic ribbon (263). The close proximity of the vesicles on the ribbon may also aid in providing steric hindrance to the syntaxin peptide in competing with the endogenous SNARE protein on the vesicle membrane.

In response to the second question of how the releasable pool vesicles, which according to our ATP□S results are tethered up the ribbon, fuse one possible explanation may be via compound exocytosis. In compound exocytosis vesicles fuse with each other piggy backing onto a docked vesicle which fuses with the plasma-membrane, thus sharing a fusion site. Membrane capacitance measurements cannot differentiate between compound exocytosis and the separate sequential fusion of the same number of vesicles at different fusion sites in neurons. Single synaptic vesicle (30nm diameter size) fusion events cannot be resolved, using whole cell recording in neurons as is possible in mast cells where the size of granules are larger. Compound exocytosis has been suggested to occur in Mb1neurons (54, 96) and at other ribbon synapses (131). Also compound exocytosis is more likely to be seen in response to strong depolarizations (96) as given by our pulse trains. Compound exocytosis would require vesicles to fuse to each other via SNARE complexes.

Another possibility is that the releasable pool of vesicles are all docked at the plasma membrane and therefore can fuse in spite of the syntaxin peptide. This would be possible if the releasable pool was formed of vesicles at the base of the ribbon and at sites away from the ribbon. Co-relation between EM reconstructions and physiology data and recent experiments where disruption of the ribbon leads to loss of the fast and sustained components (87, 131, 132, 156) and our results from chapter 3 disagree with this hypothesis.

In summary, an attractive model which may accounts for our data is that the releasable pool is resistant to the syntaxin peptide because the releasable pool vesicles are able to form SNARE complexes with each other and fuse via compound exocytosis. Limited fusion sites for ~1100 vesicles (~ 22 at the base of each ribbon) may also force the releasable pool to fuse via compound exocytosis.

4. Refilling of the rapid and releasable pool is inhibited by the Syntaxin3B peptide

Results from fig 4.7- 4.9 show that refilling of both the rapid and releasable are inhibited in the presence of the synatxin3B peptide. The syntaxin peptide could affect refilling of the pools either via a block of endocytosis or by blocking SNARE complex formation required to refill the vesicle pool.

During the pulse train the spatially averaged intra-terminal calcium exceeded 1μM (based on ratiometric calcium measurements using 0.1mM bis-fura , chapter 3). In several nerve terminals including the goldfish bipolar cell terminals, endocytosis is inhibited by the high intra cellular calcium levels such as those that are achieved during pulse trains (73, 209, 216, 221, 222). Therefore the net changes in capacitance during the pulse trains are most likely due to exocytosis alone. After the cessation of the pulse train, endocytosis was seen.

We fitted the time course of this endocytosis with a double exponential function which revealed the following averages (only the response after the first train was used, not all responses could be fit with a double exponential function): Scrambled peptide - $\tau_{fast} = 3.33s$ in 5/5terminals, $\tau_{slow} = 54.4s$ in 5/5 terminals, Syntaxin peptide - $\tau_{fast} = 2.6s$ in 5/5 terminals, $\tau_{slow} = 47.4s$ in 4/5 terminals. The time courses of endocytosis were not significantly different between the two groups. These findings suggest that the effect of the peptides on exocytosis and refilling were not likely due to an effect on the endocytosis that is seen after the cessation of the pulse train.

5. A SNAP 25 peptide block recruitment of the reserve pool vesicles while leaving the rapid and releasable pools intact

Results from fig 4.12 and 4.13suggest that the SNAP 25 peptide has a similar effect to that seen with the syntaxin peptide. The recruitment of the reserve pool is blocked but the rapid pool and releasable pool are left intact. We used a peptide based on the C-terminal of the SNARE domain. Previous studies have showed that peptides which mimic the C-terminal of SNAP 25 and span the cleavage site or are released by cleavage by Botulinum A /E, block neurotransmission in chromaffin cells and *Aplysia* (264, 265). The scrambled SNAP 25 peptide had an anomalous effect where the magnitude of exocytotic seen in response to the first pulse of the train was larger compared to that seen with the SNAP peptide and also compared to ATP controls . This could be due to the small number (n= 2) in this experiment set.

6. A Synaptobrevin peptide does not block exocytosis in retinal ribbon synapse

In our experiment an peptide based on the N-terminal of Synaptobrevin did not have any inhibitory effect. This could be due to 1) A large number of vesicles are present in the

Mb1 cytoplasm (~600,000). and protein stoichiometry show that there are 69.8 copies of Synaptobrevin on each vesicle (261). It is possible that a higher concentration of the Synaptobrevin peptide is required to out compete the high concentration of endogenous Synaptobrevin. 2) It is possible that the Synaptobrevin peptide did not load into the terminal. The Synaptobrevin peptide was not fluorescently tagged, therefore we could not monitor its loading in real time. 3) Previous studies have shown that Synaptobrevin homologue cellubrevin/VAMP3 or endobrevin/ VAMP 8 can form functional SNARE complexes and drive exocytosis (266–269). Whether these proteins can form functional SNARE complexes in the Mb 1 neuron is not known. If these proteins are able to substitute the role of Synaptobrevin in exocytosis from Mb1 neurons, a higher concentration of a peptide based on a conserved sequence between the Synaptobrevin homologues may be required to block exocytosis.

7. Effect of syntaxin on Calcium current

In our experiments we noticed a trend where the calcium currents were smaller in terminals dialyzed with the syntaxin peptide compared to the scrambled peptide in experiments in which the terminals were stimulated with the pulse train. However, we did not observe this effect with a single 1s depolarization. In conventional synapses syntaxin 1A has been shown to interact with the calcium channels. An inhibitory effect of syntaxin1 via the stabilization of calcium channel inactivation has been shown in experiments using rat cortical synaptosomes. Syntaxin was cleaved using botulinum toxin and synaptosomes were depolarized with high K+ solutions. The cleavage of syntaxin did not affect the initial calcium influx but decreased the late calcium influx. Cleavage of Synaptobrevin or SNAP 25 by botulinum toxin did not have an effect on calcium influx (270). In *Xenopus* oocyte

co-expression of syntaxin 1A and the N type calcium channel decreased the calcium influx by stabilizing calcium channel inactivation. A similar result was seen with syntaxin 1A and the Q type calcium channel but not with the presumably neuronal L type calcium channel (271). However, in another study using the *Xenopus* oocyte Syntaxin1A was shown to inhibit calcium influx via the $Ca_v 1.2$ L type channel and this inhibitory effect was regulated via two cysteine residues in the transmembrane domain of syntaxin (272–274). In pancreatic beta cell syntaxin 1 has been shown to regulate calcium influx via the α_{1D} subunit L type calcium channel (275). The inhibitory effect of syntaxin on the N type calcium channels was greater when trains of action potential like stimuli were used compared to steady depolarizations (276). This might explain the decreased I_{ca} in response to train pulses but not to single 1s pulses in our experiments.

Retinal ribbon synapses express syntaxin 3 and L-type calcium channels, $Ca_v 1.3$ and $Ca_v 1.4$ (132, 277). In retinal ribbon synapses it is not known if syntaxin 3B modulates calcium entry via $Ca_v 1.3$ or $Ca_v 1.4$ L type calcium channels. In support of the idea that syntaxin 3 may regulate calcium influx via L type calcium channels, in pancreatic islet bet cell lines over expression of syntaxin 3 inhibited the L-type calcium channels current (254). Based on these finding it would be interesting to determine if in retinal ribbon synapses syntaxin 3 B interacts with the $Ca_v 1.3$ and $Ca_v 1.4$ L type calcium channels .

In conventional synapse the carboxy transmembrane domain of Syntaxin1A is thought to be the "calcium effector domain" (274, 278). The deletion of the carboxy terminal transmembrane domain of syntaxin 1A abolished its effect of the calcium channels (271). In our experiments we used a syntaxin 3B peptide based on the N -terminal SNARE domain. If, similar to conventional synapses, syntaxin 3B does interact with the calcium channel, it

may be via the transmembrane domain and not the SNARE domain. This could explain why we do not see a stronger inhibition of the calcium current. It is possible that a short peptide is able to disrupt the formation of the SNARE complex but not the interaction of the native syntaxin 3B with the calcium channel.

It has been suggested that the SNARE complex proteins, synaptotagmin and the calcium channels form an "excitosome" that is required for evoked neurotransmitter release (279, 280). Therefore another possibility is that the syntaxin peptide's effect on disrupting the SNARE complex could have an effect on the calcium current. In pancreatic beta cells it has been shown that introduction of a peptide based on the cytosolic portion of the L type channel competes with the endogenous channel for binding with SNARE complexes and decreases depolarization evoked exocytosis (279). More experiments would be required to ascertain if in retinal ribbon synapses the Ca_v 1.3 and Ca_v 1.4 L type calcium channels are regulated via an interaction with the SNARE complex.

CHAPTER V

CONCLUSION AND FUTURE DIRECTIONS

Mechanisms underlying how ribbon synapses sustain neurotransmission is an active field of study. Two recent questions which have been debated in the field are whether the ribbon style active zones are the major site of active transmission and the role of neuronal SNARE proteins in exocytosis at ribbon synapses (82, 83, 131, 158). In the goldfish Mb1 bipolar neuron, which has served as a model for a ribbon synapse forming neuron in the retina, three components of exocytosis have been reported. The three components of release have been to attributed to three vesicle pools- a docked and ribbon tethered rapid pool , a fusion-competent, ATP primed, releasable pool and a cytoplasmic reserve pool answer. Taking advantage of the large size of the Mb1 bipolar neuron I was able to patch clamp single bipolar cell terminals and study fusion of population of vesicles as measured by changes in membrane capacitance. We sought to answer key questions underlying neurotransmission in ribbon synapses - specifically 1) whether the synaptic vesicles pools operated in a serial manner as opposed to a parallel manner and 2) which vesicle pool was associated with SNARE complexes and therefore available for immediate fast release.

1. The vesicles pools fuse in a serial manner at the ribbon style active zones

In chapter 3 we tested the hypothesis of whether the rapid pool was a subset of the releasable pool. Using ATPγS to block functional pool refilling of the releasable pool we found that depletion of rapid pool cross depletes the releasable pool and vice versa. This suggests that the rapid pool draws its vesicles from the releasable pool. In other words, a cohort of ATP primed vesicles can refill the rapid pool vesicles (docked and primed vesicles at the plasma membrane). In conventional neurons priming is thought to occur after docking

(18). In hippocampal boutons (108) and in cerebellar climbing fibers (240) not all docked vesicles can be rapidly released, suggesting that all docked vesicles may not be primed. Our results suggest that in contrast to active zones of conventional synapses, at ribbon-style active zones priming steps that require ATP hydrolysis occur before a vesicle docks to the plasma membrane (at the base of the ribbon).

In the bipolar neuron, the rapid and releasable pools are the correlates of two release components which differ in their kinetics and sensitivity to calcium buffers (72, 123, 208). This seems to be a common feature to ribbon synapses. In the cone photoreceptors, a fast component of release which is resistant to 10mM EGTA has been identified in retinal slice preparations (181). A larger, EGTA-sensitive releasable pool in cones has been identified using capacitance measurements (281). Analysis of release kinetics in hair cells in the auditory pathway have suggested at least two population of vesicles which are differentially sensitive to calcium buffers (282, 283). In the bipolar neuron it has been proposed that the two populations of vesicles are located at varying distances from the calcium channel. The base of the ribbon has been suggested to be the site of calcium entry, and the ribbons co-localize with calcium channels (85, 284). However, whether the releasable pool vesicles are located at a distance from the calcium channel by being tethered at higher rows on the ribbon or by being close to the plasma membrane but at sites away from the ribbon is not known. Midorikawa et al., 2007 have suggested that in bipolar neurons, a large portion of synaptic release may in fact occur at sites away from the ribbon. However Zenisek 2008 suggests that while vesicle fusion does occur at non-ribbon associated sites, it is rare. Therefore whether the releasable pool is ribbon tethered is an unresolved question. Calcium entry sites have been shown to be at the base of the ribbon (85, 284). We used multiple

short depolarizations which would cause fusion of only those vesicles that are near the calcium channels, and therefore ribbons, to seek the location of fusion of the vesicle pools.. In our results we find that when the refilling of the releasable pool has been blocked, several, short depolarizations deplete both the rapid and the releasable pools (fig 5.1). Therefore we suggest that both the rapid and releasable pool undergo fusion at the ribbon style active zone with the bottommost row forming the rapid pool and the ribbon tethered pool forming the releasable pool. We cannot exclude the possibility of some exocytosis at sites away from the ribbon. An upper estimate of this cohort of vesicles, as suggested by experiments, may be 14.1 ± 3.3 fF or 542 ± 126 vesicles.

Legend:
- Primed and docked vesicles -rapid pool (green)
- ATP primed vesicles -releasable pool (yellow)
- Reserve vesicles (red)
- 20 ms depolariztion step
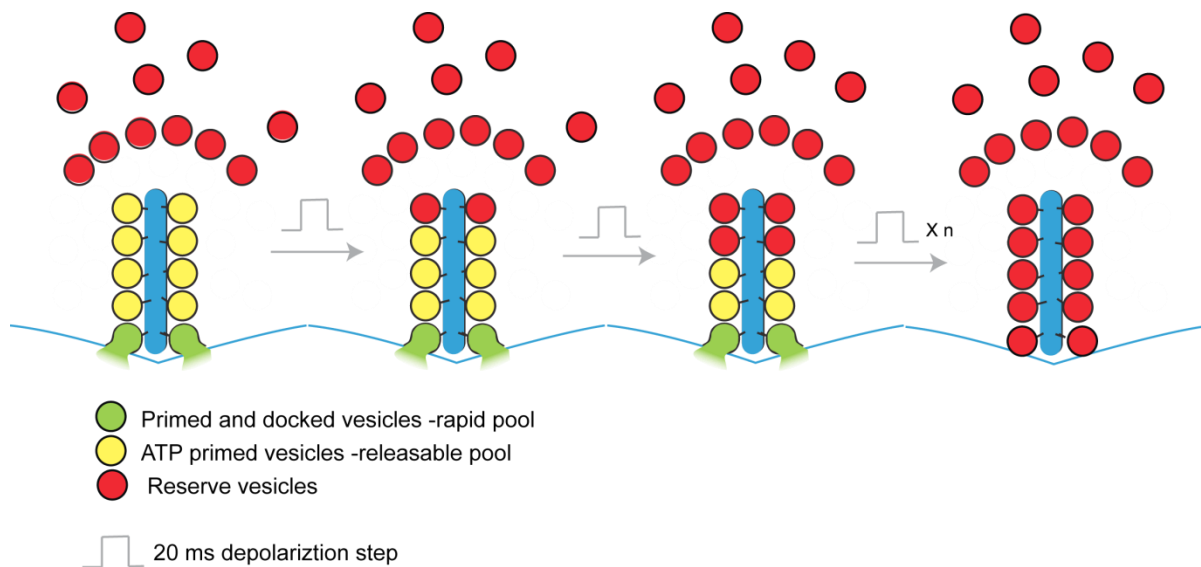
Fig 5.1 The rapid and releasable pool are ribbon tethered: In experiment 4 from chapter 3 functional refilling of the releasable pool was blocked by ATPγS. Multiple 20 ms pulses, each sufficient to deplete the rapid pool also depleted the releasable pool. This suggests an scenario where each 20 ms pulse results in fusion of the bottom most row of vesicles. After each 20 ms depolarization the ribbon may be refilled physically with vesicles (80), but these vesicles are not ATP-primed (in the absence of ATP-hydrolysis) and therefore are not fusion-competent.

An alternate possibility to the vesicles pools being located at different distances from calcium channels is two populations associated with two calcium sensors (51, 285, 286). For example the rapid pool vesicles could be associated with a high-affinity calcium sensor and therefore undergo release in response to short depolarizations, whereas the releasable pool vesicles could be associated with a low-affinity calcium sensor which requires higher levels of calcium, as would be seen with longer depolarizations. However, when exocytosis is evoked by instantaneously elevating global calcium with flash photolysis of caged calcium, the rise in capacitance can be fit with a single exponential functions suggesting a homogenous class of vesicles (54). Such a homogenous class of vesicles argues against the two-sensor hypothesis. Studies to identify the calcium sensor suggest synaptotagmin 3 as a potential candidate. Synaptotagmin 3 is expressed in the PKC labeled goldfish bipolar neurons (287). Experiments where exocytosis was monitored using FM 1-43 dyes suggest that fusion in bipolar neurons can be induced by 1-2 μM calcium (288) and synaptotagmin 3 has a higher calcium affinity and can bind to syntaxin at these concentration (289). Immunolabelling with synaptotagmin1/2 antibodies show a lack of staining in goldfish bipolar neurons (290)

In summary results from chapter 3 show that in the bipolar neuron, the correlation between estimates of pool sizes of the rapid and releasable pool from the capacitance measurements and ultra structural analysis of ribbon -tethered vesicles is not just co-incidental. Similar to the bipolar cells, studies in photoreceptors have also shown discrete vesicle pools where a good correlation exists between the capacitance measurements or post-synaptic currents and EM level estimates of ribbon-tethered vesicles (74, 142). In hair cells of several species (frog saccular hair cell, chick cochlear hair cell, turtle hair cell and

mouse inner hair cell) there seems to be a good correlation between the docked and ribbon-tethered vesicles and the first component of exocytosis or the physiological rapid pool (130, 173). However the correlate for the releasable pool is not so clear. For example in the chick cochlear hair cell ribbon synapse the releasable pool composed of ~ 8000 vesicles which is 10 times the number of vesicles tethered to the ribbon (291). This suggests that in the cochlear hair cells the releasable pool may include vesicles on the ribbon, several rounds of rapid refilling from reserve vesicles or additional release at extra-ribbon sites (282, 291). Therefore retinal ribbon synapses may differ from some hair cell synapses in their functional organization of vesicle pools.

2. Vesicles at retinal ribbon synapses undergo SNARE-mediated exocytosis

Our findings suggest that a short peptide based on the SNARE binding domain of either syntaxin 3B or SNAP 25 are able to inhibit fusion of reserve pool vesicles and block fusion of the releasable and rapid pool of vesicles in an activity-dependent manner, at retinal ribbon synapses. Our finding are in contrast to a report that suggests that in hair cells exocytosis does not require neuronal SNAREs (158). As suggested by the authors of the hair cell study, it is possible that the ribbon synapses of the auditory system differ from those in the retina as indicated by their different germ line origin (retinal ribbon synapses being neuronal in origin versus hair cells being epithelial). Retinal ribbon synapses seem more like conventional synapses in their requirement of neuronal SNAREs for exocytosis. However other possibilities also exist. In their experiments Nouvian et al., 2011, treated hair cells with Botulinum toxins for 10 minutes. Exocytosis was then elicited using repetitive depolarizations within a time scale of 10 to 30 minutes. They did not find any significant

difference between cells treated with the toxin versus controls after the first pulse.

Exocytosis in response to subsequent pulses decreased in both control and toxin treated cells (possibly due to rundown). It is possible that a longer incubation time of more that 30minutes may be required for the action of the toxin. In their supplementary data they show loading of the cells with the toxins. However it appears that after 30 minutes (the last time point tested), the concentration of the toxins tested do not reach steady state levels inside the cell. After 30 minutes, loading of none of the toxins tested were near completion or even tending to plateau. The absence of an effect on exocytosis could be due to the lack of required amounts of toxin inside the cell. The authors suggest that similar time points and concentrations of toxins were sufficient to block exocytosis in chromaffin cells. However ribbon synapses have greater number of vesicles and thus would require a larger concentrations of toxin to block exocytosis. For definitive proof that exocytosis in hair cells are not affected by Botulinum toxins, the authors should either for wait until loading of the toxin is complete (1st pulse given at time after 30minutes) and/or dialyze with a larger concentration of toxin. In fact the electrophysiological results shown in Nouvian et al., 2011 can be interpreted in another way. The total amount of exocytosis (i.e. the total membrane added in all the pulses) in cells treated with the Botulinum toxin is ~ 240 fF. If one assumes that the rapid/releasable pool of vesicles and other non ribbon associated but docked (extra-ribbon component) are associated with complexed SNAREs and therefore resistant to the Botulinum toxin, 240 fF might be the size of the vesicle pool associated with SNARE complexes. This interpretation would agree with results presented in this thesis. However significant rundown of exocytosis in both controls and cells treated with Botulinum toxin also make their data somewhat difficult to interpret. Beutner et al., 2001 has shown that

rapid elevations in $[Ca^{2+}]_i$ above 8 µM (using flash photolysis) results in a biphasic capacitance increase corresponding to the fusion of approximately 40,000 vesicles. It would be interesting to know the number of vesicles capable of fusion in the presence of Botulinum toxin using similar calcium uncaging techniques. An ideal experiment would be to allow for more than 30 minutes of incubation with the Botulinum toxin followed by elicitation of exocytosis via uncaging of calcium by flash photolysis. If synaptic vesicles of hair cells truly undergo SNARE-independent exocytosis, calcium uncaging would result in fusion of vesicles similar to controls. However, if comparable to our data a population of vesicles are associated with complexed SNAREs (thus protected from cleavage by the toxin), the exocytotic response post-flash may be decreased compared to controls. It would be interesting if the size of the vesicle pool protected from the toxin in flash experiments were ~ 240fF.

3. Vesicles in the reserve pool must form new SNARE complexes before they join the releasable pool

In response to the train stimulus, the total magnitude of exocytosis at the end of the train suggests recruitment of reserve vesicles in addition to fusion of the releasable pool of vesicles. It is unlikely that during the train newly endocytosed vesicles refill the releasable pool as 1) the 50ms IPI between each depolarization in the train is too short for endocytosis . The time constant for even the fast mode of endocytosis is 1-2 s (161, 223, 292). 2) Strong stimuli which cause increase in intracellular calcium delay the onset of endocytosis (73, 209, 212). Specifically, the intra-terminal spatially averaged calcium was elevated to more than 500 nM by the 20th pulse (1.43s) during the train pulse , a value above which endocytosis has been shown to be inhibited (209). This suggests that after the first 1.4 s of

the pulse train the change in membrane capacitance is most likely due to exocytosis alone.

In the presence of a SNARE protein competing peptide (syntaxin or SNAP 25), the total magnitude of exocytosis at the end of the train suggests that the recruitment of reserve vesicles and their subsequent fusion is blocked. This suggests that the reserve vesicles are not associated with SNARE complexes and must form new SNARE complexes to fuse (fig 5.2). Whether the SNARE peptides also blocks the actual physical translocation of reserve vesicles onto the ribbon cannot be said with certainty. However the role of SNAREs in fusion (6, 25) rather than translocation of vesicles suggests that the SNARE peptides block fusion of the reserve vesicles. SNARE proteins help to prime vesicles and Syntaxin is important for docking of vesicles (18, 19). This raises the question as to whether the ribbon functions as a site of SNARE complex formation. However SNARE proteins have been not isolated to be a associated with the synaptic ribbon (263).

4. The releasable pool of vesicles is associated with pre formed SNARE complexes

Using a SNARE-competing peptide as a tool we asked which vesicle pool was associated with SNARE complexes? Considering the classical view that a SNARE complex is formed between the v-SNARE on the vesicle and t-SNAREs on the plasma membrane, we had hypothesized that only the rapid/docked pool, which is closest to the membrane, would be resistant to the syntaxin 3B peptide. However, contrary to our hypothesis we find that the releasable and rapid pools are both initially resistant to the inhibitory peptide (fig 4.4). This suggests that the releasable and rapid pools are associated with SNARE complexes (fig 5.2), or are otherwise resistant to the effects of the peptide. Our results also showed that while initial fusion of the rapid and releasable pool was intact, subsequent fusion, which would

require refilling of the pools, was blocked. By the second pulse train the depression of the exocytotic response attributed to the rapid and releasable pools was significantly depressed (fig 4.7, 4.9). This suggests that refilling of vesicle pools required formation of new SNARE complexes

By 2 minutes the inhibitory effect of the Syntaxin 3B peptide on the rapid and releasable pool was measurable. To ascertain that the effect of the Syntaxin3B peptide on the rapid and releasable pool vesicles required activity-dependent vesicle turnover rather than a longer dialysis time, we repeated the experiments such that the first pulse train was given after 3 minutes of peptide dialysis. The results showed that in terminals dialyzed with the Syntaxin 3B peptide, when the first train was given after 3 minutes of dialysis the rapid and releasable pools were intact. The magnitude and shape of the exocytotic components seen in response to the pulse train was similar irrespective of whether the terminals were stimulated at 1 min or 3 minutes after initiation of dialysis. This further confirmed that the releasable and rapid pool vesicles but not the vesicle of the reserve pool are initially resistant to the SNARE peptide.

Vesicles sensitive to a SNARE complex inhibiting peptide.
Must assemble new SNARE complexes before they can fuse

Vesicles resistant to a SNARE complex-inhibiting peptide, likely to be in preformed complexes.

🟢 Primed and docked vesicles -rapid pool
🟡 ATP primed vesicles -releasable pool
🔴 Reserve vesicles
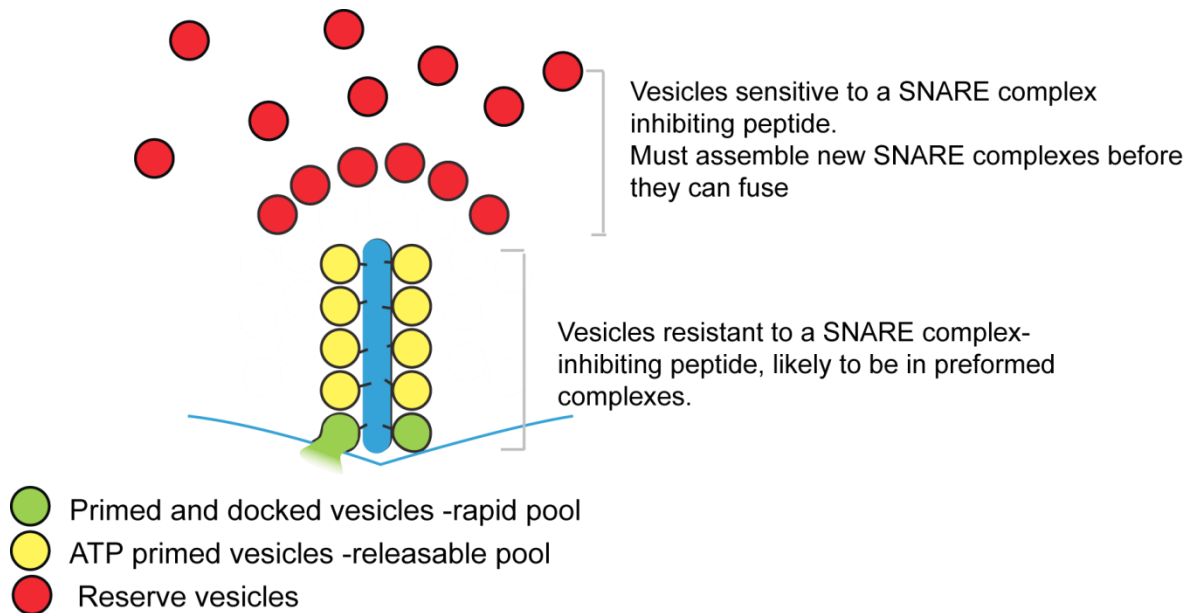
Fig 5.2 Vesicle pools associated with SNARE complexes at the bipolar neuron

5. Different fusion scenarios at the retinal ribbon synapse

Multiple models of vesicle fusion have been proposed in the retinal bipolar cells (131, 132) These include 1) progressive fusion where vesicles along the ribbon fuse one after the other These vesicles do not share the same fusion site at the same time. Higher rows of vesicles refill the lower rows. 2) Multivesicular fusion which may be synchronized - where there is synchronous fusion of multiple docked vesicles or compound fusion- where vesicles piggy-back onto each other with only the docked vesicle fusing with the plasma membrane. In compound fusion multiple vesicles share a single fusion site at the plasma membrane. In chapter 3 we show an experiment where multiple short depolarizations leads to depletion of a larger pool. In this case it is likely that the vesicles undergo the progressive mode of fusion (as seen in fig 5.1). However we also show evidence where vesicles located distally from the plasma membrane are able to undergo exocytosis that I interpret as not

needing to form new SNARE complexes. This is a possible example of the compound mode of fusion. Therefore retinal ribbon synapses might be able to undergo various modes of exocytosis.

While our study suggests a possible mechanism underlying compound fusion, the identity of specific proteins regulating this process remains unknown. Interestingly, syntaxin 3, the SNARE isoform found in retinal ribbon synapses is also found in mast cells and pancreatic acinar cells, both of which are known to undergo compound fusion (293–296).

Future Directions

Several studies have suggested the presence of t-SNAREs on vesicles (96, 259). However this has not been shown in ribbon synapses at the EM level. While compound exocytosis has been suggested to be present in the bipolar cell from EM micrographs (96), and from experiments where the fusion of a large population of vesicles in response to global elevation of calcium could be fit with a single exponential function (54). It would be interesting to see if SNARE complexes formed between vesicles could be localized by using techniques such as immunogold labeling. The synaptic ribbon is easily recognizable in EM sections as it is electron dense. The size of a vesicle is ~ 30nm and they are held at 25nm from the ribbon by tethers. Clustering of nano gold particles (10-5nm size) tagged with SNARE complex antibodies around the ribbon may suggest presence of SNARE complexes between vesicles at the ribbon. The ribbon itself may not take part in SNARE complex formation as SNARE proteins have been found absent from the ribbon complex (263).

Calcium is known to aid in pool refilling in bipolar cells (84, 208). In this thesis, terminals stimulated with the train pulse, under control conditions, show recruitment of vesicles from the reserve pool. Similar recruitment of reserve pool vesicles was not seen

with a 1 s pulse. Major differences between the train paradigm and a single 1 s depolarization include duration of depolarization and also the amount of calcium influx. The calcium influx in response to the train pulse is higher than with a 1 s depolarization (Spatially averaged $[Ca]i > 1\mu M$ during the train pulse compared to 538 ± 117 nM in response to a 1 s depolarization). The molecular mechanism underlying calcium mediated pool refilling is not known. In conventional neurons such as the calyx of Held, Calmodulin and Cam kinases may be involved in the calcium mediated pool refilling (112, 116). Calmodulin has been shown to be present in bipolar neurons (297). It would interesting to see whether Calmodulin and/or Cam kinase had an effect on the fusion and/or refilling of the vesicle pools in ribbon synapses. Calmodulin competing peptides and specific blockers of Cam kinases are commercially available. These compound could be dialyzed into terminals and their effect on fusion and recruitment of vesicle pools studied by using the pulse train paradigm.

Based on their role in inhibiting SNARE complex formation and thus exocytosis, small SNARE peptides may be used as an alternate to Botulinum toxins. One of the side effects of long term use of the Botulinum toxin is the development of neutralizing antibodies (298). Other that its well known cosmetic use, Botulinum toxin is FDA approved for the treatment of chronic migraine and has also been used to manage focal dystonias. In support of the idea that short SNARE peptides may provide a safer alternative to botulinum toxin, 'Argireline' a hexapeptide based on the N terminal of SNAP 25 (aa 12-17) has been found to be reduce wrinkles in healthy female volunteers (299).

Lastly, a rather ambitious project would be to use the SNARE peptides as a pharmacological tool in disorders resulting from excess exocytosis such as spasmodic

disorders and cell death due to excessive glutamate release. Glutamate-induced excitotoxicity has been implicated in the pathophysiology of several neurological and retinal disease including ischemia, glaucoma and diabetic retinopathies (300). Short SNARE-competing peptides that decrease exocytosis and therefore glutamate release may be an interesting approach in the management of these diseases. In hippocampal cultures, a SNAP 25 peptide has been found to be neuroprotective against glutamate mediated excitotoxicity (256).

APPENDIX A

<u>In- vitro Calcium calibration constants used:</u>

from 10/22/08 to 7/3/09
calcium= 4.53936e-6*((ratio-0.811414)/(9.17995-ratio))

from 7/3/09 to 9/15/10 use :
calcium= 8.08972e-6*((ratio-0.80031)/(14.4585-ratio))

from 9/15/10 to 9/8/11
 calcium= 4.19894e-6*((ratio-0.794362)/(11.7369-ratio))

after 1/1/2012
calcium= 1.21742e-05*((ratio-0.772027)/(9.963436-ratio))

APPENDIX B

<u>Protocols used in Igor for analysis of train pulses</u>

vg/#pragma rtGlobals=1   // Use modern global access method.
// FINDING V_AVG OF SETS IN WAVE FUNCTION: findVAvgs(w)
// --
// Function findVAvg(w) takes a given wave, w, and finds
// the average capacitances of each pulse step in the train.
// The user is given options as to what information is desired.
//
// Copyright © 2008, Ian Gemp, Proleta Datta. All Rights Reserved.
// Heidelberger Labs Inc.
// RRF Rm 407 Research Lab
// --

Function findVAvg(w)
Wave w   // wave provided by user
Variable acc = 1e-6   // approximate error in range/gap values
Variable pulse = 0.048672   //.051072 // length of the sine wave   segment . The 2nd value is from the stim traces
Variable trash = .02 //pulse/2   // this the 20msec after channel closing when Gm is still too high to get   accurate Cm   recordings
Variable range = pulse - trash// interval where average is measured i.e. the last 30msec of each Cm trace
Variable gap = 0.022464 //.019968 // this is the 20msec depolarizing pulse or gap between sets - 2nd value is from the stim traces
Variable skip = range + gap + trash // distance between end of one range to start of next
Variable s,e   // starting and ending points for the entire train
s= **0.14102**   //0.121056+trash (this is the first point after pulse not 20msec after end of pulse + trash) // start point where Cm measurement   starts , i.e. 20msec after end of depol pulse.
e= **9.7731** // end point for the entire wave

// Option Prompt
Variable whichvalues=1
Prompt whichvalues, "Do you want only stepsizes, only averages, or   everything? 1=Steps, 2=Avgs, 3=All"

DoPrompt "Options", whichvalues

// Baseline Wave Stats (last .03 seconds)
Variable base = 0.098592 // where Cm baseline ends
WaveStats/Q/R = (base-.03,base) w // calculates the wavestats for the   last 30msec of each pulse. In this line it calculating VAvgs for last 30msec   of Cm baseline, before ist pulse is given.

Variable baseave = V_avg // we decided to rename the waves to avoid confusion with the generic V_avg, this doesn't affect the calculations
print "Baseline Average = ",baseave
// Information Headings
print ""
if (whichvalues==1)
print "Calculating Stepsizes Only..."
elseif (whichvalues==2)
print "Calculating Averages Only..."
else
print "Calculating All Information..."
endif
print "-------------------------"

// Counting/Holding Variables
Variable step=0
Variable pause // what is this???not used anywhere
Variable i=1

// Gathering Set Information
do
WaveStats/Q/R = (s,s+range) w // finds WaveStats of the pulse from point s to 30 msec after
step = V_avg-baseave// calculates difference between averages of two consecutive pulses

// Presenting Information
if (whichvalues==1)
print step
elseif (whichvalues==2)
print V_avg
else
print "Set #",i
print " V_avg = ",V_avg
print " Step size = ",step
print " xRange = (",s,"-",s+range,")"
print "-------------------------"
endif
// Step up variables and reset values
s+=skip
i+=1
while (s<=(e-range+acc)) // this loops till the s is <= the 136th pulse -30 msec , a error margin of 1msec is added
print ""
print "...Done"

End

```
#pragma rtGlobals=1          // Use modern global access method.
// FINDING AVERAGE CURRENT PEAKS FROM from single train pulse
// FUNCTION:        findI(w)
// ---------------------------------------------
// Function findI(w) takes a given wave, w, which
// should represent the calcium current measured during depolarizing pulses applied to a cell
during experiment, and finds the average current peak at each pulse during a
// specified time interval.
// Ian Gemp/Proleta Datta © 2008
// Heidelberger Labs Inc.
// RRF Rm 407 Research Lab
// ---------------------------------------------
Function findI(w)
Wave w // wave provided by user
Variable gap = 0.051648 //0.0511368//0.048672 // time duration of each sine wave
Variable pulse =0.019488//0.020256//0.0192//0.022464 // time duration    between each
sine wave or the depolarizing pulse
Variable skip = gap + pulse // time between each peak measured
Variable premeas1 = 0.006  // When you want to start measuring with respect to channel
closing
Variable premeas2 = 0.001  // When you want to finish measuring with respect to channel
closing
Variable acc = 1e-5 // just in case the computer needs a little leeway - some variables aren't
accurate enough
Variable s = 0.12 //0.120192 // where the program starts, the closing of the channel of the
first pulse
Variable e = 9.7236 //9.7233//2.1119// where the program ends, the closing of the channel
of the 136th pulse
print "Calculating Averages Only..."
print "-------------------------"
Variable i=1
do
WaveStats/Q/R = (s-premeas1,s-premeas2) w // finds WaveStats of set - current peak
average
//print i
print V_avg
// Step up variables and reset values
s+=skip // s+=skip is same as s=s+skip
i+=1
while (s<=(e+acc)) // this will loop as long as value of s is<= the closing of the channel of
the 30th pulse
//print s-skip // this was a used to test if the last V-avg was taking the correct time points
//print s
End
```

```
#pragma rtGlobals=1          // Use modern global access method.
// FINDING V_AVG OF SETS IN Ca WAVE
// FUNCTION:        findCa(w)
// ---------------------------------------------
// Function findCa(w) takes a given wave, w, and finds
// the peak Calcium concentrations after each pulse
//
// Ian Gemp/Proleta Datta © 2008
// Heidelberger Labs Inc.
// UTMC MB Rm 407 Research Lab
// ---------------------------------------------


Function findCa(w,trial,trialnum)
Wave w         // wave provided by user
String trial    // holds experiment trial number// actually there is no need to put string
variables if you use the 'O' after wavestats as that erases any previous wave with same name
Variable trialnum     // hold experiment trial number as text
// Prompt asking for the F1&F2 baseline values
Variable f1base
Variable f2base
Prompt f1base, "F1 Baseline"
Prompt f2base, "F2 Baseline"
DoPrompt "Baseline Values", f1base, f2base // these are input by user . User has to
calculate this from f1 and f2 waves from Xchart


// Sets up time ranges for both F1 sets
Variable tstart1 = 0.0072 // start point for f1 measurement of the train
Variable tend1 = 0.05568 // end point of f1 measurement of the train (remember that the
2nd trace (from high res) is constructed such that the first 50msec are f1 (360) and the rest is
f2 (388))
//Variable tstart2 = 2.16557 // this is from previous procedures where we were taking f1
avg before and after the pulse , averaging them to get the f1avg
//Variable tend2 = 2.21923


// Calculates F1 avg
WaveStats/Q/R = (tstart1,tend1) w
Variable f1befavg = V_avg // we renamed the wave to avoid confusion between this and
the generic V_avg
Variable f1avg = f1befavg - f1base // Subtracts baseline from F1 avg
// Creates F2 wave with trial as suffix
String f2wave = "f2avg"+trial
Duplicate/O w,$f2wave
Wave f2temp = $f2wave
f2temp = w-f2base


// Creates ratio wave with trial as suffix
```

```
String ratiowave = "ratio"+trial
Duplicate/O w,$ratiowave  // overwirtes wave
Wave rtemp = $ratiowave
rtemp = f1avg/f2temp // calculates ratio for the trace. f2 temp is from entire trace while f1
avg is from the first 100 ms

// Coefficients for Ca(ratio)
Variable Keff = 8.08972e-6 //5.30336e-6
Variable Rmin = 0.80031 //0.8897435
Variable Rmax = 14.4585 //9.17995

// Creates Ca wave with trial as suffix
String Cawave = "Ca"+trial
Duplicate/O w,$Cawave  // overwrites previous wave
Wave Catemp = $Cawave
Catemp = Keff*((rtemp-Rmin)/(Rmax-rtemp))

// Defines variables for specifying measurement ranges
Variable skip = 0.071136 // distance between each Ca measurement
Variable acc = 1e-6 // gives program leeway (in case skip isn't perfect)
Variable s = 0.1199 //0.121056 // where program starts
Variable e = 9.7549 // where program ends
// how far left and right of the channel closing the Ca should be measured
Variable premeas = .020
Variable postmeas = .045

print "Calculating Averages Only..."
print "-------------------------"

// Counting/Holding Variables
Variable i=1

do
WaveStats/Q/R = (s+premeas,s+postmeas) Catemp
// finds WaveStats of train      //print i
print V_avg

// Step up variables and reset values
s+=skip
i+=1
while (s<=(e+acc))
print ""
print "...Done
End
```

REFERENCES

1.   Eccles, J.C. 1982. The synapse: from electrical to chemical transmission. Annual review of neuroscience. 5: 325-39.

2.   Cowan, W.M., and E.R. Kandel. 2001. A brief history of synapses and synaptic transmission. In: Synapses. .

3.   Fodstad, H. 2001. The neuron theory. Stereotactic and functional neurosurgery. 77: 20-4.

4.   Cajal, S.R. y. 1906. The structure and connexions of neurons. Nobel Lectures, Physiology or Medicine 1901-1921, Elsevier Publishing Company, Amsterdam, 1967. .

5.   Sherrington, C.S. The Integrative Action of the Nervous System. by]. New York: Charles Scribner's Sons, 1906. Hardcover, 1st Edition - Ted Kottler, Bookseller. .

6.   Sudhof, T.C. 2004. The synaptic vesicle cycle. Annual review of neuroscience. 27: 509-47.

7.   Sjostrand, F.S. 1958. Ultrastructure of retinal rod synapses of the guinea pig eye as revealed by three-dimensional reconstructions from serial sections. Journal of ultrastructure research. 2: 122-70.

8.   Sjostrand, F.S. 1953. The ultrastructure of the innersegments of the retinal rods of the guinea pig eye as revealed by electron microscopy. Journal of cellular physiology. 42: 45-70.

9.   Kidd, M. 1962. Electron microscopy of the inner plexiform layer of the retina in the cat and the pigeon. Journal of anatomy. 96: 179-87.

10.   Dowling, J.E., and B.B. Boycott. 1966. Organization of the primate retina: electron microscopy. Proc R Soc Lond B Biol Sci. 166: 80-111.

11.   Wersäll, J., A. Flock, and P.G. Lundquist. 1965. Structural basis for directional sensitivity in cochlear and vestibular sensory receptors. Cold Spring Harbor symposia on quantitative biology. 30: 115-32.

12.   Hama, K. 1965. Some Observations on the Fine Structure of the Lateral Line Organ of the Japanese Sea Eel Lycozymba Nystromi. The Journal of cell biology. 24: 193-210.

13.   Vollrath, L., and H. Huss. 1973. The synaptic ribbons of the guinea-pig pineal gland under normal and experimental conditions. Zeitschrift für Zellforschung und mikroskopische Anatomie (Vienna, Austria : 1948). 139: 417-29.

14.   Velden, Van Der, H.A. 1946. The number of quanta necessary for the perception of light of the human eye. Ophthalmologica. Journal international d'ophtalmologie. International journal of ophthalmology. Zeitschrift für Augenheilkunde. 111: 321-31.

15.   Sakitt, B. 1972. Counting every quantum. The Journal of physiology. 223: 131-50.

16. Rieke, F., and D.A. Baylor. 1998. Origin of reproducibility in the responses of retinal rods to single photons. Biophysical journal. 75: 1836-57.

17. Ahnert-Hilger, G., M. Höltje, I. Pahner, S. Winter, and I. Brunk. 2003. Regulation of vesicular neurotransmitter transporters. Reviews of physiology, biochemistry and pharmacology. 150: 140-60.

18. Becherer, U., and J. Rettig. 2006. Vesicle pools, docking, priming, and release. Cell and tissue research. 326: 393-407.

19. Verhage, M., and J.B. Sørensen. 2008. Vesicle docking in regulated exocytosis. Traffic (Copenhagen, Denmark). 9: 1414-24.

20. Toonen, R.F., O. Kochubey, H. de Wit, A. Gulyas-Kovacs, B. Konijnenburg, et al. 2006. Dissecting docking and tethering of secretory vesicles at the target membrane. The EMBO journal. 25: 3725-37.

21. Borisovska, M., Y. Zhao, Y. Tsytsyura, N. Glyvuk, S. Takamori, et al. 2005. v-SNAREs control exocytosis of vesicles from priming to fusion. The EMBO journal. 24: 2114-26.

22. Betz, A., P. Thakur, H.J. Junge, U. Ashery, J.S. Rhee, et al. 2001. Functional interaction of the active zone proteins Munc13-1 and RIM1 in synaptic vesicle priming. Neuron. 30: 183-96.

23. Gulyás-Kovács, A., H. de Wit, I. Milosevic, O. Kochubey, R. Toonen, et al. 2007. Munc18-1: sequential interactions with the fusion machinery stimulate vesicle

docking and priming. The Journal of neuroscience : the official journal of the Society for Neuroscience. 27: 8676-86.

24. Carr, C.M., and J. Rizo. 2010. At the junction of SNARE and SM protein function. Current opinion in cell biology. 22: 488-95.

25. Jahn, R., and R.H. Scheller. 2006. SNAREs--engines for membrane fusion. Nature reviews. Molecular cell biology. 7: 631-43.

26. Jahn, R., T. Lang, and T.C. Südhof. 2003. Membrane fusion. Cell. 112: 519-33.

27. Südhof, T.C., and J.E. Rothman. 2009. Membrane fusion: grappling with SNARE and SM proteins. Science (New York, N.Y.). 323: 474-7.

28. Shupliakov, O., and L. Brodin. 2010. Recent insights into the building and cycling of synaptic vesicles. Experimental cell research. 316: 1344-50.

29. Chen, Y.A., and R.H. Scheller. 2001. SNARE-mediated membrane fusion. Nature reviews. Molecular cell biology. 2: 98-106.

30. Misura, K.M., R.H. Scheller, and W.I. Weis. 2000. Three-dimensional structure of the neuronal-Sec1-syntaxin 1a complex. Nature. 404: 355-62.

31. Dulubova, I., S. Sugita, S. Hill, M. Hosaka, I. Fernandez, et al. 1999. A conformational switch in syntaxin during exocytosis: role of munc18. The EMBO journal. 18: 4372-82.

32.   Grosshans, B.L., D. Ortiz, and P. Novick. 2006. Rabs and their effectors: achieving specificity in membrane traffic. Proceedings of the National Academy of Sciences of the United States of America. 103: 11821-7.

33.   Chen, X., D.R. Tomchick, E. Kovrigin, D. Araç, M. Machius, et al. 2002. Three-dimensional structure of the complexin/SNARE complex. Neuron. 33: 397-409.

34.   Reim, K., H. Wegmeyer, J.H. Brandstätter, M. Xue, C. Rosenmund, et al. 2005. Structurally and functionally unique complexins at retinal ribbon synapses. The Journal of cell biology. 169: 669-80.

35.   Reim, K., M. Mansour, F. Varoqueaux, H.T. McMahon, T.C. Südhof, et al. 2001. Complexins regulate a late step in Ca2+-dependent neurotransmitter release. Cell. 104: 71-81.

36.   Schaub, J.R., X. Lu, B. Doneske, Y.-K. Shin, and J.A. McNew. 2006. Hemifusion arrest by complexin is relieved by Ca2+-synaptotagmin I. Nature structural & molecular biology. 13: 748-50.

37.   Giraudo, C.G., W.S. Eng, T.J. Melia, and J.E. Rothman. 2006. A clamping mechanism involved in SNARE-dependent exocytosis. Science (New York, N.Y.). 313: 676-80.

38.   Tang, J., A. Maximov, O.-H. Shin, H. Dai, J. Rizo, et al. 2006. A complexin/synaptotagmin 1 switch controls fast synaptic vesicle exocytosis. Cell. 126: 1175-87.

39. Huntwork, S., and J.T. Littleton. 2007. A complexin fusion clamp regulates spontaneous neurotransmitter release and synaptic growth. Nature neuroscience. 10: 1235-7.

40. Xue, M., A. Stradomska, H. Chen, N. Brose, W. Zhang, et al. 2008. Complexins facilitate neurotransmitter release at excitatory and inhibitory synapses in mammalian central nervous system. Proceedings of the National Academy of Sciences of the United States of America. 105: 7875-80.

41. Krishnakumar, S.S., D.T. Radoff, D. Kümmel, C.G. Giraudo, F. Li, et al. 2011. A conformational switch in complexin is required for synaptotagmin to trigger synaptic fusion. Nature structural & molecular biology. 18: 934-40.

42. Kümmel, D., S.S. Krishnakumar, D.T. Radoff, F. Li, C.G. Giraudo, et al. 2011. Complexin cross-links prefusion SNAREs into a zigzag array. Nature structural & molecular biology. 18: 927-33.

43. Li, F., F. Pincet, E. Perez, C.G. Giraudo, D. Tareste, et al. 2011. Complexin activates and clamps SNAREpins by a common mechanism involving an intermediate energetic state. Nature structural & molecular biology. 18: 941-6.

44. Perin, M.S., V.A. Fried, G.A. Mignery, R. Jahn, and T.C. Südhof. 1990. Phospholipid binding by a synaptic vesicle protein homologous to the regulatory region of protein kinase C. Nature. 345: 260-3.

45. Brose, N., A.G. Petrenko, T.C. Südhof, and R. Jahn. 1992. Synaptotagmin: a calcium sensor on the synaptic vesicle surface. Science (New York, N.Y.). 256: 1021-5.

46. Pang, Z.P., E. Melicoff, D. Padgett, Y. Liu, A.F. Teich, et al. 2006. Synaptotagmin-2 is essential for survival and contributes to Ca2+ triggering of neurotransmitter release in central and neuromuscular synapses. The Journal of neuroscience : the official journal of the Society for Neuroscience. 26: 13493-504.

47. Xu, J., T. Mashimo, and T.C. Südhof. 2007. Synaptotagmin-1, -2, and -9: Ca(2+) sensors for fast release that specify distinct presynaptic properties in subsets of neurons. Neuron. 54: 567-81.

48. Roux, I., S. Safieddine, R. Nouvian, M. Grati, M.-C. Simmler, et al. 2006. Otoferlin, defective in a human deafness form, is essential for exocytosis at the auditory ribbon synapse. Cell. 127: 277-289.

49. Dulon, D., S. Safieddine, S.M. Jones, and C. Petit. 2009. Otoferlin is critical for a highly sensitive and linear calcium-dependent exocytosis at vestibular hair cell ribbon synapses. The Journal of neuroscience : the official journal of the Society for Neuroscience. 29: 10474-87.

50. Geppert, M., Y. Goda, R.E. Hammer, C. Li, T.W. Rosahl, et al. 1994. Synaptotagmin I: a major Ca2+ sensor for transmitter release at a central synapse. Cell. 79: 717-27.

51. Sun, J., Z.P. Pang, D. Qin, A.T. Fahim, R. Adachi, et al. 2007. A dual-Ca2+-sensor model for neurotransmitter release in a central synapse. Nature. 450: 676-82.

52.　Young, S.M., and E. Neher. 2009. Synaptotagmin has an essential function in synaptic vesicle positioning for synchronous release in addition to its role as a calcium sensor. Neuron. 63: 482-96.

53.　Katz, B., and R. Miledi. 1965. The effect of temperature on the synaptic delay at the neuromuscular junction. The Journal of physiology. 181: 656-70.

54.　Heidelberger, R., C. Heinemann, E. Neher, and G. Matthews. 1994. Calcium dependence of the rate of exocytosis in a synaptic terminal. Nature. 371: 513-515.

55.　Borst, J.G., F. Helmchen, and B. Sakmann. 1995. Pre- and postsynaptic whole-cell recordings in the medial nucleus of the trapezoid body of the rat. The Journal of physiology. 489 (Pt 3: 825-40.

56.　Palmer, M.J. 2010. Characterisation of bipolar cell synaptic transmission in goldfish retina using paired recordings. The Journal of physiology. 588: 1489-98.

57.　Pang, Z.P., J. Sun, J. Rizo, A. Maximov, and T.C. Südhof. 2006. Genetic analysis of synaptotagmin 2 in spontaneous and Ca2+-triggered neurotransmitter release. The EMBO journal. 25: 2039-50.

58.　von Gersdorff, H., T. Sakaba, K. Berglund, and M. Tachibana. 1998. Submillisecond kinetics of glutamate release from a sensory synapse. Neuron. 21: 1177-88.

59.　Rahamimoff, R., and Y. Yaari. 1973. Delayed release of transmitter at the frog neuromuscular junction. The Journal of physiology. 228: 241-57.

60.   Atluri, P.P., and W.G. Regehr. 1998. Delayed release of neurotransmitter from cerebellar granule cells. The Journal of neuroscience : the official journal of the Society for Neuroscience. 18: 8214-27.

61.   Best, A.R., and W.G. Regehr. 2009. Inhibitory regulation of electrically coupled neurons in the inferior olive is mediated by asynchronous release of GABA. Neuron. 62: 555-65.

62.   Daw, M.I., L. Tricoire, F. Erdelyi, G. Szabo, and C.J. McBain. 2009. Asynchronous transmitter release from cholecystokinin-containing inhibitory interneurons is widespread and target-cell independent. The Journal of neuroscience : the official journal of the Society for Neuroscience. 29: 11112-22.

63.   Hefft, S., and P. Jonas. 2005. Asynchronous GABA release generates long-lasting inhibition at a hippocampal interneuron-principal neuron synapse. Nature neuroscience. 8: 1319-28.

64.   Katz, B., and R. Miledi. 1967. Tetrodotoxin and neuromuscular transmission. Proceedings of the Royal Society of London. Series B, Containing papers of a Biological character. Royal Society (Great Britain). 167: 8-22.

65.   Llano, I., J. González, C. Caputo, F.A. Lai, L.M. Blayney, et al. 2000. Presynaptic calcium stores underlie large-amplitude miniature IPSCs and spontaneous calcium transients. Nature neuroscience. 3: 1256-65.

66. Denker, A., and S.O. Rizzoli. 2010. Synaptic vesicle pools: an update. Frontiers in synaptic neuroscience. 2: 135.

67. Hua, Z., S. Leal-Ortiz, S.M. Foss, C.L. Waites, C.C. Garner, et al. 2011. v-SNARE Composition Distinguishes Synaptic Vesicle Pools. Neuron. 71: 474-87.

68. Birks, R., and F.C. MacIntosh. 1961. Acetylcholine Metabolism of a Sympathetic Ganglion. .

69. Rizzoli, S.O., and W.J. Betz. 2005. Synaptic vesicle pools. Nature reviews. Neuroscience. 6: 57-69.

70. Hanse, E., and B. Gustafsson. 2001. Vesicle release probability and pre-primed pool at glutamatergic synapses in area CA1 of the rat neonatal hippocampus. The Journal of physiology. 531: 481-93.

71. Schneggenburger, R., A.C. Meyer, and E. Neher. 1999. Released fraction and total size of a pool of immediately available transmitter quanta at a calyx synapse. Neuron. 23: 399-409.

72. Mennerick, S., and G. Matthews. 1996. Ultrafast exocytosis elicited by calcium current in synaptic terminals of retinal bipolar neurons. Neuron. 17: 1241-1249.

73. Neves, G., and L. Lagnado. 1999. The kinetics of exocytosis and endocytosis in the synaptic terminal of goldfish retinal bipolar cells. The Journal of physiology. 515 (Pt 1: 181-202.

74. Bartoletti, T.M., N. Babai, and W.B. Thoreson. 2010. Vesicle pool size at the salamander cone ribbon synapse. Journal of Neurophysiology. 103: 419-423.

75. von Gersdorff, H., E. Vardi, G. Matthews, and P. Sterling. 1996. Evidence that vesicles on the synaptic ribbon of retinal bipolar neurons can be rapidly released. Neuron. 16: 1221-7.

76. Schikorski, T., and C.F. Stevens. 2001. Morphological correlates of functionally defined synaptic vesicle populations. Nature neuroscience. 4: 391-5.

77. Satzler, K., L.F. Sohl, J.H. Bollmann, J.G.G. Borst, M. Frotscher, et al. 2002. Three-Dimensional Reconstruction of a Calyx of Held and Its Postsynaptic Principal Neuron in the Medial Nucleus of the Trapezoid Body. The Journal of neuroscience : the official journal of the Society for Neuroscience. 22: 10567-10579.

78. Kuromi, H., and Y. Kidokoro. 1998. Two distinct pools of synaptic vesicles in single presynaptic boutons in a temperature-sensitive Drosophila mutant, shibire. Neuron. 20: 917-25.

79. de Lange, R.P.J., A.D.G. de Roos, and J.G.G. Borst. 2003. Two modes of vesicle recycling in the rat calyx of Held. The Journal of neuroscience : the official journal of the Society for Neuroscience. 23: 10164-73.

80. Heidelberger, R., P. Sterling, and G. Matthews. 2002. Roles of ATP in depletion and replenishment of the releasable pool of synaptic vesicles. Journal of Neurophysiology. 88: 98-106.

81.   Heidelberger, R. 1998. Adenosine triphosphate and the late steps in calcium-dependent exocytosis at a ribbon synapse. The Journal of general physiology. 111: 225-41.

82.   Midorikawa, M., Y. Tsukamoto, K. Berglund, M. Ishii, and M. Tachibana. 2007. Different roles of ribbon-associated and ribbon-free active zones in retinal bipolar cells. Nature Neuroscience. 10: 1268-1276.

83.   Zenisek, D. 2008. Vesicle association and exocytosis at ribbon and extraribbon sites in retinal bipolar cell presynaptic terminals. Proceedings of the National Academy of Sciences of the United States of America. 105: 4922-4927.

84.   von Gersdorff, H., and G. Matthews. 1997. Depletion and replenishment of vesicle pools at a ribbon-type synaptic terminal. The Journal of neuroscience : the official journal of the Society for Neuroscience. 17: 1919-27.

85.   Zenisek, D., V. Davila, L. Wan, and W. Almers. 2003. Imaging calcium entry sites and ribbon structures in two presynaptic cells. Journal of Neuroscience. 23: 2538-48.

86.   Holt, M., A. Cooke, A. Neef, and L. Lagnado. 2004. High mobility of vesicles supports continuous exocytosis at a ribbon synapse. Current Biology. 14: 173-183.

87.   LoGiudice, L., P. Sterling, and G. Matthews. 2008. Mobility and turnover of vesicles at the synaptic ribbon. Journal of Neuroscience. 28: 3150-3158.

88.   Hilfiker, S., V.A. Pieribone, A.J. Czernik, H.T. Kao, G.J. Augustine, et al. 1999. Synapsins as regulators of neurotransmitter release. Philosophical transactions of the Royal Society of London. Series B, Biological sciences. 354: 269-79.

89.   Li, L., L.S. Chin, O. Shupliakov, L. Brodin, T.S. Sihra, et al. 1995. Impairment of synaptic vesicle clustering and of synaptic transmission, and increased seizure propensity, in synapsin I-deficient mice. Proceedings of the National Academy of Sciences of the United States of America. 92: 9235-9.

90.   Rosahl, T.W., D. Spillane, M. Missler, J. Herz, D.K. Selig, et al. 1995. Essential functions of synapsins I and II in synaptic vesicle regulation. Nature. 375: 488-93.

91.   Mozhayeva, M.G., Y. Sara, X. Liu, and E.T. Kavalali. 2002. Development of vesicle pools during maturation of hippocampal synapses. The Journal of neuroscience : the official journal of the Society for Neuroscience. 22: 654-65.

92.   Mandell, J.W., E. Townes-Anderson, A.J. Czernik, R. Cameron, P. Greengard, et al. 1990. Synapsins in the vertebrate retina: absence from ribbon synapses and heterogeneous distribution among conventional synapses. Neuron. 5: 19-33.

93.   Ullrich, B., and T.C. Südhof. 1994. Distribution of synaptic markers in the retina: implications for synaptic vesicle traffic in ribbon synapses. Journal of physiology, Paris. 88: 249-57.

94. Safieddine, S., and R.J. Wenthold. 1999. SNARE complex at the ribbon synapses of cochlear hair cells: analysis of synaptic vesicle- and synaptic membrane-associated proteins. The European journal of neuroscience. 11: 803-12.

95. Usukura, J., and E. Yamada. 1987. Ultrastructure of the synaptic ribbons in photoreceptor cells of Rana catesbeiana revealed by freeze-etching and freeze-substitution. Cell and tissue research. 247: 483-8.

96. Matthews, G., and P. Sterling. 2008. Evidence that vesicles undergo compound fusion on the synaptic ribbon. Journal of Neuroscience. 28: 5403-5411.

97. Chung, C., B. Barylko, J. Leitz, X. Liu, and E.T. Kavalali. 2010. Acute dynamin inhibition dissects synaptic vesicle recycling pathways that drive spontaneous and evoked neurotransmission. The Journal of neuroscience : the official journal of the Society for Neuroscience. 30: 1363-76.

98. Mathew, S.S., L. Pozzo-Miller, and J.J. Hablitz. 2008. Kainate modulates presynaptic GABA release from two vesicle pools. The Journal of neuroscience : the official journal of the Society for Neuroscience. 28: 725-31.

99. Fredj, N.B., and J. Burrone. 2009. A resting pool of vesicles is responsible for spontaneous vesicle fusion at the synapse. Nature neuroscience. 12: 751-8.

100. Wilhelm, B.G., T.W. Groemer, and S.O. Rizzoli. 2010. The same synaptic vesicles drive active and spontaneous release. Nature neuroscience. 13: 1454-6.

101. Gandhi, S.P., and C.F. Stevens. 2003. Three modes of synaptic vesicular recycling revealed by single-vesicle imaging. Nature. 423: 607-13.

102. Opazo, F., A. Punge, J. Bückers, P. Hoopmann, L. Kastrup, et al. 2010. Limited intermixing of synaptic vesicle components upon vesicle recycling. Traffic (Copenhagen, Denmark). 11: 800-12.

103. Wienisch, M., and J. Klingauf. 2006. Vesicular proteins exocytosed and subsequently retrieved by compensatory endocytosis are nonidentical. Nature neuroscience. 9: 1019-27.

104. Kamin, D., M.A. Lauterbach, V. Westphal, J. Keller, A. Schönle, et al. 2010. High- and low-mobility stages in the synaptic vesicle cycle. Biophysical journal. 99: 675-84.

105. Westphal, V., S.O. Rizzoli, M.A. Lauterbach, D. Kamin, R. Jahn, et al. 2008. Video-rate far-field optical nanoscopy dissects synaptic vesicle movement. Science (New York, N.Y.). 320: 246-9.

106. Staras, K., T. Branco, J.J. Burden, K. Pozo, K. Darcy, et al. 2010. A vesicle superpool spans multiple presynaptic terminals in hippocampal neurons. Neuron. 66: 37-44.

107. Fernandez-Alfonso, T., and T.A. Ryan. 2008. A heterogeneous "resting" pool of synaptic vesicles that is dynamically interchanged across boutons in mammalian CNS synapses. Brain cell biology. 36: 87-100.

108.	Rizzoli, S.O., and W.J. Betz. 2004. The structural organization of the readily releasable pool of synaptic vesicles. Science (New York, N.Y.). 303: 2037-9.

109.	Rosenmund, C., and C.F. Stevens. 1996. Definition of the readily releasable pool of vesicles at hippocampal synapses. Neuron. 16: 1197-207.

110.	von Gersdorff, H., R. Schneggenburger, S. Weis, and E. Neher. 1997. Presynaptic depression at a calyx synapse: the small contribution of metabotropic glutamate receptors. The Journal of neuroscience : the official journal of the Society for Neuroscience. 17: 8137-46.

111.	Wang, L.Y., and L.K. Kaczmarek. 1998. High-frequency firing helps replenish the readily releasable pool of synaptic vesicles. Nature. 394: 384-8.

112.	Sakaba, T., and E. Neher. 2001. Calmodulin mediates rapid recruitment of fast-releasing synaptic vesicles at a calyx-type synapse. Neuron. 32: 1119-31.

113.	Richards, D.A., C. Guatimosim, and W.J. Betz. 2000. Two endocytic recycling routes selectively fill two vesicle pools in frog motor nerve terminals. Neuron. 27: 551-9.

114.	Richards, D.A., C. Guatimosim, S.O. Rizzoli, and W.J. Betz. 2003. Synaptic vesicle pools at the frog neuromuscular junction. Neuron. 39: 529-41.

115.	Sakaba, T., R. Schneggenburger, and E. Neher. 2002. Estimation of quantal parameters at the calyx of Held synapse. Neuroscience research. 44: 343-56.

116. Hosoi, N., T. Sakaba, and E. Neher. 2007. Quantitative analysis of calcium-dependent vesicle recruitment and its functional role at the calyx of Held synapse. The Journal of neuroscience : the official journal of the Society for Neuroscience. 27: 14286-98.

117. Stevens, C.F., and T. Tsujimoto. 1995. Estimates for the pool size of releasable quanta at a single central synapse and for the time required to refill the pool. Proceedings of the National Academy of Sciences of the United States of America. 92: 846-9.

118. Suyama, S., T. Hikima, H. Sakagami, T. Ishizuka, and H. Yawo. 2007. Synaptic vesicle dynamics in the mossy fiber-CA3 presynaptic terminals of mouse hippocampus. Neuroscience research. 59: 481-90.

119. Trommershäuser, J., R. Schneggenburger, A. Zippelius, and E. Neher. 2003. Heterogeneous presynaptic release probabilities: functional relevance for short-term plasticity. Biophysical journal. 84: 1563-79.

120. Pyle, J.L., E.T. Kavalali, E.S. Piedras-Rentería, and R.W. Tsien. 2000. Rapid reuse of readily releasable pool vesicles at hippocampal synapses. Neuron. 28: 221-31.

121. Harata, N., J.L. Pyle, A.M. Aravanis, M. Mozhayeva, E.T. Kavalali, et al. 2001. Limited numbers of recycling vesicles in small CNS nerve terminals: implications for neural signaling and vesicular cycling. Trends in neurosciences. 24: 637-43.

122. Ryan, T.A., H. Reuter, and S.J. Smith. 1997. Optical detection of a quantal presynaptic membrane turnover. Nature. 388: 478-82.

123. von Gersdorff, H., and G. Matthews. 1994. Dynamics of synaptic vesicle fusion and membrane retrieval in synaptic terminals. Nature. 367: 735-9.

124. Hull, C., K. Studholme, S. Yazulla, and H. Von Gersdorff. 2006. Diurnal changes in exocytosis and the number of synaptic ribbons at active zones of an ON-type bipolar cell terminal. Journal of Neurophysiology. 96: 2025-2033.

125. Harata, N., T.A. Ryan, S.J. Smith, J. Buchanan, and R.W. Tsien. 2001. Visualizing recycling synaptic vesicles in hippocampal neurons by FM 1-43 photoconversion. Proceedings of the National Academy of Sciences of the United States of America. 98: 12748-53.

126. Aravanis, A.M., J.L. Pyle, and R.W. Tsien. 2003. Single synaptic vesicles fusing transiently and successively without loss of identity. Nature. 423: 643-7.

127. Schikorski, T., and C.F. Stevens. 1997. Quantitative ultrastructural analysis of hippocampal excitatory synapses. The Journal of neuroscience : the official journal of the Society for Neuroscience. 17: 5858-67.

128. Satzler, K., L.F. Sohl, J.H. Bollmann, J.G.G. Borst, M. Frotscher, et al. 2002. Three-Dimensional Reconstruction of a Calyx of Held and Its Postsynaptic Principal Neuron in the Medial Nucleus of the Trapezoid Body. J. Neurosci. 22: 10567-10579.

129. Takei, K., O. Mundigl, L. Daniell, and P. De Camilli. 1996. The synaptic vesicle cycle: a single vesicle budding step involving clathrin and dynamin. The Journal of cell biology. 133: 1237-50.

130. Moser, T., A. Brandt, and A. Lysakowski. 2006. Hair cell ribbon synapses. Cell and tissue research. 326: 347-59.

131. Matthews, G., and P. Fuchs. 2010. The diverse roles of ribbon synapses in sensory neurotransmission. Nature Reviews Neuroscience. 11: 812-822.

132. Heidelberger, R., W.B. Thoreson, and P. Witkovsky. 2005. Synaptic transmission at retinal ribbon synapses. Progress in retinal and eye research. 24: 682-720.

133. Schmitz, F., A. Königstorfer, and T.C. Südhof. 2000. RIBEYE, a component of synaptic ribbons: a protein's journey through evolution provides insight into synaptic ribbon function. Neuron. 28: 857-72.

134. Zenisek, D., N.K. Horst, C. Merrifield, P. Sterling, and G. Matthews. 2004. Visualizing synaptic ribbons in the living cell. Journal of Neuroscience. 24: 9752-9759.

135. Tom Dieck, S., W.D. Altrock, M.M. Kessels, B. Qualmann, H. Regus, et al. 2005. Molecular dissection of the photoreceptor ribbon synapse: physical interaction of Bassoon and RIBEYE is essential for the assembly of the ribbon complex. The Journal of Cell Biology. 168: 825-36.

136. Uthaiah, R.C., and A.J. Hudspeth. 2010. Molecular anatomy of the hair cell's ribbon synapse. Journal of Neuroscience. 30: 12387-12399.

137. Dick, O., I. Hack, W.D. Altrock, C.C. Garner, E.D. Gundelfinger, et al. 2001. Localization of the presynaptic cytomatrix protein Piccolo at ribbon and conventional

synapses in the rat retina: comparison with Bassoon. The Journal of comparative neurology. 439: 224-34.

138. Frank, T., M.A. Rutherford, N. Strenzke, A. Neef, T. Pangršič, et al. 2010. Bassoon and the synaptic ribbon organize Ca^2+ channels and vesicles to add release sites and promote refilling. Neuron. 68: 724-38.

139. Dick, O., S. Tom Dieck, W.D. Altrock, J. Ammermüller, R. Weiler, et al. 2003. The presynaptic active zone protein bassoon is essential for photoreceptor ribbon synapse formation in the retina. Neuron. 37: 775-786.

140. Joselevitch, C., and D. Zenisek. 2010. The cytomatrix protein bassoon contributes to fast transmission at conventional and ribbon synapses. Neuron. 68: 604-606.

141. Venkatesan, J.K., S. Natarajan, K. Schwarz, S.I. Mayer, K. Alpadi, et al. 2010. Nicotinamide adenine dinucleotide-dependent binding of the neuronal Ca2+ sensor protein GCAP2 to photoreceptor synaptic ribbons. The Journal of neuroscience : the official journal of the Society for Neuroscience. 30: 6559-76.

142. Thoreson, W.B., K. Rabl, E. Townes-Anderson, and R. Heidelberger. 2004. A highly Ca2+-sensitive pool of vesicles contributes to linearity at the rod photoreceptor ribbon synapse. Neuron. 42: 595-605.

143. Sejnowski, T.J., and M.L. Yodlowski. 1982. A freeze-fracture study of the skate electroreceptor. Journal of neurocytology. 11: 897-912.

144. Lenzi, D., J.W. Runyeon, J. Crum, M.H. Ellisman, and W.M. Roberts. 1999. Synaptic vesicle populations in saccular hair cells reconstructed by electron tomography. The Journal of neuroscience : the official journal of the Society for Neuroscience. 19: 119-32.

145. Sterling, P., and G. Matthews. 2005. Structure and function of ribbon synapses. Trends in Neurosciences. 28: 20-29.

146. Morgans, C.W. 2001. Localization of the alpha(1F) calcium channel subunit in the rat retina. Investigative ophthalmology & visual science. 42: 2414-8.

147. Issa, N.P., and A.J. Hudspeth. 1994. Clustering of Ca2+ channels and Ca(2+)-activated K+ channels at fluorescently labeled presynaptic active zones of hair cells. Proceedings of the National Academy of Sciences of the United States of America. 91: 7578-82.

148. Alle, H., and J.R.P. Geiger. 2008. Analog signalling in mammalian cortical axons. Current opinion in neurobiology. 18: 314-20.

149. Morgans, C.W., J.H. Brandstätter, J. Kellerman, H. Betz, and H. Wässle. 1996. A SNARE complex containing syntaxin 3 is present in ribbon synapses of the retina. Journal of Neuroscience. 16: 6713-6721.

150. Curtis, L.B., B. Doneske, X. Liu, C. Thaller, J.A. McNew, et al. 2008. Syntaxin 3b is a t-SNARE specific for ribbon synapses of the retina. J Comp Neurol. 510: 550-559.

151. Curtis, L., P. Datta, X. Liu, N. Bogdanova, R. Heidelberger, et al. 2010. Syntaxin 3B is essential for the exocytosis of synaptic vesicles in ribbon synapses of the retina. Neuroscience. 166: 832-841.

152. Zanazzi, G., and G. Matthews. 2010. Enrichment and differential targeting of complexins 3 and 4 in ribbon-containing sensory neurons during zebrafish development. Neural development. 5: 24.

153. Reim, K., H. Regus-Leidig, J. Ammermüller, A. El-Kordi, K. Radyushkin, et al. 2009. Aberrant function and structure of retinal ribbon synapses in the absence of complexin 3 and complexin 4. Journal of cell science. 122: 1352-61.

154. Lenzi, D., and H. von Gersdorff. 2001. Structure suggests function: the case for synaptic ribbons as exocytotic nanomachines. BioEssays : news and reviews in molecular, cellular and developmental biology. 23: 831-40.

155. Muresan, V., A. Lyass, and B.J. Schnapp. 1999. The kinesin motor KIF3A is a component of the presynaptic ribbon in vertebrate photoreceptors. The Journal of neuroscience : the official journal of the Society for Neuroscience. 19: 1027-37.

156. Snellman, J., B. Mehta, N. Babai, T.M. Bartoletti, W. Akmentin, et al. 2011. Acute destruction of the synaptic ribbon reveals a role for the ribbon in vesicle priming. Nature Neuroscience. 14: 1135-1141.

157. Edmonds, B.W., F.D. Gregory, and F.E. Schweizer. 2004. Evidence that fast exocytosis can be predominantly mediated by vesicles not docked at active zones in frog saccular hair cells. The Journal of physiology. 560: 439-50.

158. Nouvian, R., J. Neef, A.V. Bulankina, E. Reisinger, T. Pangršič, et al. 2011. Exocytosis at the hair cell ribbon synapse apparently operates without neuronal SNARE proteins. Nature Neuroscience. 14: 411-413.

159. Heidelberger, R., and G. Matthews. 1992. Calcium influx and calcium current in single synaptic terminals of goldfish retinal bipolar neurons. The Journal of physiology. 447: 235-56.

160. Kaneko, A., and M. Tachibana. 1985. A voltage-clamp analysis of membrane currents in solitary bipolar cells dissociated from Carassius auratus. The Journal of Physiology. 358: 131-152.

161. Heidelberger, R., Z.-Y. Zhou, and G. Matthews. 2002. Multiple components of membrane retrieval in synaptic terminals revealed by changes in hydrostatic pressure. Journal of Neurophysiology. 88: 2509-2517.

162. Lindau, M., and E. Neher. 1988. Patch-clamp techniques for time-resolved capacitance measurements in single cells. Pflügers Archiv : European journal of physiology. 411: 137-46.

163. Gillis KD. 1995. Techniques for membrane capacitance measurements. In: Single Channel Recording (Neher E, Sakmann B), New York: Plenum Press. . pp. 155-198.

164. Augustine, G.J., and E. Neher. 1992. Calcium requirements for secretion in bovine chromaffin cells. The Journal of physiology. 450: 247-71.

165. Pusch, M., and E. Neher. 1988. Rates of diffusional exchange between small cells and a measuring patch pipette. Pflügers Archiv : European journal of physiology. 411: 204-11.

166. Marty, A., and J. Zimmerberg. 1989. Diffusion into the patch-clamp recording pipette of a factor necessary for muscarinic current response. Cellular signalling. 1: 259-68.

167. Khvotchev, M., I. Dulubova, J. Sun, H. Dai, J. Rizo, et al. 2007. Dual modes of Munc18-1/SNARE interactions are coupled by functionally critical binding to syntaxin-1 N terminus. The Journal of neuroscience : the official journal of the Society for Neuroscience. 27: 12147-55.

168. Messler, P., H. Harz, and R. Uhl. 1996. Instrumentation for multiwavelengths excitation imaging. Journal of neuroscience methods. 69: 137-47.

169. Grynkiewicz, G., M. Poenie, and R.Y. Tsien. 1985. A new generation of Ca2+ indicators with greatly improved fluorescence properties. The Journal of biological chemistry. 260: 3440-50.

170. Thoreson, W.B. 2007. Kinetics of synaptic transmission at ribbon synapses of rods and cones. Molecular neurobiology. 36: 205-23.

171. Wan, Q.-F., and R. Heidelberger. 2011. Synaptic release at mammalian bipolar cell terminals. Visual neuroscience. 28: 109-19.

172. Heidelberger, R. 2007. Mechanisms of tonic, graded release: lessons from the vertebrate photoreceptor. The Journal of physiology. 585: 663-7.

173. Nouvian, R., D. Beutner, T.D. Parsons, and T. Moser. 2006. Structure and Function of the Hair Cell Ribbon Synapse. The Journal of membrane biology. 209: 153-165.

174. Barlow, H.B., W.R. Levick, and M. Yoon. 1971. Responses to single quanta of light in retinal ganglion cells of the cat. Vision Res. Suppl 3: 87-101.

175. Kolb, H., K.A. Linberg, and S.K. Fisher. 1992. Neurons of the human retina: a Golgi study. The Journal of comparative neurology. 318: 147-87.

176. Ayoub, G.S., and D.R. Copenhagen. 1991. Application of a fluorometric method to measure glutamate release from single retinal photoreceptors. Journal of neuroscience methods. 37: 7-14.

177. Baylor, D.A., and M.G. Fuortes. 1970. Electrical responses of single cones in the retina of the turtle. The Journal of physiology. 207: 77-92.

178. Dacheux, R.F., and R.F. Miller. 1976. Photoreceptor-bipolar cell transmission in the perfused retina eyecup of the mudpuppy. Science (New York, N.Y.). 191: 963-4.

179. Nomura, A., R. Shigemoto, Y. Nakamura, N. Okamoto, N. Mizuno, et al. 1994. Developmentally regulated postsynaptic localization of a metabotropic glutamate receptor in rat rod bipolar cells. Cell. 77: 361-9.

180. Nakajima, Y., H. Iwakabe, C. Akazawa, H. Nawa, R. Shigemoto, et al. 1993. Molecular characterization of a novel retinal metabotropic glutamate receptor mGluR6 with a high agonist selectivity for L-2-amino-4-phosphonobutyrate. The Journal of biological chemistry. 268: 11868-73.

181. DeVries, S.H. 2000. Bipolar cells use kainate and AMPA receptors to filter visual information into separate channels. Neuron. 28: 847-56.

182. Greferath, U., U. Grünert, and H. Wässle. 1990. Rod bipolar cells in the mammalian retina show protein kinase C-like immunoreactivity. The Journal of comparative neurology. 301: 433-42.

183. Berglund, K., M. Midorikawa, and M. Tachibana. 2002. Increase in the pool size of releasable synaptic vesicles by the activation of protein kinase C in goldfish retinal bipolar cells. The Journal of Neuroscience The Official Journal of the Society for Neuroscience. 22: 4776-4785.

184. Kolb, H., L. Zhang, and L. Dekorver. 1993. Differential staining of neurons in the human retina with antibodies to protein kinase C isozymes. Visual neuroscience. 10: 341-51.

185. Amthor, F.R., E.S. Takahashi, and C.W. Oyster. 1989. Morphologies of rabbit retinal ganglion cells with concentric receptive fields. The Journal of comparative neurology. 280: 72-96.

186. Bloomfield, S.A., and R.F. Miller. 1986. A functional organization of ON and OFF pathways in the rabbit retina. The Journal of neuroscience : the official journal of the Society for Neuroscience. 6: 1-13.

187. Kolb, H., and E.V. Famiglietti. 1974. Rod and cone pathways in the inner plexiform layer of cat retina. Science (New York, N.Y.). 186: 47-9.

188. Ammermüller, J., and H. Kolb. 1995. The organization of the turtle inner retina. I. ON- and OFF-center pathways. The Journal of comparative neurology. 358: 1-34.

189. Tachibana, M., and T. Okada. 1991. Release of endogenous excitatory amino acids from ON-type bipolar cells isolated from the goldfish retina. Journal of Neuroscience. 11: 2199-2208.

190. Tachibana, M., T. Okada, T. Arimura, K. Kobayashi, and M. Piccolino. 1993. Dihydropyridine-sensitive calcium current mediates neurotransmitter release from bipolar cells of the goldfish retina. The Journal of neuroscience : the official journal of the Society for Neuroscience. 13: 359-361.

191. Hu, C., A. Bi, and Z.-H. Pan. 2009. Differential expression of three T-type calcium channels in retinal bipolar cells in rats. Visual neuroscience. 26: 177-87.

192. Pan, Z.H. 2000. Differential expression of high- and two types of low-voltage-activated calcium currents in rod and cone bipolar cells of the rat retina. Journal of neurophysiology. 83: 513-27.

193. Pan, Z.H., H.J. Hu, P. Perring, and R. Andrade. 2001. T-type Ca(2+) channels mediate neurotransmitter release in retinal bipolar cells. Neuron. 32: 89-98.

194. de la Villa, P., C.F. Vaquero, and A. Kaneko. 1998. Two types of calcium currents of the mouse bipolar cells recorded in the retinal slice preparation. The European journal of neuroscience. 10: 317-23.

195. Logiudice, L., D. Henry, and G. Matthews. 2006. Identification of calcium channel alpha1 subunit mRNA expressed in retinal bipolar neurons. Molecular vision. 12: 184-9.

196. Protti, D.A., and I. Llano. 1998. Calcium currents and calcium signaling in rod bipolar cells of rat retinal slices. The Journal of neuroscience : the official journal of the Society for Neuroscience. 18: 3715-24.

197. Snellman, J., D. Zenisek, and S. Nawy. 2009. Switching between transient and sustained signalling at the rod bipolar-AII amacrine cell synapse of the mouse retina. The Journal of Physiology. 587: 2443-2455.

198. Singer, J.H., and J.S. Diamond. 2003. Sustained Ca2+ entry elicits transient postsynaptic currents at a retinal ribbon synapse. Journal of Neuroscience. 23: 10923-10933.

199. Jarsky, T., M. Cembrowski, S.M. Logan, W.L. Kath, H. Riecke, et al. 2011. A synaptic mechanism for retinal adaptation to luminance and contrast. The Journal of neuroscience : the official journal of the Society for Neuroscience. 31: 11003-15.

200. Zenisek, D., and G. Matthews. 1998. Calcium action potentials in retinal bipolar neurons. Visual neuroscience. 15: 69-75.

201. Protti, D.A., N. Flores-Herr, and H. von Gersdorff. 2000. Light evokes Ca2+ spikes in the axon terminal of a retinal bipolar cell. Neuron. 25: 215-27.

202. Palmer, M.J. 2006. Modulation of Ca(2+)-activated K+ currents and Ca(2+)-dependent action potentials by exocytosis in goldfish bipolar cell terminals. The Journal of physiology. 572: 747-62.

203. Saito, T., H. Kondo, and J.I. Toyoda. 1979. Ionic mechanisms of two types of on-center bipolar cells in the carp retina. I. The responses to central illumination. The Journal of general physiology. 73: 73-90.

204. Yazulla, S., K.M. Studholme, and J.Y. Wu. 1987. GABAergic input to the synaptic terminals of mb1 bipolar cells in the goldfish retina. Brain research. 411: 400-5.

205. Zimov, S., and S. Yazulla. 2008. Novel processes invaginate the pre-synaptic terminal of retinal bipolar cells. Cell and tissue research. 333: 1-16.

206. Sherry, D.M., and S. Yazulla. 1993. Goldfish bipolar cells and axon terminal patterns: a Golgi study. The Journal of comparative neurology. 329: 188-200.

207. von Gersdorff, H., and G. Matthews. 1999. Electrophysiology of synaptic vesicle cycling. Annual review of physiology. 61: 725-52.

208. Gomis, A., J. Burrone, and L. Lagnado. 1999. Two actions of calcium regulate the supply of releasable vesicles at the ribbon synapse of retinal bipolar cells. The Journal of neuroscience : the official journal of the Society for Neuroscience. 19: 6309-17.

209. von Gersdorff, H., and G. Matthews. 1994. Inhibition of endocytosis by elevated internal calcium in a synaptic terminal. Nature. 370: 652-5.

210. Jockusch, W.J., G.J.K. Praefcke, H.T. McMahon, and L. Lagnado. 2005. Clathrin-dependent and clathrin-independent retrieval of synaptic vesicles in retinal bipolar cells. Neuron. 46: 869-78.

211. Rouze, N.C., and E.A. Schwartz. 1998. Continuous and transient vesicle cycling at a ribbon synapse. Journal of Neuroscience. 18: 8614-8624.

212. Heidelberger, R. 2001. ATP is required at an early step in compensatory endocytosis in synaptic terminals. The Journal of neuroscience : the official journal of the Society for Neuroscience. 21: 6467-74.

213. Yamashita, T., T. Hige, and T. Takahashi. 2005. Vesicle endocytosis requires dynamin-dependent GTP hydrolysis at a fast CNS synapse. Science (New York, N.Y.). 307: 124-7.

214. Marks, B., M.H. Stowell, Y. Vallis, I.G. Mills, A. Gibson, et al. 2001. GTPase activity of dynamin and resulting conformation change are essential for endocytosis. Nature. 410: 231-5.

215. Shupliakov, O., P. Löw, D. Grabs, H. Gad, H. Chen, et al. 1997. Synaptic vesicle endocytosis impaired by disruption of dynamin-SH3 domain interactions. Science (New York, N.Y.). 276: 259-63.

216. Cousin, M.A., and P.J. Robinson. 2000. Ca(2+) influx inhibits dynamin and arrests synaptic vesicle endocytosis at the active zone. The Journal of neuroscience : the official journal of the Society for Neuroscience. 20: 949-57.

217. Xu, J., B. McNeil, W. Wu, D. Nees, L. Bai, et al. 2008. GTP-independent rapid and slow endocytosis at a central synapse. Nature neuroscience. 11: 45-53.

218. Wan, Q.-F., A. Vila, Z.-Y. Zhou, and R. Heidelberger. 2008. Synaptic vesicle dynamics in mouse rod bipolar cells. Visual neuroscience. 25: 523-33.

219. Wan, Q.-F., Z.-Y. Zhou, P. Thakur, A. Vila, D.M. Sherry, et al. 2010. SV2 acts via presynaptic calcium to regulate neurotransmitter release. Neuron. 66: 884-95.

220. Zenisek, D., and G. Matthews. 2000. The role of mitochondria in presynaptic calcium handling at a ribbon synapse. Neuron. 25: 229-237.

221. Hsu, S.F., and M.B. Jackson. 1996. Rapid exocytosis and endocytosis in nerve terminals of the rat posterior pituitary. The Journal of physiology. 494 (Pt 2: 539-53.

222. Leitz, J., and E.T. Kavalali. 2011. Ca^{2+} influx slows single synaptic vesicle endocytosis. The Journal of neuroscience : the official journal of the Society for Neuroscience. 31: 16318-26.

223. Burrone, J., G. Neves, A. Gomis, A. Cooke, and L. Lagnado. 2002. Endogenous calcium buffers regulate fast exocytosis in the synaptic terminal of retinal bipolar cells. Neuron. 33: 101-112.

224. Saviane, C., and R.A. Silver. 2006. Fast vesicle reloading and a large pool sustain high bandwidth transmission at a central synapse. Nature. 439: 983-7.

225. Taschenberger, H., R.M. Leão, K.C. Rowland, G.A. Spirou, and H. von Gersdorff. 2002. Optimizing synaptic architecture and efficiency for high-frequency transmission. Neuron. 36: 1127-43.

226. Lonart, G., and T.C. Südhof. 2000. Assembly of SNARE core complexes prior to neurotransmitter release sets the readily releasable pool of synaptic vesicles. The Journal of biological chemistry. 275: 27703-7.

227. Söllner, T., S.W. Whiteheart, M. Brunner, H. Erdjument-Bromage, S. Geromanos, et al. 1993. SNAP receptors implicated in vesicle targeting and fusion. Nature. 362: 318-24.

228. Fasshauer, D., H. Otto, W.K. Eliason, R. Jahn, and A.T. Brünger. 1997. Structural changes are associated with soluble N-ethylmaleimide-sensitive fusion protein attachment protein receptor complex formation. The Journal of biological chemistry. 272: 28036-41.

229. Pobbati, A.V., A. Stein, and D. Fasshauer. 2006. N- to C-terminal SNARE complex assembly promotes rapid membrane fusion. Science (New York, N.Y.). 313: 673-6.

230. Sørensen, J.B., K. Wiederhold, E.M. Müller, I. Milosevic, G. Nagy, et al. 2006. Sequential N- to C-terminal SNARE complex assembly drives priming and fusion of secretory vesicles. The EMBO journal. 25: 955-66.

231. Benfenati, F., F. Onofri, and S. Giovedí. 1999. Protein-protein interactions and protein modules in the control of neurotransmitter release. Philosophical transactions of the Royal Society of London. Series B, Biological sciences. 354: 243-57.

232. Redecker, P., H. Pabst, A. Gebert, and S. Steinlechner. 1997. Expression of synaptic membrane proteins in gerbil pinealocytes in primary culture. Journal of neuroscience research. 47: 509-20.

233. Redecker, P., C. Weyer, and D. Grube. 1996. Rat and gerbil pinealocytes contain the synaptosomal-associated protein 25 (SNAP-25). Journal of pineal research. 21: 29-34.

234. Sherry, D.M., H. Yang, and K.M. Standifer. 2001. Vesicle-associated membrane protein isoforms in the tiger salamander retina. The Journal of comparative neurology. 431: 424-36.

235. Sherry, D.M., M.M. Wang, and L.J. Frishman. 2003. Differential distribution of vesicle associated membrane protein isoforms in the mouse retina. Molecular vision. 9: 673-88.

236. Brandstatter, J.H., H. Wassle, H. Betz, C.W. Morgans, J.H. Brandstätter, et al. 1996. The plasma membrane protein SNAP-25, but not syntaxin, is present at photoreceptor and bipolar cell synapses in the rat retina. Eur J Neurosci. 8: 823-828.

237. Greenlee, M.H., C.B. Roosevelt, and D.S. Sakaguchi. 2001. Differential localization of SNARE complex proteins SNAP-25, syntaxin, and VAMP during development of the mammalian retina. The Journal of comparative neurology. 430: 306-20.

238. Broadie, K., A. Prokop, H.J. Bellen, C.J. O'Kane, K.L. Schulze, et al. 1995. Syntaxin and synaptobrevin function downstream of vesicle docking in Drosophila. Neuron. 15: 663-73.

239. O'Connor, V., C. Heuss, W.M. De Bello, T. Dresbach, M.P. Charlton, et al. 1997. Disruption of syntaxin-mediated protein interactions blocks neurotransmitter secretion. Proceedings of the National Academy of Sciences of the United States of America. 94: 12186-91.

240. Xu-Friedman, M.A., K.M. Harris, and W.G. Regehr. 2001. Three-dimensional comparison of ultrastructural characteristics at depressing and facilitating synapses onto cerebellar Purkinje cells. The Journal of neuroscience : the official journal of the Society for Neuroscience. 21: 6666-72.

241. Toonen, R.F.G., K. Wierda, M.S. Sons, H. de Wit, L.N. Cornelisse, et al. 2006. Munc18-1 expression levels control synapse recovery by regulating readily releasable pool size. Proceedings of the National Academy of Sciences of the United States of America. 103: 18332-7.

242. Hay, J.C., and T.F. Martin. 1992. Resolution of regulated secretion into sequential MgATP-dependent and calcium-dependent stages mediated by distinct cytosolic proteins. The Journal of cell biology. 119: 139-51.

243.   von Rüden, L., and E. Neher. 1993. A Ca-dependent early step in the release of catecholamines from adrenal chromaffin cells. Science (New York, N.Y.). 262: 1061-5.

244.   Eberhard, D.A., C.L. Cooper, M.G. Low, and R.W. Holz. 1990. Evidence that the inositol phospholipids are necessary for exocytosis. Loss of inositol phospholipids and inhibition of secretion in permeabilized cells caused by a bacterial phospholipase C and removal of ATP. The Biochemical journal. 268: 15-25.

245.   Hay, J.C., P.L. Fisette, G.H. Jenkins, K. Fukami, T. Takenawa, et al. 1995. ATP-dependent inositide phosphorylation required for Ca(2+)-activated secretion. Nature. 374: 173-7.

246.   Wang, Y., M. Okamoto, F. Schmitz, K. Hofmann, and T.C. Südhof. 1997. Rim is a putative Rab3 effector in regulating synaptic-vesicle fusion. Nature. 388: 593-8.

247.   Gerber, S.H., J.-C. Rah, S.-W. Min, X. Liu, H. de Wit, et al. 2008. Conformational switch of syntaxin-1 controls synaptic vesicle fusion. Science (New York, N.Y.). 321: 1507-10.

248.   Walter, A.M., K. Wiederhold, D. Bruns, D. Fasshauer, and J.B. Sørensen. 2010. Synaptobrevin N-terminally bound to syntaxin-SNAP-25 defines the primed vesicle state in regulated exocytosis. The Journal of cell biology. 188: 401-13.

249. Ma, C., W. Li, Y. Xu, and J. Rizo. 2011. Munc13 mediates the transition from the closed syntaxin-Munc18 complex to the SNARE complex. Nature structural & molecular biology. 18: 542-9.

250. Hunt, J.M., K. Bommert, M.P. Charlton, A. Kistner, E. Habermann, et al. 1994. A post-docking role for synaptobrevin in synaptic vesicle fusion. Neuron. 12: 1269-79.

251. Zenisek, D., J.A. Steyer, and W. Almers. 2000. Transport, capture and exocytosis of single synaptic vesicles at active zones. Nature. 406: 849-54.

252. Hayashi, T., H. McMahon, S. Yamasaki, T. Binz, Y. Hata, et al. 1994. Synaptic vesicle membrane fusion complex: action of clostridial neurotoxins on assembly. The EMBO journal. 13: 5051-61.

253. von Gersdorff, H., and G. Matthews. 1996. Calcium-dependent inactivation of calcium current in synaptic terminals of retinal bipolar neurons. The Journal of neuroscience : the official journal of the Society for Neuroscience. 16: 115-22.

254. Kang, Y., X. Huang, E.A. Pasyk, J. Ji, G.G. Holz, et al. 2002. Syntaxin-3 and syntaxin-1A inhibit L-type calcium channel activity, insulin biosynthesis and exocytosis in beta-cell lines. Diabetologia. 45: 231-41.

255. Fergestad, T., M.N. Wu, K.L. Schulze, T.E. Lloyd, H.J. Bellen, et al. 2001. Targeted mutations in the syntaxin H3 domain specifically disrupt SNARE complex function in synaptic transmission. The Journal of neuroscience : the official journal of the Society for Neuroscience. 21: 9142-50.

256. Blanes-Mira, C., J.M. Merino, E. Valera, G. Fernández-Ballester, L.M. Gutiérrez, et al. 2004. Small peptides patterned after the N-terminus domain of SNAP25 inhibit SNARE complex assembly and regulated exocytosis. Journal of neurochemistry. 88: 124-35.

257. Zampighi, G.A., C. Schietroma, L.M. Zampighi, M. Woodruff, E.M. Wright, et al. 2011. Conical Tomography of a Ribbon Synapse: Structural Evidence for Vesicle Fusion. PLoS ONE. 6: 12.

258. Jackman, S.L., S.-Y. Choi, W.B. Thoreson, K. Rabl, T.M. Bartoletti, et al. 2009. Role of the synaptic ribbon in transmitting the cone light response. Nature neuroscience. 12: 303-10.

259. Walch-Solimena, C., J. Blasi, L. Edelmann, E.R. Chapman, G.F. von Mollard, et al. 1995. The t-SNAREs syntaxin 1 and SNAP-25 are present on organelles that participate in synaptic vesicle recycling. The Journal of cell biology. 128: 637-45.

260. Kretzschmar, S., W. Volknandt, and H. Zimmermann. 1996. Colocalization on the same synaptic vesicles of syntaxin and SNAP-25 with synaptic vesicle proteins: a re-evaluation of functional models required? Neuroscience research. 26: 141-8.

261. Takamori, S., M. Holt, K. Stenius, E.A. Lemke, M. Grønborg, et al. 2006. Molecular anatomy of a trafficking organelle. Cell. 127: 831-46.

262. Sinha, R., S. Ahmed, R. Jahn, and J. Klingauf. 2011. Two synaptobrevin molecules are sufficient for vesicle fusion in central nervous system synapses. Proceedings of the National Academy of Sciences of the United States of America. 108: 14318-23.

263. Kantardzhieva, A.V., M. Peppi, W.S. Lane, and W.F. Sewell. 2011. Protein composition of immunoprecipitated synaptic ribbons. Journal of proteome research. 11: 1163-74.

264. Apland, J.P., J.A. Biser, M. Adler, A.V. Ferrer-Montiel, M. Montal, et al. 1999. Peptides that mimic the carboxy-terminal domain of SNAP-25 block acetylcholine release at an Aplysia synapse. Journal of applied toxicology : JAT. 19 Suppl 1: S23-6.

265. Ferrer-Montiel, A.V., L.M. Gutiérrez, J.P. Apland, J.M. Canaves, A. Gil, et al. 1998. The 26-mer peptide released from SNAP-25 cleavage by botulinum neurotoxin E inhibits vesicle docking. FEBS letters. 435: 84-8.

266. McMahon, H.T., Y.A. Ushkaryov, L. Edelmann, E. Link, T. Binz, et al. 1993. Cellubrevin is a ubiquitous tetanus-toxin substrate homologous to a putative synaptic vesicle fusion protein. Nature. 364: 346-9.

267. Schoch, S., F. Deák, A. Königstorfer, M. Mozhayeva, Y. Sara, et al. 2001. SNARE function analyzed in synaptobrevin/VAMP knockout mice. Science (New York, N.Y.). 294: 1117-22.

268. Yang, B., L. Gonzalez, R. Prekeris, M. Steegmaier, R.J. Advani, et al. 1999. SNARE interactions are not selective. Implications for membrane fusion specificity. The Journal of biological chemistry. 274: 5649-53.

269. Fasshauer, D., W. Antonin, M. Margittai, S. Pabst, and R. Jahn. 1999. Mixed and non-cognate SNARE complexes. Characterization of assembly and biophysical properties. The Journal of biological chemistry. 274: 15440-6.

270. Bergsman, J.B., and R.W. Tsien. 2000. Syntaxin modulation of calcium channels in cortical synaptosomes as revealed by botulinum toxin C1. The Journal of neuroscience : the official journal of the Society for Neuroscience. 20: 4368-78.

271. Bezprozvanny, I., R.H. Scheller, and R.W. Tsien. 1995. Functional impact of syntaxin on gating of N-type and Q-type calcium channels. Nature. 378: 623-6.

272. Trus, M., O. Wiser, M.C. Goodnough, and D. Atlas. 2001. The transmembrane domain of syntaxin 1A negatively regulates voltage-sensitive Ca(2+) channels. Neuroscience. 104: 599-607.

273. Atlas, D., O. Wiser, and M. Trus. 2001. The voltage-gated Ca2+ channel is the Ca2+ sensor of fast neurotransmitter release. Cellular and molecular neurobiology. 21: 717-31.

274. Arien, H., O. Wiser, I.T. Arkin, H. Leonov, and D. Atlas. 2003. Syntaxin 1A modulates the voltage-gated L-type calcium channel (Ca(v)1.2) in a cooperative manner. The Journal of biological chemistry. 278: 29231-9.

275. Yang, S.N., O. Larsson, R. Bränström, A.M. Bertorello, B. Leibiger, et al. 1999. Syntaxin 1 interacts with the L(D) subtype of voltage-gated Ca(2+) channels in pancreatic beta cells. Proceedings of the National Academy of Sciences of the United States of America. 96: 10164-9.

276. Degtiar, V.E., R.H. Scheller, and R.W. Tsien. 2000. Syntaxin modulation of slow inactivation of N-type calcium channels. The Journal of neuroscience : the official journal of the Society for Neuroscience. 20: 4355-67.

277. Zanazzi, G., and G. Matthews. 2009. The molecular architecture of ribbon presynaptic terminals. Molecular Neurobiology. 39: 130-48.

278. Wu, M.N., T. Fergestad, T.E. Lloyd, Y. He, K. Broadie, et al. 1999. Syntaxin 1A interacts with multiple exocytic proteins to regulate neurotransmitter release in vivo. Neuron. 23: 593-605.

279. Wiser, O., M. Trus, A. Hernández, E. Renström, S. Barg, et al. 1999. The voltage sensitive Lc-type Ca2+ channel is functionally coupled to the exocytotic machinery. Proceedings of the National Academy of Sciences of the United States of America. 96: 248-53.

280. Kim, D.K., and W.A. Catterall. 1997. Ca2+-dependent and -independent interactions of the isoforms of the alpha1A subunit of brain Ca2+ channels with presynaptic SNARE proteins. Proceedings of the National Academy of Sciences of the United States of America. 94: 14782-6.

281. Innocenti, B., and R. Heidelberger. 2008. Mechanisms contributing to tonic release at the cone photoreceptor ribbon synapse. Journal of neurophysiology. 99: 25-36.

282. Spassova, M.A., M. Avissar, A.C. Furman, M.A. Crumling, J.C. Saunders, et al. 2004. Evidence that rapid vesicle replenishment of the synaptic ribbon mediates recovery from short-term adaptation at the hair cell afferent synapse. Journal of the Association for Research in Otolaryngology : JARO. 5: 376-90.

283. Moser, T., and D. Beutner. 2000. Kinetics of exocytosis and endocytosis at the cochlear inner hair cell afferent synapse of the mouse. Proceedings of the National Academy of Sciences of the United States of America. 97: 883-8.

284. Raviola, E., and N.B. Gilula. 1975. Intramembrane organization of specialized contacts in the outer plexiform layer of the retina. A freeze-fracture study in monkeys and rabbits. The Journal of cell biology. 65: 192-222.

285. Blank, P.S., M.S. Cho, S.S. Vogel, D. Kaplan, A. Kang, et al. 1998. Submaximal responses in calcium-triggered exocytosis are explained by differences in the calcium sensitivity of individual secretory vesicles. The Journal of general physiology. 112: 559-67.

286. Goda, Y., and C.F. Stevens. 1994. Two components of transmitter release at a central synapse. Proceedings of the National Academy of Sciences of the United States of America. 91: 12942-6.

287. Berntson, Amy K Morgans, C.W. 2003. Distribution of the presynaptic calcium sensors, synaptotagmin I/II and synaptotagmin III, in the goldfish and rodent retinas. Journal of vision. 3: 274-80.

288. Lagnado, L., A. Gomis, and C. Job. 1996. Continuous vesicle cycling in the synaptic terminal of retinal bipolar cells. Neuron. 17: 957-67.

289. Li, C., B.A. Davletov, and T.C. Südhof. 1995. Distinct Ca2+ and Sr2+ binding properties of synaptotagmins. Definition of candidate Ca2+ sensors for the fast and slow components of neurotransmitter release. The Journal of biological chemistry. 270: 24898-902.

290. Heidelberger, R., M.M. Wang, and D.M. Sherry. 2003. Differential distribution of synaptotagmin immunoreactivity among synapses in the goldfish, salamander, and mouse retina. Visual neuroscience. 20: 37-49.

291. Eisen, M.D., M. Spassova, and T.D. Parsons. 2004. Large releasable pool of synaptic vesicles in chick cochlear hair cells. Journal of neurophysiology. 91: 2422-8.

292. Smith, S.M., R. Renden, and H. Von Gersdorff. 2008. Synaptic vesicle endocytosis: fast and slow modes of membrane retrieval. Trends in Neurosciences. 31: 559-568.

293. Frank, S.P.C., K.-P. Thon, S.C. Bischoff, and A. Lorentz. 2011. SNAP-23 and syntaxin-3 are required for chemokine release by mature human mast cells. Molecular immunology. 49: 353-8.

294. Pombo, I., J. Rivera, and U. Blank. 2003. Munc18-2/syntaxin3 complexes are spatially separated from syntaxin3-containing SNARE complexes. FEBS letters. 550: 144-8.

295. Guo, Z., C. Turner, and D. Castle. 1998. Relocation of the t-SNARE SNAP-23 from lamellipodia-like cell surface projections regulates compound exocytosis in mast cells. Cell. 94: 537-48.

296. Behrendorff, N., S. Dolai, W. Hong, H.Y. Gaisano, and P. Thorn. 2011. Vesicle-associated membrane protein 8 (VAMP8) is a SNARE (soluble N-ethylmaleimide-sensitive factor attachment protein receptor) selectively required for sequential granule-to-granule fusion. The Journal of biological chemistry. 286: 29627-34.

297. Pochet, R., B. Pasteels, A. Seto-Ohshima, E. Bastianelli, S. Kitajima, et al. 1991. Calmodulin and calbindin localization in retina from six vertebrate species. The Journal of comparative neurology. 314: 750-62.

298. Colosimo, C., D. Tiple, and A. Berardelli. 2012. Efficacy and Safety of Long-term Botulinum Toxin Treatment in Craniocervical Dystonia: A Systematic Review. Neurotoxicity research. .

299. Blanes-Mira, C., J. Clemente, G. Jodas, A. Gil, G. Fernández-Ballester, et al. 2002. A synthetic hexapeptide (Argireline) with antiwrinkle activity. International journal of cosmetic science. 24: 303-10.

300. Baltmr, A., J. Duggan, S. Nizari, T.E. Salt, and M.F. Cordeiro. 2010. Neuroprotection in glaucoma - Is there a future role? Experimental eye research. 91: 554-66.

VITA

Proleta Datta was born in Bangalore, India on June 27th 1980 to Dr. Indira Ghosh and Dr. Santanu Datta. Proleta received her medical training and completed her internship from Kasturba Medical College, Mangalore in 2004. She subsequently entered the Neuroscience Graduate program at the University of Texas -Medical School at Houston in 2005. She joined the laboratory of Dr. Ruth Heidelberger where she explored mechanisms underlying neurotransmitter release from ribbon synapses of the retina.

Permanent Address:

B-302, RV Enclave

15 cross Malleshwaram

Bangalore   560003

This is a License Agreement between Proleta Datta ("You") and Elsevier ("Elsevier") provided by Copyright Clearance Center ("CCC"). The license consists of your order details, the terms and conditions provided by Elsevier, and the payment terms and conditions.

All payments must be made in full to CCC. For payment instructions, please see information listed at the bottom of this form.

Supplier	Elsevier Limited The Boulevard,Langford Lane Kidlington,Oxford,OX5 1GB,UK
Registered Company Number	1982084
Customer name	Proleta Datta
Customer address	Dept of Neurobiology and Anatomy Houston, TX 77030
License number	2847270750722
License date	Feb 13, 2012
Licensed content publisher	Elsevier
Licensed content publication	Neuron
Licensed content title	A Highly Ca-Sensitive Pool of Vesicles Contributes to Linearity at the Rod Photoreceptor Ribbon Synapse
Licensed content author	Wallace B Thoreson,Katalin Rabl,Ellen Townes-Anderson,Ruth Heidelberger
Licensed content date	27 May 2004
Licensed content volume number	42
Licensed content issue	4

number

Number of pages	11
Start Page	595
End Page	605
Type of Use	reuse in a thesis/dissertation
Portion	figures/tables/illustrations
Number of figures/tables/illustrations	1
Format	both print and electronic
Are you the author of this Elsevier article?	No
Will you be translating?	No
Order reference number	None
Title of your thesis/dissertation	THE FUNCTIONAL ORGANIZATION OF SYNAPTIC VESICLE POOLS IN A RETINAL BIPOLAR NEURON
Expected completion date	Apr 2012
Estimated size (number of pages)	100
Elsevier VAT number	GB 494 6272 12
Permissions price	0.00 USD
VAT/Local Sales Tax	0.0 USD / 0.0 GBP
Total	0.00 USD
Terms and Conditions	

Gratis licenses (referencing $0 in the Total field) are free. Please retain this printable license for your reference. No payment is required.